PB82-196924

Mechanisms of Dry SO2 Control Processes

Radian Corp.
Durham, NC

Prepared for

Industrial Environmental Research Lab.
Research Triangle Park, NC

Apr 82

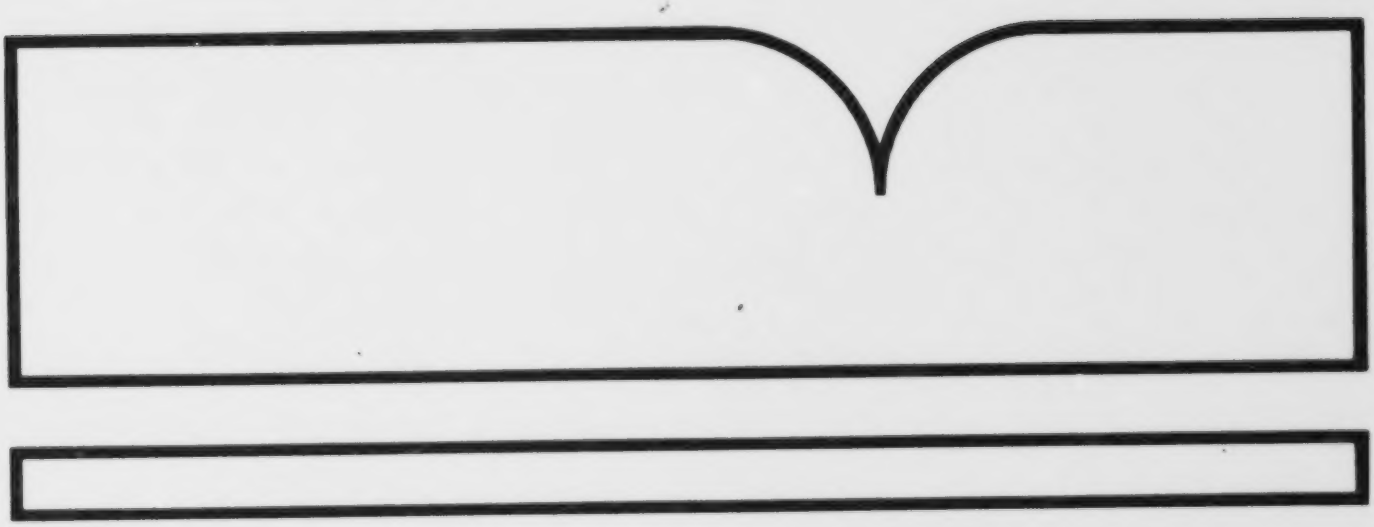

U.S. Department of Commerce
National Technical Information Service
NTIS.

PB82-196924

EPA-600/7-82-026
April 1982

MECHANISMS OF DRY SO_2 CONTROL PROCESSES

by

Cathy Apple and Mary E. Kelly

Radian Corporation
3024 Pickett Road
Durham, North Carolina 27705

EPA Contract No. 68-02-3171, Task 15

Project Officer

Theodore G. Brna

Utilities and Industrial Power Division
Industrial Environmental Research Laboratory
Research Triangle Park, North Carolina 27711

REPRODUCED BY
NATIONAL TECHNICAL
INFORMATION SERVICE
U.S. DEPARTMENT OF COMMERCE
SPRINGFIELD, VA. 22161

Prepared for

OFFICE OF ENVIRONMENTAL ENGINEERING AND TECHNOLOGY
OFFICE OF RESEARCH AND DEVELOPMENT
U. S. ENVIRONMENTAL PROTECTION AGENCY
WASHINGTON, DC 20460

TECHNICAL REPORT DATA
(Please read Instructions on the reverse before completing)

1. REPORT NO.	2.	3. RECIPIENT'S ACCESSION NO.
EPA-600/7-82-026	ORD Report	PB82 176924

4. TITLE AND SUBTITLE	5. REPORT DATE
Mechanisms of Dry SO_2 Control Processes	April 1982
	6. PERFORMING ORGANIZATION CODE
7. AUTHOR(S)	8. PERFORMING ORGANIZATION REPORT NO.
Cathy Apple and Mary E. Kelly	
9. PERFORMING ORGANIZATION NAME AND ADDRESS	10. PROGRAM ELEMENT NO.
Radian Corporation 3024 Pickett Road Durham, North Carolina 27705	11. CONTRACT/GRANT NO. 68-02-3171, Task 15
12. SPONSORING AGENCY NAME AND ADDRESS	13. TYPE OF REPORT AND PERIOD COVERED
EPA, Office of Research and Development Industrial Environmental Research Laboratory Research Triangle Park, NC 27711	Task Final; 9/80 - 9/81 14. SPONSORING AGENCY CODE EPA/600/13

15. SUPPLEMENTARY NOTES IERL-RTP project officer is Theodore G. Brna, Mail Drop 61, 919/541-2683.

16. ABSTRACT The report discusses physical and chemical processes and reaction mechanisms for lime spray drying and dry injection of sodium compounds in dry flue gas desulfurization (FGD) processes. It includes: chemical reactions, physical changes, proposed reaction mechanisms and mathematical models, process parameters affecting reactions and their rates, and data needed to verify proposed reaction mechanisms and models. Published technical papers were the primary reference sources. The report focuses on coal-fired boiler dry FGD applications. Lime spray drying reactions are primarily gas/liquid-phase reactions, with SO2 removal depending on moisture in the lime slurry droplet. Initially, the moisture content is high, and the reaction rate is controlled by diffusion of SO2 to the droplet surface; most SO2 removal occurs during this phase. As evaporation reduces the moisture, the dissolution of Ca(OH)2 into ions limits the SO2 removal rate. Later, the precipitation of of $CaSO_3 \cdot 1/2\ H_2O$ onto the surface of the lime particles retards diffusion of SO2 to the unreacted sorbent. Injecting sodium compound powders into flue gas removes SO2 via gas/solid reactions. First, NaHCO3 is thermally decomposed to Na2CO3 (small pores in the sorbent particles increase the particles' surface area and reactivity). Then the SO2 reacts with Na2CO3 to form Na2SO3, starting at the particle surface.

17. KEY WORDS AND DOCUMENT ANALYSIS

a. DESCRIPTORS		b. IDENTIFIERS/OPEN ENDED TERMS	c. COSATI Field/Group	
Pollution	Sodium	Pollution Control	13B	
Sulfur Dioxide	Mathematical Models	Stationary Sources	07B	12A
Flue Gases	Coal	Dry Processes	21B	21D
Desulfurization	Combustion	Reaction Mechanisms	07A, 07D	
Calcium Oxides		Lime Spray Drying		
Spray Drying			13H	

18. DISTRIBUTION STATEMENT	19. SECURITY CLASS (This Report)	21. NO. OF PAGES
Release to Public	Unclassified	
	20. SECURITY CLASS (This page) Unclassified	22

EPA Form 2220-1 (9-73)

ABSTRACT

This report identifies and evaluates the postulated physical changes, chemical reactions, and reaction mechanisms involved in two dry flue gas desulfurization (FGD) technologies: lime spray drying and dry injection of sodium compounds. Topics covered are: (1) chemical reactions and physical changes, (2) proposed reaction mechanisms and mathematical models, (3) process parameters which affect the reactions and rate controlling steps, and (4) needs for additional data to verify the proposed mechanisms and the effects of the various process parameters. The information used in developing this report was obtained from a review of published articles and technical papers.

The reactions involved in lime spray drying are gas-liquid phase reactions. SO_2 removal is dependent on the moisture content of the drying lime slurry droplet. Initially, the moisture content of the droplet is high and the rate of reaction is controlled by the diffusion of SO_2 to the surface of the slurry droplet. It appears that the greatest amount of SO_2 is removed at this time, and Babcock and Wilcox has mathematically modelled SO_2 removal during this period. As the moisture content of the droplet is reduced by evaporation the dissolution of $Ca(OH)_2$ into ions becomes the rate limiting factor. SO_2 removal by the spray-dried solids is limited by the dissolution of $Ca(OH)_2$, and by the diffusion of SO_2 through the $CaSO_3 \cdot \frac{1}{2}H_2O$ product that has precipitated on the surface of the lime particle.

The reactions involved in the removal of SO_2 by the dry injection of finely ground sodium compounds are gas-solid phase reactions. Two steps are involved in the removal of SO_2. First, $NaHCO_3$ is thermally decomposed to Na_2CO_3. This reaction produces small pores in the sorbent particles, which increases the available surface area and the reactivity of the sorbent. Then the SO_2 reacts with Na_2CO_3 to produce Na_2SO_3. This reaction begins at the surface of the particle and moves inward leaving behind a layer of reacted ash. This ash layer tends to plug the pores that were formed by thermal decomposition, reducing the reactivity of the sorbent. Therefore, it has been postulated that initially the rate of reaction is controlled by the thermal decomposition of $NaHCO_3$ to Na_2CO_3, and then becomes controlled by the diffusion of SO_2 through the ash layer. Mathematical models describing SO_2 removal for these cases can be derived from the classical unreacted core model.

CONTENTS

Abstract ii
Tables v
Figures vi
Acknowledgements viii

1.0 Summary 1

1.1 Lime Spray Drying 2
1.2 Sodium Dry Injection 6
1.3 Summary References 11

2.0 Lime Spray Drying 12

2.1 Reactions and Reaction Models for Lime Spray Drying 14
2.1.1 Physical Changes and Chemical Reactions 14
2.1.1.1 Physical Changes 15
2.1.1.1.1 Stages of Drying 15
2.1.1.1.2 Physical Properties of the Droplet during Drying 18
2.1.1.2 Chemical Reactions 20
2.1.2 Reaction Models 21
2.1.2.1 Qualitative Models 23
2.1.2.2 Quantitative Models 25
2.1.2.2.1 Diffusion Model 28
2.1.2.2.2 Stoichiometric Ratio Correlation (Transfer Area Model) 33
2.2 Process Parameters Affecting the Spray Drying Process . . . 36
2.2.1 Approach to Saturation Temperature 37
2.2.2 Slurry Droplet Size - Method of Atomization 38
2.2.3 Residence Time of the Flue Gas in the Dryer 41
2.2.4 Stoichiometric Ratio 41
2.2.5 Droplet - Gas Mixing 42
2.2.6 Lime Slaking 43
2.2.7 Inlet SO_2 Concentration 44
2.2.8 Flue Gas Inlet Temperature 44
2.2.9 Spray-Dried Off-Product Recycle 48
2.2.10 Fabric Filter versus ESP Particulate Collection . . . 53
2.3 Data Gaps in Literature 55
2.4 Literature Cited for Spray Drying 56

3.0 Sodium Dry Injection 58

3.1 Reactions and Reaction Models for Sodium Dry Injection . . . 60
3.1.1 Chemical Reactions and Physical Changes 61
3.1.1.1 Chemical Reactions 61
3.1.1.2 Physical Changes 63

CONTENTS (Continued)

3.1.2 Reaction Models 65
3.1.2.1 Qualitative Models 65
3.1.2.2 Quantitative Models 67
3.1.2.2.1 Unreacted-Core Model 67
3.1.2.2.2 Empirical Models 75
3.2 Process Parameters Affecting the Dry Injection Process . . . 79
3.2.1 Sorbent Type 80
3.2.2 Sorbent Preparation 87
3.2.3 Particle Size 89
3.2.4 Temperature 92
3.2.5 Stoichiometric Ratio 95
3.2.6 Mode of Injection 97
3.2.7 Residence Time of Flue Gas in the Duct 98
3.2.8 Filter Cleaning Intervals 98
3.2.9 Inlet SO_2 Concentration 98
3.2.10 Gas Velocity and Air-to-Cloth Ratio 100
3.3 Data Gaps in Literature 100
3.4 Literature Cited for Dry Injection 102

4.0 Bibliography 104

Appendix A Derivation of Diffusion Model 111
Appendix B Derivation of the Unreacted-Core Model 119
Appendix C Conversion Factors 127

TABLES

Number		Page
2-1a	Chemical Composition of the Spray-Dried FGD Waste Product (Research-Cottrell)	22
2-1b	Chemical Composition of the Spray-Dried FGD Waste Product (Buell)	22
2-2	Spray Dryer FGD Performance Using Cooling Tower Blowdown Water	44
2-3	Hopper Ash Analyses Comparison	50
3-1a	Laboratory Studies of FGD by Injection of Dry Adsorbent	81
3-1b	Studies of FGD by Injection of Dry Adsorbent on Pilot Plant Equipment	82
3-2	Chemical Composition of Sodium Compounds used in Dry Injection	83
3-3	SO_2 Removal Results with $NaHCO_3$ and Nahcolite	88
3-4	Effect of Temperature on Dry Injection SO_2 Removal	93

FIGURES

Number		Page
2-1	Typical spray dryer/particulate collection flow diagram	13
2-2	Stages of spray drying: drying rate versus time	17
2-3	Drying and reaction sequence of atomized droplets	19
2-4	Scanning electron micrographs (SEM's) and elemental analysis of spray-dried solids	26-27
2-5a	Babcock and Wilcox's test of the constant rate period absorption model	32
2-5b	Buell's test of the constant rate period absorption model	32
2-6a	Babcock and Wilcox's test of the stoichiometry correlation model	35
2-6b	Buell's test of the stoichiometry correlation model	35
2-7a	Effect of approach to adiabatic saturation temperature on spray dryer SO_2 removal (Research-Cottrell)	39
2-7b	Effect of approach to adiabatic saturation temperature on spray dryer SO_2 removal (Buell)	40
2-8a	Effect of inlet SO_2 concentration on spray dryer SO_2 removal (Research-Cottrell)	45
2-8b	Effect of inlet SO_2 concentration on spray dryer SO_2 removal (Buell)	46
2-9	Effect of flue gas inlet temperature on spray dryer SO_2 removal (Buell)	47
2-10a	Effect of recycle ratio on overall SO_2 removal (Research-Cottrell)	51
2-10b	Effect of recycle on overall SO_2 removal (Buell)	52
2-11a	Spray dryer only SO_2 removal	54
2-11b	Overall SO_2 removal	54

FIGURES (Continued)

Number		Page
3-1	Nahcolite dry injection flow diagram	59
3-2a	Representation of a reacting particle when gas film diffusion is the rate controlling step	68
3-2b	Representation of a reacting particle when ash diffusion is the rate controlling step	70
3-2c	Representation of a reacting particle when chemical reaction is the rate controlling step	72
3-3	Progress of reaction of a single spherical particle with surrounding gas measured in terms of time for complete conversion	74
3-4a	Reaction rate as a function of the extent of sorbent conversion	77
3-4b	Extent of solid conversion with time for reaction of SO_2 with sodium bicarbonate	78
3-5a	SO_2 removal with dry injection of nahcolite into the duct of the pilot system	84
3-5b	SO_2 removal with dry injection of trona into the duct of the pilot system	85
3-5c	SO_2 removal with dry injection of refined trona into the duct of the pilot system	86
3-6	SO_2 removal as a function of $NaHCO_3$ stoichiometric ratio for different particle sizes	91
3-7	Effect of temperature on SO_2 removal efficiency	94
3-8	Effect of stoichiometric ratio on SO_2 removal efficiency with nahcolite	96
3-9	SO_2 removal efficiency versus residence time in the duct	99

ACKNOWLEDGEMENTS

The authors of this report would like to express their gratitude to all the organizations that have provided information used in the preparation of this report. Special thanks are extended to William Downs and Babcock and Wilcox for their cooperation and assistance. Thanks also go to Dr. T.G. Brna, the EPA Project Officer, for his thorough and constructive review.

SECTION 1

SUMMARY

This report identifies and evaluates the postulated physical changes, chemical reactions, and reaction mechanisms involved in dry flue gas desulfurization (FGD). Basically, this work is a review of the available published theories describing the reactions involved in lime spray drying and dry injection of sodium compounds. The topics that are covered in this report are:

1) The physical changes and chemical reactions that occur in the dry scrubbing systems.

2) Proposed reaction mechanisms and mathematical models.

3) Process parameters which affect the reactions and the rate controlling steps.

4) Additional data needed to verify or expand on the proposed mechanisms and the affects of the various process parameters.

The information used in developing this report was obtained from previously published articles and technical papers. Much of the information was obtained from papers presented at the October 1980 EPA Symposium on Flue Gas Desulfurization. A bibliography of valuable literature sources used in the preparation of this report is presented in Section 4.

The information on spray drying is more complete and consistent than the information on dry injection. Spray drying has been investigated more thoroughly and is presently being applied to commercial-scale units. Dry injection is still being investigated on the pilot scale, although recent tests have been conducted on a system designed to treat 20 MWe equivalent of flue gas.[1]

It should be noted that the term stoichiometry used in this report represents the moles of fresh sorbent introduced to the system divided by the moles of SO_2 entering the system. For lime the moles of sorbent is based on the equivalent moles of CaO introduced, and for sodium compounds the moles of sorbent is based on the equivalent moles of Na_2O entering the system. This method of describing dry scrubbing stoichiometry is commonly used by system vendors and the results they report are based

upon this definition. The conventional FGD definition for stoichiometry in wet systems is the moles of sorbent introduced to the system divided by the moles of SO_2 removed by the system. Compared with the conventional FGD definition of stoichiometry, the definition used by dry scrubbing vendors tends to make the system look more favorable because it does not account for SO_2 removal efficiency. However, it should be noted that the dry scrubbing definition of stoichiometry is the same definition that is conventionally used in chemistry (i.e. the moles of A needed to react completely with B without accounting for efficiency).

It should also be noted that English Engineering units are used in this report. Although it is EPA policy to use metric units in all Agency documents, it was felt that the English system would be more useful to users of this report. However, a list of Metric-English conversion factors is provided in Appendix C.

1.1 LIME SPRAY DRYING

Spray drying involves contacting SO_2 laden flue gas with an atomized sorbent slurry in a spray dryer. The SO_2 is absorbed by the slurry droplets, while the droplets are dried by the hot flue gas. An ESP or fabric filter is used to collect the dried solids exiting the spray dryer.

Information on dry flue gas desulfurization (FGD) with lime spray drying was evaluated in order to determine the reactions and reaction mechanisms involved in the removal of SO_2. The results of pilot-scale lime spray drying tests were examined in order to establish the reaction mechanisms and rate controlling steps. Proposed qualitative and quantitative models describing the spray drying process were also evaluated. Additionally, the important process parameters affecting the spray drying reactions were qualitatively evaluated to determine their influence on the rate controlling steps of the reaction and on the degree of SO_2 removal achievable. Finally, data gaps in published literature were identified. These data gaps tend to prevent complete verification and expansion of the proposed models.

1.1.1 Qualitative and Quantitative Reaction Models for Lime Spray Drying

Models developed for lime spray drying must take into account the simultaneous physical changes and chemical reactions that occur in the spray dryer. The overall chemical reaction takes place between the gaseous SO_2 and the dissoluted lime sorbent to form calcium sulfate and sulfite salts:

$$Ca(OH)_{2(s)} + SO_{2(g)} + H_2O_{(l)} \rightleftharpoons CaSO_3 \cdot \tfrac{1}{2}H_2O_{(s)} + 3/2\ H_2O_{(l)} \qquad (1\text{-}1)$$

$$CaSO_3 \cdot \tfrac{1}{2}H_2O_{(s)} + \tfrac{1}{2}O_{2(g)} + 3/2\ H_2O_{(l)} \rightleftharpoons CaSO_4 \cdot 2H_2O_{(s)} \qquad (1\text{-}2)$$

Simultaneously, the reaction surface is physically changed as the slurry droplet dries.

The reactions that occur are basically gas-liquid phase reactions, because moisture must be present for the reactions to occur. Thus, the moisture content and composition of the slurry droplet during and after drying are extremely important in determining the nature of the rate controlling steps. The slurry droplet is typically composed of many small particles of porous solid lime in an aqueous medium. As the slurry droplet dries, water evaporates from the surface of the droplet, leaving behind a solid agglomerate composed mainly of sulfite and sulfate product solids and unreacted lime. The dried solids also may contain significant amounts of residual moisture, depending on the length of drying time and the approach to saturation at the dryer outlet.

The most widely accepted qualitative model suggests that the chemical reactions that occur are intimately linked to three stages of droplet drying.[2] These drying stages have been characterized as follows:

1) Constant rate period. The greatest amount of water is evaporated from the droplet during this period, and drying is controlled by the rate of diffusion of water vapor from the saturated surface of the droplet.

2) First falling rate period. During this period, the lime particles in the slurry droplet begin to touch one another due to the loss of moisture, and drying is controlled by the rate of diffusion of water vapor from an unsaturated surface.

3) Second falling rate period. Drying during this period is controlled by the rate of diffusion of moisture through and around the tightly packed lime particles.

During the constant rate stage of drying, the rate of SO_2 removal appears to be controlled by the diffusion of the SO_2 in the flue gas to the surface of the slurry droplet. The reaction that occurs between the gaseous SO_2 and the water in the droplet is characterized by the following equation:

$$SO_{2(g)} \rightleftharpoons SO_{2(aq)} \qquad (1\text{-}3)$$

As evaporation proceeds during the two falling rate periods, less water is available for the dissolution of the solid $Ca(OH)_2$ into ions;[3] therefore the dissolution of the $Ca(OH)_2$ becomes the rate limiting factor.

If the spray-dried solids maintain adequate moisture, further reaction may continue in the downstream collection device. This is termed the pseudo-equilibrium period. Reactions during this period are limited by the rate of diffusion of SO_2 through the $CaSO_3 \cdot \frac{1}{2}H_2O$ that has formed on the surface of the lime particles and through the pore system of the lime particles.

This qualitative model provides the basis for development of theoretical and empirical quantitative (mathematical) models. Once these models have been evaluated and verified against test data, they can be used with confidence to predict SO_2 removal under given conditions.

A mathematical model was developed by Babcock and Wilcox (B&W)[4] to characterize the reactions that occur during the constant rate drying period. The qualitative model states that the rate of reaction is controlled by the diffusion of SO_2 to the slurry droplets during this period. From this assumption the following mathematical relationship was developed:

$$E = 1 - \left(\frac{t_p}{Tin-Tsat}\right)^{0.62} \qquad (1\text{-}4)$$

where: E = SO_2 removal efficiency, fraction

Tsat = Adiabatic saturation temperature of the flue gas, °F

Tin = Inlet temperature of the flue gas, °F

t_p = Approach to the adiabatic saturation temperature at the spray dryer outlet (Tout-Tsat), °F

Tout = Spray dryer outlet temperature of the flue gas, °F

Test data obtained by Buell at the Martin Drake Station seem to show that the model is valid for relatively large spray dryers (greater than 8,500 acfm), but it underpredicted SO_2 removal at B&W's Alliance Research Center 1500-acfm spray dryer. These conflicting results may be due to the different spray dryer designs used by Buell and B&W, or they may be due to "wall effects." These wall effects involve chemical reactions between the SO_2 and the lime that coats the walls of the spray dryer. This coating provides sites for additional SO_2 removal. There is more wall surface area per molecule of gas in a small spray dryer, so that more reaction sites are available per SO_2 molecule. Therefore, under the same test conditions greater SO_2 removal would be expected in a small dryer.

Another mathematical model developed by B&W correlates SO_2 removal efficiency with the stoichiometric ratio. The model states that

$$E = 1-e^{-K'SR} \qquad (1\text{-}5)$$

where: E = SO_2 removal efficiency, fraction

SR = Stoichiometric ratio = $\frac{\text{moles CaO in}}{\text{moles } SO_2 \text{ in}}$

K' = Correlation coefficient

The variable K' is a function of the specific surface of the lime (in ft^2 of surface per lb of lime) and the residence time of the flue gas in the spray dryer. Test data collected by B&W[4] and Buell[2], utilizing a close approach to saturation temperature and SO_2 concentrations less than 2000 ppm, fit the above relationship extremely well. Therefore, it seems that this general correlation can be used to predict SO_2 removal efficiency for these operating conditions.

1.1.2 Process Parameters Affecting the Lime Spray Drying Reactions

It has been postulated that the spray drying reaction rate is controlled initially by the diffusion of SO_2 into the droplet and then becomes controlled by the dissolution of $Ca(OH)_2$ into ions. The rate of dissolution of $Ca(OH)_2$ changes as the slurry droplet dries. Initially, Ca^{++} and OH^- ions saturate the slurry droplet and are easily dissoluted, but as the droplet dries dissolution becomes limited by the amount of moisture left in the droplet. Therefore, three major processes can be postulated:

1) Gas-phase SO_2 absorption into the slurry droplet.
2) $Ca(OH)_2$ dissolution in the slurry droplet.
3) $Ca(OH)_2$ dissolution in the spray-dried solid.

The parameters that affect these processes are presented below.

Both the approach to saturation temperature and the size of the initial slurry droplet affect mass transfer during these three processes and are therefore crucial process variables. The process variables can be categorized as follows:

1) Variables affecting SO_2 mass transfer into the slurry droplet
   - Approach to saturation temperature
   - Size of the slurry droplet-method of atomization
   - Mixing of the gas and droplets
   - Residence time of flue gas in the dryer
   - Inlet SO_2 concentration
   - Inlet flue gas temperature
2) Variables affecting Ca^{++} mass transfer in the slurry droplet
   - Stoichiometric ratio
   - Approach to saturation temperature
   - Size of the slurry droplet
   - Residence time of flue gas in the dryer

3) Variables affecting Ca^{++} mass transfer in the spray-dried solids

Approach to saturation temperature

Size of the initial slurry droplet

Slaking

Stoichiometric ratio

Off-product recycle

These variables and their effects are analyzed in Section 2.2. Reported test results that indicate the effect these variables have on SO_2 removal efficiency are also discussed.

1.1.3 Data Gaps in Literature

In order to test the proposed mathematical models and the effects of the variables listed above, detailed test data are required. Much of the published test data lacks detailed and complete information on inlet SO_2 concentration, stoichiometric ratio, or approach to saturation.

There is a particular lack of information on spray dryer performance when the SO_2 concentration exceeds 2500 to 3000 ppm SO_2. This information is necessary to test the applicability of lime spray drying for use in units firing coals containing more than 3 percent sulfur. Additional analysis might also be required to resolve conflicting theories on the effects of certain variables (i.e., inlet gas temperature, off-product recycle) on SO_2 removal efficiency.

1.2 DRY INJECTION OF SODIUM COMPOUNDS

Dry injection involves contacting SO_2 laden flue gas with a dry sorbent. The sorbent is pneumatically injected into the duct carrying the flue gas and/or precoated on fabric filter bags. The SO_2 is removed from the flue gas by adsorption by the sorbent.

Information on the dry injection of sodium compounds was evaluated in order to characterize the reactions and reaction mechanisms involved in the desulfurization process. The sodium sorbents that were investigated were nahcolite ore (predominantly $NaHCO_3$) and trona ore ($Na_2CO_3 \cdot NaHCO_3 \cdot 2H_2O$). The results of laboratory-scale and pilot-scale dry injection tests were evaluated in order to establish the reaction mechanism and rate controlling steps. There was a great deal of inconsistency in the experimental results, which made it difficult to draw conclusions about the dry injection process. However, qualitative and quantitative models describing the dry injection process have been proposed[5,6] and are presented in this report. In addition, important process parameters which influence the dry injection reactions were qualitatively evaluated. Finally, data gaps and conflicting results identified in published literature are discussed in order to identify areas that may require further investigation.

1.2.1 Qualitative and Quantitative Reaction Models for Sodium Compound Dry Injection

The dry injection reactions that occur when the SO_2 is contacted with the sorbent are strictly gas-solid phase reactions.[2] The overall chemical reactions that occur during dry injection are shown below for nahcolite and trona respectively.

$$2\ NaHCO_{3(s)} + SO_{2(g)} + 1/2\ O_{2(g)} \longrightarrow Na_2SO_{4(s)} + 2\ CO_{2(g)} + H_2O_{(g)} \quad (1\text{-}6)$$

$$2(Na_2CO_3 \cdot NaHCO_3 \cdot 2H_2O)_{(s)} + 3SO_{2(g)} + 3/2\ O_{2(g)} \longrightarrow 3Na_2SO_4 + 4CO_{2(g)} + 5H_2O_{(g)} \quad (1\text{-}7)$$

These reactions do not occur in single steps as they are written above, but instead involve a series of three steps: (1) thermal decomposition of $NaHCO_3$ to Na_2CO_3, (2) reaction between Na_2CO_3 and SO_2 to form Na_2SO_3, and (3) oxidation of Na_2SO_3 to Na_2SO_4. Several changes in physical characteristics of the sorbent accompany these reactions.

When the $NaHCO_3$ is thermally decomposed to Na_2CO_3, small pores (approximately 0.3 μm in diameter) develop in the sorbent particle as H_2O and CO_2 gas are evolved. These pores provide an increased surface area for chemical reaction, thus increasing the reactivity of the sorbent. The rate of decomposition of $NaHCO_3$ is extremely temperature dependent, and temperatures between 300° and 600°F are required for adequate pore development.

Test results have shown that trona is less reactive than nahcolite.[7] It is postulated that trona is less reactive because it already contains one mole of Na_2CO_3 for every mole of $NaHCO_3$ present. Therefore, trona does not contain as much $NaHCO_3$ as nahcolite, and the decomposition of the sorbent does not generate as much pore volume per particle of trona. It has been found that the sorbent with the greatest amount of sodium bicarbonate ($NaHCO_3$) parts for total sodium parts present will generally be the most effective for SO_2 removal.

The reaction of the SO_2 with the sodium sorbent proceeds from the exterior of the sorbent particle inward, leaving behind an inert layer of Na_2SO_4 on the surface of the sorbent particle. The molar volume of this reacted Na_2SO_4 layer is approximately 26 percent greater than the molar volume of the unreacted Na_2CO_3. This increase in the molar volume tends to plug the internal pores that were generated by the decomposition of the sorbent. Scanning electron micrograph's (SEM's) of halved sorbent particles recovered after reaction with SO_2 showed that there was a surface zone of Na_2SO_4, an intermediate reaction zone, and a central unreacted core of Na_2CO_3.

The SEM's of the reacted sorbent particles warrant the application of the classical unreacted-core model. This model proposes that three major steps are involved in the reaction of SO_2 with the sorbent:

1) Diffusion of gaseous SO_2 to the surface of the sorbent particle through the stagnant gas film surrounding the the particle.

2) Penetration and diffusion of gaseous SO_2 through the Na_2SO_4 ash layer to the unreacted core.[2]

3) Chemical reaction of gaseous SO_2 with the sorbent at the reaction surface.

Each of these steps has a different resistance to the rate of reaction, but the step with the highest resistance is considered to be rate controlling. Test results indicate that the diffusion of gaseous SO_2 through the stagnant gas film is not a rate controlling step.[6] It has been proposed[6] that initially the rate of reaction is controlled by chemical reaction, and as the ash layer builds up the rate of reaction becomes controlled by the diffusion of SO_2 through the ash layer.

The rate of chemical reaction may be controlled by either the rate of thermal decomposition of $NaHCO_3$ to Na_2CO_3 or the rate of uptake of SO_2 by the Na_2CO_3 to form Na_2SO_3.[3] However, most experimental results[5,6,7] seem to indicate that thermal decomposition is the rate controlling chemical reaction.

Mathematical relationships have been developed[8] for the case where each of the three reaction steps (gas film diffusion, ash layer diffusion, and chemical reaction) controls the rate of reaction. However, for the dry injection process the rate of SO_2 removal is controlled by either the rate of chemical reaction or diffusion through the ash layer. Expressions describing SO_2 removal efficiency as a function of reaction time for these two cases are presented below.

Ash Layer Diffusion Controls

$$\frac{t}{\tau} = 1 - 3(1-E/SR)^{2/3} + 2(1-E/SR) \qquad (1\text{-}8)$$

where:

$$\tau = \frac{\rho \, R^2}{6 \, D_v \, C_{SO_2\text{-}g}(MW)} \qquad (1\text{-}9)$$

(The above equation cannot be solved directly for E.)

Chemical Reaction Controls

$$E = \left[1-\left(1- \frac{t}{\tau}\right)^3 SR \right] \quad (1\text{-}10)$$

where:

$$\tau = \frac{\rho R}{k_s C_{SO_2\text{-}g}(MW)} \quad (1\text{-}11)$$

A definition of the variables included in these equations is presented below.

t	=	Time, sec
τ	=	Time needed for complete conversion of the sorbent, sec
E	=	SO_2 removal efficiency, $\frac{\text{mole } SO_2 \text{ removed}}{\text{mole } SO_2 \text{ in flue gas}}$
SR	=	Stoichiometric ratio, $\frac{\text{mole } Na_2O \text{ injected}}{\text{mole } SO_2 \text{ in flue gas}}$
R	=	Initial particle radius, ft
ρ	=	Density of the sorbent, lb/ft^3
$C_{SO_2\text{-}g}$	=	Concentration of SO_2 in the gas phase, $lb\text{-}mole/ft^3$
(MW)	=	Molecular weight of sorbent, lb/lb-mole
D_v	=	Mass diffusivity of SO_2 through the ash layer, ft^2/sec
k_s	=	First-order rate constant for chemical reaction, ft/sec

These mathematical models were not evaluated because test data published thus far have been incomplete, and many of the variables required for the determination of τ, (i.e., D_v, k_s, R, and ρ) were not provided and could not be easily estimated from the available literature.

1.2.2 Process Parameters Affecting the Dry Injection Process

There are many process parameters which affect SO_2 removal efficiency in the dry injection processes. These parameters were evaluated and were ranked in the approximate order of their relative importance.

In general, the parameters that may effect SO_2 removal in dry injection are those that affect the diffusion of SO_2 to the surface of the sorbent particle, diffusion of SO_2 through the inert ash layer on

the particle surface, or chemical reaction. Parameters that influence these three reaction steps are characterized below.

1) Variables affecting SO_2 mass transfer to the sorbent particles
   - Particle size
   - Residence time of the reactants in the duct
   - Inlet SO_2 concentration
   - Gas velocity and air-to-cloth ratio
   - Mode of sorbent injection
   - Gas temperature

2) Variables affecting SO_2 mass transfer through the inert ash layer
   - Sorbent preparation
   - Particle size
   - Residence time of the reactants in the duct
   - Filter cleaning intervals
   - Stoichiometric ratio

3) Variables affecting chemical reaction
   - Sorbent type
   - Sorbent preparation
   - Temperature
   - Stoichiometric ratio

These parameters and their effects are discussed in Section 3.2. Reported test results indicating the effect these parameters have on SO_2 removal efficiency are also presented.

1.2.3 Data Gaps in Literature

It is proposed that the unreacted core model can be applied to the reactions that occur during dry injection.[7] However, this model was not evaluated against experimental data, therefore it may not be valid. In order to evaluate the applicability of the unreacted core model, experimental data describing sorbent conversion versus time will be required. The mechanism by which the desulfurization reaction

$$Na_2CO_{3(s)} + SO_{2(g)} \longrightarrow Na_2SO_{3(s)} + CO_{2(g)} \qquad (1\text{-}12)$$

proceeds also needs to be established, and the influence of the flue gas moisture content on desulfurization should be examined.

It would be useful to characterize SO_2 removal at inlet SO_2 concentrations greater than 2000 ppm to determine if dry injection is applicable to systems that burn coal with a higher sulfur content. In addition, parametric testing should be performed to clear up conflicting experimental results concerning the effects of particle size, injection temperature, and thermal predecomposition of the sorbent on SO_2 removal. Finally, it may be beneficial to test dry injection on a flue gas produced from combustion under low excess air conditions. Minimizing the oxygen content of the flue gas could reduce the oxidation of Na_2SO_3 to Na_2SO_4. If in fact the oxidation of Na_2SO_3 causes the pores in the sorbent particle to plug, then a reduction in the amount of Na_2SO_4 generated should reduce plugging and allow for better SO_2 removal.

1.3 LITERATURE CITED

1. Kelly, M.E. and S.A. Shareef, Third Survey of Dry SO_2 Control Systems. EPA-600/7-81-097, (NTIS PB # 81 218976). July 1981.

2. Parsons, E.L., et al. "SO_2 Removal by Dry FGD." In: Proceedings of Sixth Symposium on Flue Gas Desulfurization. Houston, Texas. EPA-600/9-81-019b, Vol. 2, pp. 801-852. April 1981.

3. Getler, J.L. et al. "Modelling the Spray Absorption Process for SO_2 removal." In: Journal of the Air Pollution Control Association 29:12. December 1979. pp. 1270-1274.

4. Downs, W., W.J. Sanders, and C.E. Miller. "Control of SO_2 Emissions by Dry Scrubbing." (Presented at the American Power Conference. Chicago, Illinois. April 21-23, 1980.)

5. Dickerman, J.C., et al. "Evaluation of Dry Alkali FGD Systems." Radian report: DCN-78-200-226-03. March 31, 1978.

6. Davis, W.T. and T.C. Keener, "Phase I: Chemical Kinetic Studies on Dry Sorbents, Literature Review." University of Tennessee. August 10, 1980.

7. Samuel, E.A. and D.E. Lapp, "Testing and Assessment of a Baghouse for Dry SO_2 removal, Task 4: SO_2 Removal Using Dry Sodium Compounds." September 1980. Draft report prepared by Buell Emission Control Division, Envirotech Corporation, for U. S. EPA, Contract No. 68-02-3119.

8. Levenspiel, O. Chemical Reaction Engineering. 2nd edition. New York: John Wiley and Sons, Inc., 1972. pp. 357-377.

SECTION 2

LIME SPRAY DRYING

Presently, lime and soda ash spray drying are the only commercially developed dry FGD technologies. The majority of operating and planned spray drying systems utilize lime as the sorbent; therefore, this report will concentrate on lime spray drying systems. Spray drying is being applied to both utility and industrial units that fire low sulfur and medium sulfur coals (generally less than 2 percent sulfur).[1] A basic schematic of the spray drying process using a lime sorbent is presented in Figure 2-1.

Flue gas at a temperature of 275°F to 325°F, or higher for industrial systems, and containing 250 to 2500 ppm SO_2 (typically less than 1000 ppm SO_2) is contacted with a lime slurry in the spray dryer. The 15 to 25 weight percent solids slurry is atomized into fine droplets which are dispersed in the flue gas. Liquid-to-gas ratios of about 0.3 gal slurry/1000 acf gas are common. The finely atomized slurry droplets provide a large surface area for mass transfer. Water evaporates from the slurry and adiabatically humidifies the flue gas to within 20° to 50°F of its saturation temperature. An adequate margin above saturation must be maintained at the dryer outlet to prevent flow obstruction by agglomerated moist solids and damage to downstream particulate collection equipment, particularly if a fabric filter is used. The amount of water which can be evaporated into the flue gas, and thus the amount of sorbent that can be added at a given slurry concentration, is set by energy balance considerations.[1] The flue gas residence time in the dryer must be long enough to allow adequate drying of the solids. Typical residence times are approximately 10 seconds, the solids generally being dried to less than one percent free moisture, with a total residual moisture content between 2 and 5 percent. The spray dryer produces an off-product which is composed of reacted and unreacted sorbent, and fly ash. Some of this off-product is collected in the bottom of the spray dryer, while most of it is collected in the downstream particulate collection device.

SO_2 removal in the spray dryer ranges between 40 and 90 percent depending upon the inlet SO_2 concentration, residence time, approach to saturation temperature at the dryer outlet, and the stoichiometric ratio of sorbent to SO_2. Sixty-five to 70 percent SO_2 removal in the spray dryer is typical at a 20°F approach and a stoichiometric ratio of 1.2 when the inlet SO_2 is below 1500 ppm.[2] Without increasing the amount of fresh lime added per mole of inlet SO_2, removal can be increased by

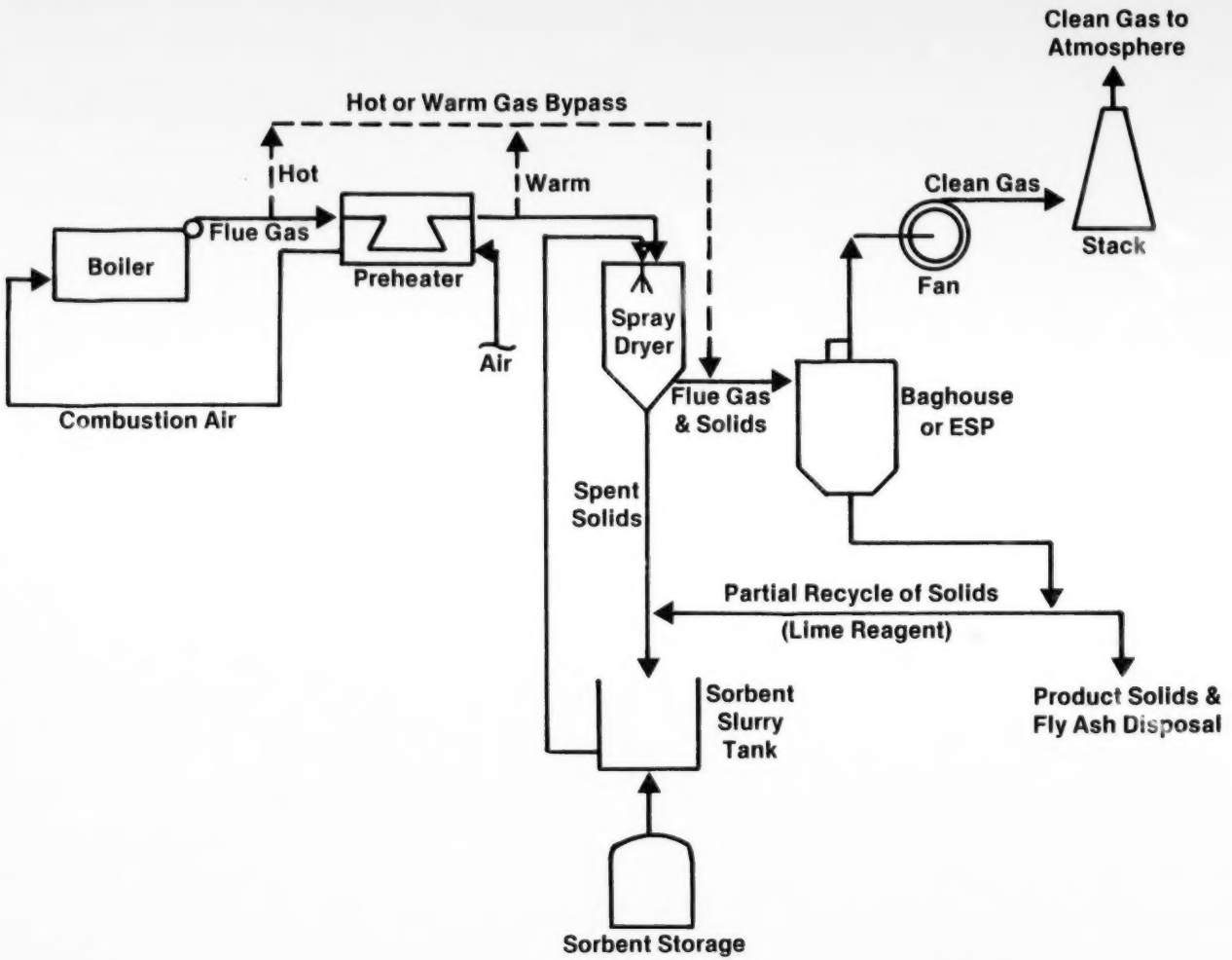

Figure 2-1. Typical spray dryer/particulate collection flow diagram.[1]

approximately 10 percent by recycling the spray-dried solids and fly ash.[2] Removal of SO_2 can also occur in the downstream collection device. Some tests have indicated that approximately 10 percent of the total SO_2 removal achieved by the spray dryer system can occur in the collection device.[3] The spray-dried solids can be removed by either an ESP or a fabric filter. The advantages and disadvantages of these two collection devices are discussed in Section 2.2.10.

SO_2 removal is enhanced by a very close approach to saturation temperature at the spray dryer outlet. A close approach increases the moisture content of the spray-dried solids, which increases SO_2 removal but also reduces the spray dryer outlet gas temperature.[2] The reduction in outlet temperature may cause maintenance problems in a downstream fabric filter collection device; therefore, the minimum recommended approach to saturation is 20°F[2] when lime sorbent is used.

These maintenance problems can be eliminated by heating the flue gas before it enters the fabric filter, thus allowing a closer approach to saturation at the dryer outlet. This reheat is usually supplied by warm or hot flue gas which bypasses the spray dryer (see Figure 2-1). The amount of flue gas available for reheat is, however, limited by the overall SO_2 removal equipment.

2.1 REACTIONS AND REACTION MODELS FOR LIME SPRAY DRYING

This section presents the current theories on the reactions that occur during lime spray drying with a fabric filter collection device. The physical changes that occur when the slurry droplet is dried and the chemical reactions between the gaseous SO_2 and the atomized lime slurry are discussed. Current theories on the mechanisms involved in the spray drying reactions, including both qualitative and quantitative reaction models, are also presented.

2.1.1 Physical Changes and Chemical Reactions

This section analyzes the physical changes and chemical reactions that occur when flue gas is desulfurized in a spray dryer with a lime slurry. The physical changes are those that involve the drying of the slurry droplet, and the chemical reactions are those that occur between the SO_2 and the $Ca(OH)_2$. The drying of the lime solids with the simultaneous diffusion of SO_2 to the evaporating droplet, such as is required in this dry scrubbing process, is a relatively complex process. In addition, SO_2 removal can occur in three places:

1) The spray dryer
2) The duct between the spray dryer and the fabric filter
3) Across the filter cake in the fabric filter

As the composition of the slurry droplet changes in the spray dryer, the types of reactions that occur also change. Three steps have been postulated to describe the reactions that take place as the droplet dries:

1) First, there is reaction between gas phase SO_2 and the liquid phase lime as it exits the atomizer.
2) Second, there is absorption of gas phase SO_2 into the finely atomized droplets being dried.
3) Third, there is reaction between gas phase SO_2 and the slightly moist spray-dried solids.

The overall reaction that occurs is basically a gas-liquid phase reaction. If the slurry droplets were completely dried, the reaction would be a gas-solid phase reaction. When the droplet is completely dried, no further SO_2 absorption takes place.[4] Experience has shown that this dry SO_2-lime reaction is ineffective at spray drying temperatures (the reaction rate falls off below 1000°F).[5] Therefore, some surface moisture must exist on the particle in order for SO_2 to be absorbed.[4]

The degree of SO_2 removal achievable under given conditions depends upon the physical changes in the slurry droplet and the chemical reactions that occur. These physical and chemical processes are discussed in the following sections.

2.1.1.1 Physical Changes. The physical changes that have the greatest effect on the overall reaction are those that occur during the drying of the slurry droplet. In spray drying, heat and mass transfer are accomplished simultaneously by direct contact of the hot flue gas and dispersed slurry droplets. The droplets are dried as water vapor diffuses from the surface due to the liquid being heated to a temperature at which its vapor pressure exceeds the partial pressure of the vapor in the surrounding gas. The rates of heat and mass transfer during evaporation are functions of temperature, humidity, and the transport properties of the flue gas surrounding each droplet. Droplet diameter and the relative velocity between the droplet and the flue gas are also important parameters. The slurry droplet undergoes several physical changes during the various stages of the drying process. These changes contribute significantly to the nature and degree of completion of the reaction in the spray dryer.

2.1.1.1.1 Stages of Drying. Initially, each slurry droplet contains a large number of insoluble discrete lime particles with interspacial distances equivalent to several particle diameters. These individual particles are in constant random motion within the droplet.[6] At first, the droplets lose moisture by evaporation from a saturated surface. The droplet surface decreases in area, and in the final stages water evaporates from the interior of the solid. The evaporation rate varies with time and moisture content, with different mechanisms controlling distinct periods in the drying process.

Three drying stages are encountered during the evaporation of the slurry droplet:[2]

1) Constant rate period
2) First falling rate period
3) Second falling rate period

These stages are presented graphically in Figure 2-2.

Following an initial warmup period, represented by segment AB in Figure 2-2, there is the constant rate period, represented by segment BC. During this constant rate period, drying proceeds by diffusion of water vapor from a saturated surface into the flue gas. The surface of the droplet maintains approximately constant temperature, the wet bulb temperature, while the gas is being cooled. The drying rate during this period is governed by heat and mass transfer, available surface area, and gradients of temperature and vapor pressure, which drive the heat and mass transfer processes. The drying rate during the constant rate period may be expressed as:

$$\frac{dm}{d\theta} = \frac{h_t \, A \, \Delta T}{\lambda} = k_g'' \, A \, \Delta p \qquad (2\text{-}1)$$

where:

$\frac{dm}{d\theta}$ = drying rate, lb/hr

h_t = average heat transfer coefficient, Btu/hr-ft^2-°F

A = area for heat and mass transfer, ft^2

ΔT = temperature potential, (Tout - Tsat), °F

λ = latent heat of vaporization, Btu/lb

k_g'' = mass transfer coefficient, lb/ft^2-hr-atm

Δp = pressure potential, (sat. press. — partial press.), atm

For a single drying droplet, the area for heat and mass transfer (A) is continuously shrinking as the droplet dries during the constant rate period. However, if the spray dryer is examined as a whole the total surface area of the droplets at any time should remain constant. Therefore, Equation 2-1 is useful in predicting the total rate of drying in the spray dryer, but it may not be applicable to the drying of a single droplet.

Most of the droplet moisture is removed during the constant rate period. As the droplet dries, several factors tend to reduce the rate of evaporation. As evaporation proceeds the droplet begins to shrink

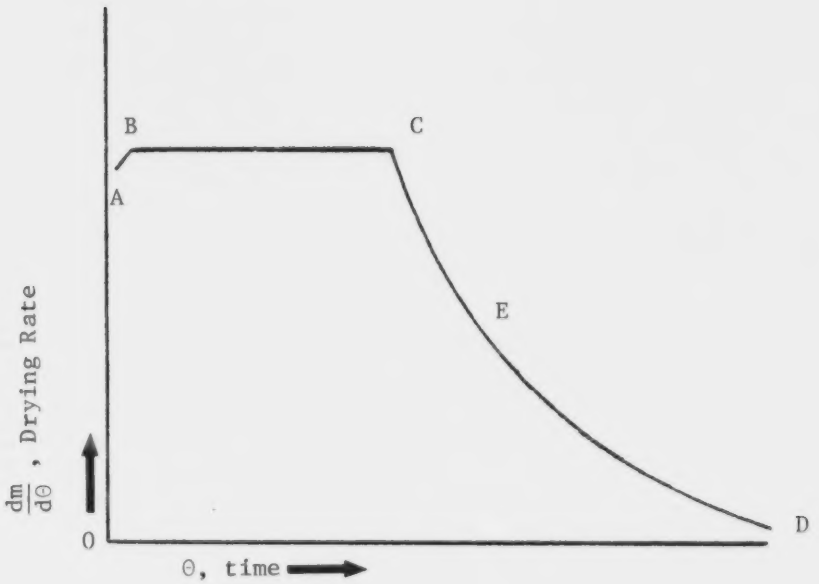

A-B Warmup
B-C Constant Rate Drying Period
C-E First Falling Rate Drying Period
E-D Second Falling Rate Drying Period

Figure 2-2. Stages of spray drying: drying rate versus time.[2]

and the distance between discrete lime particles is reduced until the particle surfaces touch, restricting particle motion.[6] Approximately 75 percent of the water has been evaporated by this time.[6] Also, the cooling of the flue gas reduces the temperature gradient, thus reducing the driving force for heat transfer and slowing the evaporation rate.

At a certain point a "critical" moisture content is reached, and saturated conditions cannot be maintained over the entire surface of the droplet (point C on Figure 2-2). This marks the beginning of the falling rate period. The falling rate period is subdivided into the first falling rate period, represented by Segment CE in Figure 2-2, where unsaturated surface drying prevails, and the second falling rate period, segment DE, where internal movement of moisture in the solid controls.

In the first falling rate period the surface temperature increases because saturated conditions can no longer be maintained. The drying rate, however, is still governed by factors affecting the diffusion of moisture away from the evaporating surface. As moisture is removed from the surface of the droplet, a dried layer forms which becomes a barrier to further moisture transfer. Internal moisture movement becomes increasingly important as the plane of evaporation retreats below the surface of the dried outer layer.

Since the lime particles touch one another, the paths for diffusion of water to the particle surface become restricted, making the remaining moisture more difficult to remove. Diffusion through and around the particles becomes the limiting factor for further moisture removal. This condition is represented by point E in Figure 2-2 and marks the beginning of the second falling rate period. The evaporation rate continues to drop as the diffusion path of moisture through the particle is lengthened. By the conclusion of the second falling rate period, the moisture content of the dried lime agglomerate will essentially be in equilibrium with the surrounding gas.[2]

2.1.1.1.2 Physical Properties of the Droplet During Drying. As the slurry droplet dries, its physical characteristics change. Initially, the lime-water slurry enters the spray dryer through an atomizer which produces droplets with a mean diameter between 50 to 100 μm.[4,6] These droplets shrink in size during the constant rate period. The slurry droplets are composed of many fine particles of $Ca(OH)_2$ between 0.5 and 4.0 μm in diameter.[6] During the falling rate period, these elementary lime particles touch one another, thus the size of the lime droplet/agglomerate remains relatively constant. Spray-dried solids collected in the bottom of the spray dryer have been found to have a particle diameter of approximately 30 to 35 μm, and solids collected in the fabric filter were found to have a diameter of approximately 10 μm.[11] The droplets exit the atomizer with an approximate velocity of 450 ft/sec and decelerate to below 30 ft/sec in less than 0.1 sec.[6] The initial pH of the droplets is very high, but the pH drops as the reaction proceeds.[2] Figure 2-3 shows the relative size of the droplet and the lime particles as the droplet dries.

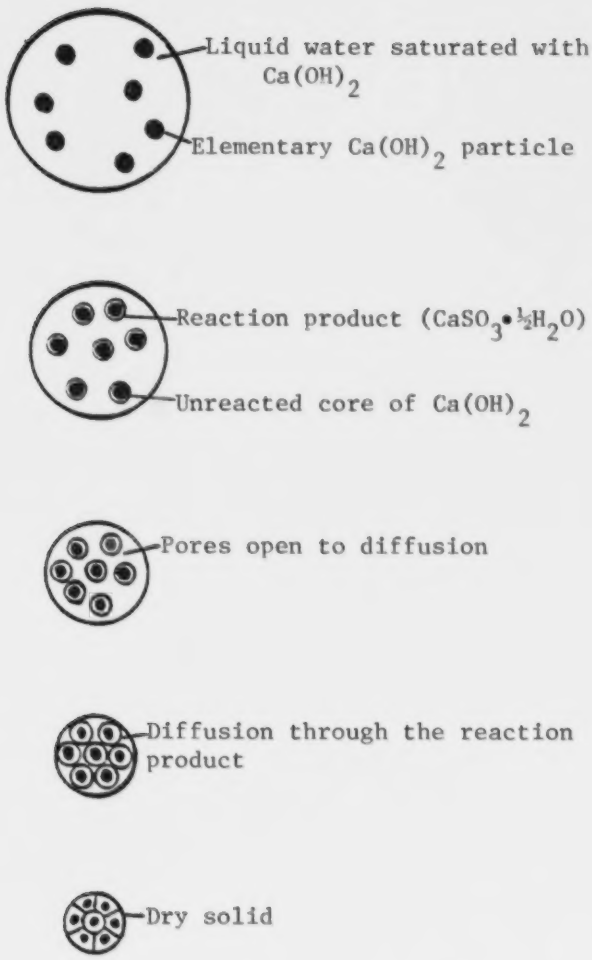
Liquid water saturated with $Ca(OH)_2$
Elementary $Ca(OH)_2$ particle
Reaction product ($CaSO_3 \cdot \frac{1}{2}H_2O$)
Unreacted core of $Ca(OH)_2$
Pores open to diffusion
Diffusion through the reaction product
Dry solid

Figure 2-3. Drying and reaction sequence of atomized droplets.[6]

2.1.1.2 Chemical Reactions. The chemical reaction of the lime slurry with gaseous SO_2 in the spray dryer is similar in most respects to the reactions that occur in a wet lime scrubber. However, the kinetics of the process are more involved due to the influence of the simultaneous drying process. The spray drying reactions are also complicated by the presence of CO_2 in the flue gas. The CO_2 can react with the lime to form calcium carbonate, $CaCO_3$, which reduces the amount of lime available for SO_2 removal. This section presents the chemical reactions that occur in the spray dryer. The limiting reactions and rate controlling steps will be identified in Section 2.1.2, Reaction Models.

The overall reactions that occur in the spray dryer are presented in Equations 2-2 and 2-3.[6]

$$Ca(OH)_2 + SO_2 + H_2O \rightleftharpoons CaSO_3 \cdot \tfrac{1}{2}H_2O + 3/2\ H_2O \qquad (2\text{-}2)$$

$$CaCO_3 + SO_2 + H_2O \rightleftharpoons CaSO_3 \cdot \tfrac{1}{2}H_2O + CO_2 + \tfrac{1}{2}H_2O \qquad (2\text{-}3)$$

These reactions do not occur in a single step but involve a series of reactions which can be expressed by the following equations proposed by Getler:[6]

1. Diffusion of SO_2 and CO_2 through the gas film boundary surrounding the liquid surface of the atomized droplet

$$SO_{2(g)} \rightleftharpoons SO_{2(aq)} \qquad (2\text{-}4)$$

$$CO_{2(g)} \rightleftharpoons CO_{2(aq)} \qquad (2\text{-}5)$$

2. Dissolution of SO_2 and CO_2

$$SO_2 + H_2O \rightleftharpoons H_2SO_3 \qquad (2\text{-}6)$$

$$CO_2 + H_2O \rightleftharpoons H_2CO_3 \qquad (2\text{-}7)$$

3. Dissociation in alkaline medium

$$H_2SO_3 \rightleftharpoons H^+ + HSO_3^- \rightleftharpoons 2H^+ + SO_3^= \qquad (2\text{-}8)$$

$$H_2CO_3 \rightleftharpoons H^+ + HCO_3^- \rightleftharpoons 2H^+ + CO_3^= \qquad (2\text{-}9)$$

$$SO_2 + H_2O + SO_3^= \rightleftharpoons 2HSO_3^- \qquad (2\text{-}10)$$

$$SO_2 + HCO_3^- \rightleftharpoons HSO_3^- + CO_2 \qquad (2\text{-}11)$$

$$2SO_2 + H_2O + CO_3^= \rightleftharpoons 2HSO_3^- + CO_2 \qquad (2\text{-}12)$$

4. Dissolution of Solids

$$CaCO_3 + H^+ + HCO_3^- \rightleftharpoons Ca^{++} + 2H^+ + 2CO_3^= \quad (2\text{-}13)$$

$$Ca(OH)_2 \rightleftharpoons Ca^{++} + 2OH^- \quad (2\text{-}14)$$

5. Formation of Salts

$$Ca^{++} + SO_3^= + \tfrac{1}{2}H_2O \rightleftharpoons CaSO_3 \cdot \tfrac{1}{2}H_2O\ (s) \quad (2\text{-}15)$$

$$Ca^{++} + CO_3^= \rightleftharpoons CaCO_{3(s)} \quad (2\text{-}16)$$

$$CaSO_3 \cdot \tfrac{1}{2}H_2O + \tfrac{1}{2}O_2 + 3/2\ H_2O \rightleftharpoons CaSO_4 \cdot 2H_2O\ (s) \quad (2\text{-}17)$$

All of the above reactions require an aqueous medium; therefore the moisture content of the slurry droplet and the spray-dried solids is an extremely important factor. The final products are relatively insoluble and consist of $CaSO_3 \cdot \tfrac{1}{2}H_2O$, $CaSO_4 \cdot 2H_2O$, and $CaCO_3$. These solid end products precipitate from solution onto the surfaces of the sorbent particles.[2]

From the above reaction equations it can be seen that both SO_2 and CO_2 react with the available lime. The importance of the competition between SO_2 and CO_2 for reaction sites has not been thoroughly investigated. The partial pressure of CO_2 in the flue gas is typically at least two orders of magnitude higher than that of SO_2, but the CO_2 has a lower solubility and forms a weaker acid in solution than SO_2.[2] Many investigators have treated the CO_2 as an inert gas, but several tests on the spray dryer off-product have shown that a substantial portion of the lime not reacted with SO_2 was converted to $CaCO_3$.[2] Two analyses of the chemical composition of the spray-dried product solids have shown significant concentrations of $CaCO_3$ in spray dryer and fabric filter solids. These results are presented in Tables 2-1a and 2-1b. Prototype tests have indicated that the sorbent "lost" to CO_2 may be recovered by means of partial off-product recycle.[2] As can be seen from Table 2-1a, Research-Cottrell found a 50 percent reduction in the $CaCO_3$ content of the product solids when they used an off-product recycle. Buell, on the other hand, found no significant change in the $CaCO_3$ content of the product solids when a recycle was employed (See Table 2-1b). However, Buell's results are not directly comparable because the tests with straight through lime and 50 percent recycle were conducted at different stoichiometric ratios (see Table 2-1b).

2.1.2 Reaction Models

Theories on the reaction mechanisms that govern flue gas desulfurization in a spray dryer utilizing a lime sorbent have been developed in several technical papers.[2,5,6] These qualitative descriptions attempt to characterize the reaction models and possible rate limiting steps involved in the spray drying reactions. The qualitative models provide a basis

TABLE 2-1a. CHEMICAL COMPOSITION OF THE SPRAY-DRIED FGD WASTE PRODUCT.[11] (Research-Cottrell)

Component	Weight Percent			
	Lime Only		Lime with Recycle	
	Spray Dryer	Fabric Filter	Spray Dryer	Fabric Filter
$CaSO_3 \cdot 1/2\ H_2O$	23.9	23.0	18.6	21.0
$CaSO_4$	4.8	4.9	6.7	10.5
$Ca(OH)_2$	< 0.1	1.3	0.5	< 0.1
$CaCO_3$	17.5	13.2	8.7	6.7
Flyash	53.7	57.6	65.5	61.7
	100.0	100.0	100.0	100.0

TABLE 2-1b. CHEMICAL COMPOSITION OF THE SPRAY-DRIED FGD WASTE PRODUCT.[12] (Buell)

Component	Weight Percent			
	Lime Only Low Stoichiometry		Lime with 50% recycle High Stoichiometry	
	Spray Dryer	Fabric Filter	Spray Dryer	Fabric Filter
Solids	99.9	99.7	96.8	98.5
$CaSO_3 \cdot 1/2\ H_2O$	3.9	2.3	19.2	20.8
$CaSO_4 \cdot 2H_2O$	1.2	2.2	9.3	2.3
$CaCO_3$	10.7	10.7	9.9	11.9
$Ca(OH)_2$	5.4	4.4	13.0	9.6
Mg	0.9	1.0	0.2	3.0
Acid Insoluble	80.4	77.5	59.6	62.1

for developing quantitative (mathematical) models to predict SO_2 removal under given reaction conditions. The available information on both qualitative and quantitative models is summarized in the following sections. In addition, the various mathematical models are applied to available data in an effort to briefly evaluate the validity of the model. In many cases, however, the available data are not sufficient to thoroughly evaluate the proposed models.

2.1.2.1 Qualitative Models. The reactions that occur in the spray dryer are intimately linked to the droplet drying stages which were discussed earlier in Section 2.1.1.1.1. Reaction models have been developed for three stages in the drying of the droplet:

1) Constant rate period
2) Falling rate period
3) Pseudo-equilibrium period

The constant rate and falling rate periods have been defined in Section 2.1.1.1.1. The pseudo-equilibrium period does not occur within the spray dryer, but represents the properties of the spray-dried solids. If the droplets are not completely evaporated but instead establish a pseudo-equilibrium within the cool and humid environment of the dry scrubber, then aqueous phase reactions between lime and SO_2 could theoretically continue in the ductwork from the spray dryer and in the downstream collection device.

The first stage of the reaction occurs in the absorber vessel during the warmup and constant rate drying periods (see Figure 2-2, segment AC). During this period the drying rate is controlled by heat transfer to the droplets, as water vapor simultaneously diffuses from the saturated droplet surface. Since the liquid is saturated with Ca^{++} ions in equilibrium with the solid $Ca(OH)_2$ particles, the pH is high and the reaction rate is controlled by the diffusion of gaseous SO_2 and CO_2 to the droplet

$$SO_{2(g)} \rightleftharpoons SO_{2(aq)} \qquad (2\text{-}4)$$

$$CO_{2(g)} \rightleftharpoons CO_{2(aq)} \qquad (2\text{-}5)$$

Once the SO_2 is absorbed by the droplet, it is rapidly dissoluted into H_2SO_3 (Equation 2-6) and then dissociates into H^+ and $SO_3^=$ ions (Equation 2-8). The calcium ions (Ca^{++}), which saturate the water in the droplet, react with the sulfite ions ($SO_3^=$) (See Equation 2-15). The solid reaction product then precipitates out of the solution onto the surface of the elementary lime particles. The diffusion of SO_2 and CO_2 into the droplet tends to be impeded by the counter-diffusion of water vapor. SO_2 removal can be increased by effective mixing of the droplets and the

gas stream, high humidity to lengthen evaporation time, and fine atomization of the slurry which promotes mass transfer (but not so fine that the droplets dry too rapidly).[2]

During the reaction between the dissoluted $Ca(OH)_2$ and the dissociated H_2SO_3, a solid, discrete reaction product $CaSO_3 \cdot \frac{1}{2} H_2O$[2] forms on the surface of each elementary particle. This surface reaction is represented in Figure 2-3. As more reaction product forms on the surface of the elementary lime particles, the reaction rate begins to be limited by resistance to diffusion through the sulfite reaction product layer on the particle surface.[6]

During the falling rate periods (Figure 2-2, segments CE and ED) the sorbent particles touch one another due to evaporation of moisture from the droplet. The pH has dropped because of the dissolution of SO_2 and CO_2 into acids and the precipitation of calcium salts. The rate of dissolution of fresh $Ca(OH)_2$[2] (Equation 2-14) now begins to be the rate-limiting factor.

$$CaCO_3 + H^+ + HCO_3^- \rightleftharpoons Ca^{++} + 2H^+ + 2CO_3^= \qquad (2\text{-}13)$$

$$Ca(OH)_2 \rightleftharpoons Ca^{++} + 2OH^- \qquad (2\text{-}14)$$

As the reaction proceeds, the interstices between adjacent sorbent particles become clogged with crystalline precipitates of the reaction products. The solid reaction product has a higher molar volume than the solid reactant which causes the sulfite-coated particle formed to expand. The reaction continues as mass transport takes place through void volumes and interstices between elementary unreacted particles. The particles continue to expand during the reaction, causing diffusion resistance through the sulfite product layer formed around the elementary particles to increase. Consequently, diffusion of moisture through the pores becomes progressively more restricted. Eventually each elementary particle in the dried agglomerate has a completely reacted surface and an unreacted core.[6]

When evaporation has virtually ceased, the "dry" sorbent particles leave the spray dryer with an "equilibrium" moisture content. This stage is termed pseudo-equilibrium. The equilibrium moisture may allow for further SO_2 removal downstream of the spray dryer in the collection device. This equilibrium moisture is critical for any reaction to occur. If the sorbent particles have adequate moisture to allow for dissolution of the solid $Ca(OH)_2$, then it appears that pore diffusion is the major rate limiting step. SO_2 removal in the fabric filter has been found to be a strong function of the approach to saturation temperature (t_p) at the spray dryer outlet. Low values of t_p (i.e., a close approach to saturation) will result in high equilibrium moisture content in the spray dryer off-product and tends to promote further reaction.[2]

The surface reaction between the elementary lime particles and the SO_2 as represented in Figure 2-3 has been supported[6] by scanning electron micrographs (SEM's) of the spray dryer off-product. An elemental analysis of the spray-dried particles clearly shows calcium distributed evenly across the diameter while the sulfur distribution reflects a highly reacted surface and virtually unreacted core (see Figure 2-4, Frames C, D, E and F). Figure 2-4, Frames A and B, also show the relative size of unreacted spray-dried lime and lime spray-dried in the presence of a 1,000 ppm SO_2 flue gas. From these figures it can be seen that the particles expand when reacted with SO_2.[6]

According to Downs et al.,[5] SO_2 removal during the three drying periods (constant rate, falling rate, and pseudo-equilibrium) may be enhanced by maximizing the parameters listed below for these drying periods.

Constant Rate Period and Falling Rate Period:

1) Large mass transfer surface area via
   - Fine atomization
   - High lime flow rate
2) Long evaporation (reaction) period via
   - High percent solids
   - Coarse atomization
   - Close approach to saturation

Pseudo-equilibrium period

1) Large total surface via
   - Fine atomization
   - Good slaking
   - High lime flow
2) High humidity via
   - Close approach to saturation

Increasing flue gas residence time in the spray dryer is most beneficial to SO_2 removal during the constant rate and falling rate periods. SO_2 removal during the pseudo-equilibrium period benefits most by a close approach to saturation temperature which appears to increase the residual moisture content of the product solids, thus increasing the potential for additional SO_2 removal in the downstream duct and the fabric filter.

2.1.2.2 Quantitative Models. Once the qualitative nature of the spray drying reactions are understood, mathematical models can be developed

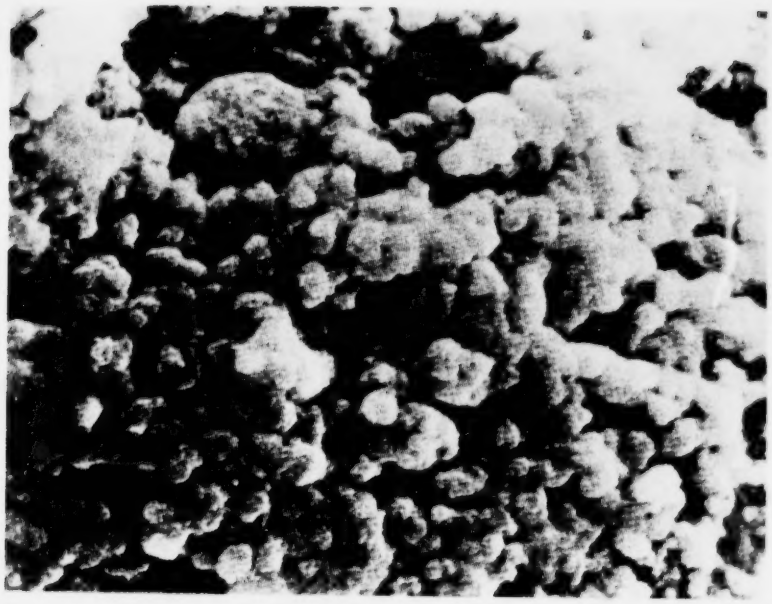

A) SEM micrograph of spray-dried lime (12,000 x magnification).

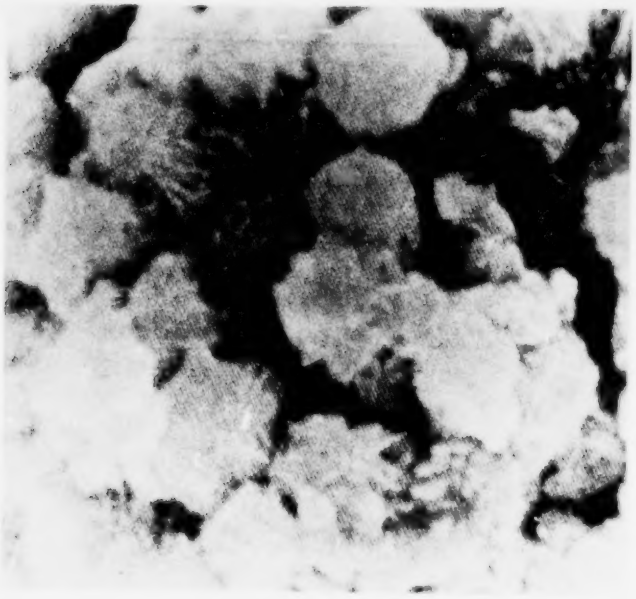

B) SEM micrograph of lime particle spray-dried with simulated 1,000 ppm flue gas (12,000 magnification).

Figure 2-4. Scanning electron micrographs (SEM's) and elemental analysis of spray-dried solids.[6]

C) Ca elemental analysis of particles.

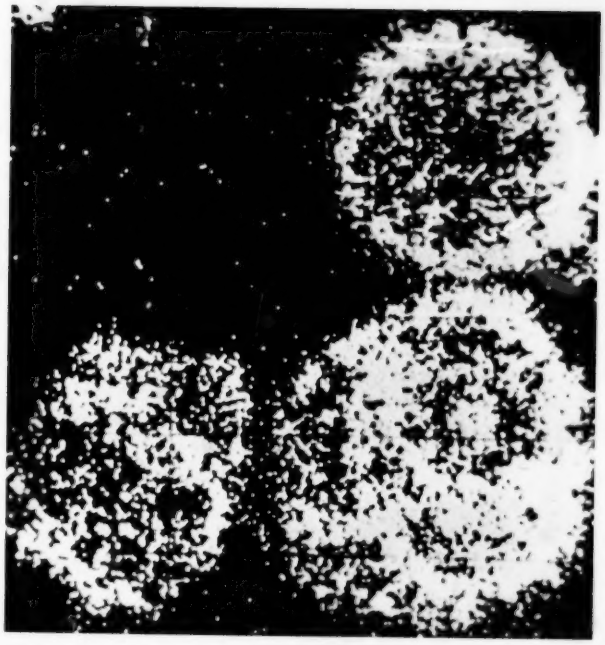

D) S elemental analysis of particles.

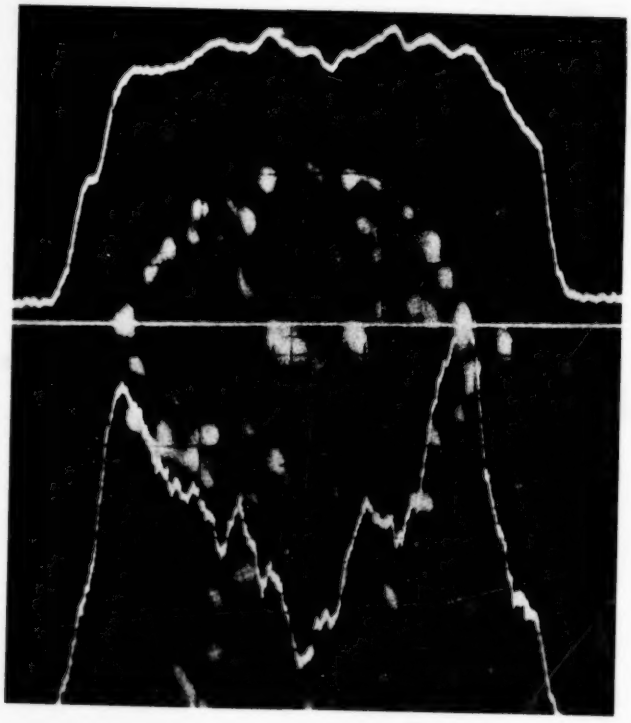

E) Ca distribution across diameter of one particle.

F) S distribution across diameter of one particle.

Figure 2-4. (Continued) Scanning electron micrographs (SEM's) and elemental analysis of spray-dried solids.[6]

to quantify the extent of SO_2 removal under given process and design conditions. The derivation of mathematical models is complicated by the fact that the reaction zone changes physically as well as chemically. Any mathematical model must take into account the changes in temperature and mass transport phenomena that occur in the spray dryer.

The majority of published work to date containing mathematical expressions that describe SO_2 removal during the spray drying process has been provided by Babcock and Wilcox (B&W).[2] B&W has developed a simple diffusion model, a general empirical correlation, and is presently developing models to describe the SO_2 absorption process during all three reaction periods (constant rate, falling rate, and pseudo-equilibrium).[5] The diffusion and correlation models will be presented in the following sections, along with data that support or conflict with these models.

These models are only applicable to the range of inlet SO_2 concentrations that have been studied (less than 2000 ppm SO_2). The applicability of these models to higher inlet SO_2 concentrations has not been demonstrated.

2.1.2.2.1 Diffusion Model. A common theory presented in recent spray drying literature is that most of the SO_2 is absorbed during the first drying stage, the constant rate period.[2] A simple mathematical model was devised by B&W on this premise. The model stated that SO_2 was absorbed by a continuously shrinking droplet of water which had an infinite capacity for SO_2. The assumption of infinite capacity for SO_2 absorption requires that the stoichiometric ratio of lime to SO_2 be relatively large (at least 1.0). By assuming that the droplet has an infinite capacity for SO_2, dissolution of $Ca(OH)_2$ is eliminated as the rate controlling step. Therefore, SO_2 absorption is controlled only by gas phase diffusion.[5]

Downs et al.[5] developed a mathematical model based upon these assumptions. The development of this mathematical model required solving mass and energy balances simultaneously. Other assumptions used in the derivation of the mathematical model were that the relative velocity between the liquid droplets and the flue gas is zero, that the flow through the spray dryer is plug flow, and that the gas flowrate is constant. From this Downs et al., developed the following expression:

$$N_T = -\frac{Dv}{\alpha}\,\frac{N_{SH}}{N_{NU}}\,\ln\left(\frac{Tin - Tsat}{Tout - Tsat}\right) \qquad (2\text{-}18)$$

N_T = Number of transfer units for SO_2 absorption

Tin = Inlet gas temperature to spray dryer, °F

Tsat = Adiabatic saturation temperature of gas, °F

Tout = Outlet gas temperature from spray dryer, °F

Dv = Mass diffusivity for SO_2 diffusion to droplet, ft^2/sec

α = Thermal diffusivity of SO_2 to droplet, ft^2/sec

N_{SH} = Sherwood number for SO_2 absorption

N_{NU} = Nusselt number for convective heat transfer

The derivation of Equation 2-18 is presented in Appendix A.

It would be helpful to relate the number of transfer units (N_T) to some measurable quantity, such as the SO_2 absorption efficiency. It is stated in Equation A-13 of Appendix A that

$$N_T = \int_{y_i}^{y_f} \frac{dy}{\Delta y}, \text{ where } \Delta y = y - y^* \qquad (2\text{-}19)$$

y = mole fraction of SO_2 in the flue gas, lb mole SO_2/lb mole flue gas

subscripts:

i = initial condition

f = final condition

The variable y* is the mole fraction of SO_2 at the liquid/gas interface. During the constant rate drying period, it is assumed that the SO_2 reacts immediately upon absorption into the slurry droplet; therefore, y* = 0 at the interface. Thus,

$$N_T = \int_{y_i}^{y_f} \frac{dy}{y} = \ln y_f - \ln y_i = \ln\left(\frac{y_f}{y_i}\right) \qquad (2\text{-}20)$$

This can easily be manipulated into a function of absorption efficiency.

$$\ln\left[\frac{y_f}{y_i} + \left(1 - \frac{y_i}{y_i}\right)\right] = \ln\left[1 - \left(\frac{y_i}{y_i} - \frac{y_f}{y_i}\right)\right] = \ln(1-E) \qquad (2\text{-}21)$$

Therefore, the Downs et al. equation becomes

$$-\ln(1-E) = \frac{Dv}{\alpha}\left(\frac{N_{SH}}{N_{NU}}\right) \ln\left(\frac{Tin - Tsat}{Tout - Tsat}\right) \qquad (2\text{-}22)$$

From tabulated data, it was determined that for real flue gases the ratio Dv/α is approximately 0.62 and is moderately independent of temperature in the operating range of dry scrubbers.[5] Also for this system the flue gas is assumed to flow past single spheres (slurry droplets). For either laminar or turbulent flow past spheres, the Sherwood and Nusselt numbers can be determined from the following relationships:

$$N_{SH} = 2.0 + 0.6 (N_{RE})^{1/2} (N_{SC})^{1/3} \quad (2\text{-}23)$$

$$N_{NU} = 2.0 + 0.6 (N_{RE})^{1/2} (N_{PR})^{1/3} \quad (2\text{-}24)$$

where:

N_{RE} = Reynolds number ($\rho ud/\mu$)

N_{SC} = Schmidt number ($\mu/\rho Dv$)

N_{PR} = Prandtl number ($C_p \mu/k_h$)

and:

ρ = Density of the flue gas, lb/ft^3

u = Relative velocity between flue gas and droplet, ft/hr

μ = Viscosity of the flue gas, lb/ft-hr

d = Diameter of the slurry droplet, ft

C_p = Specific heat at constant pressure of the flue gas, Btu/lb-°F

k_h = Thermal conductivity of the flue gas, Btu/hr-ft-°F

These Sherwood and Nusselt numbers are also dimensionless groups which describe the mass transfer and heat transfer characteristics of the system. One of the assumptions of this model was that the relative velocity between the flue gas and the liquid droplets was zero; therefore, N_{RE} becomes zero and the ratio N_{SH}/N_{NU} approximates unity. This leaves the outlet gas temperature as the only independent variable.[5] Thus, the mathematical expression reduces to

$$-\ln (1-E) = 0.62 \ln\left(\frac{Tin - Tsat}{Tout - Tsat}\right) \quad (2\text{-}25)$$

Therefore, if this model predicts actual operation, a plot of

$$-\ln (1-E) \text{ versus } \ln \left(\frac{Tin - Tsat}{Tout - Tsat}\right)$$

should give a line with a slope of 0.62.

By solving Equation 2-25 for E, a relationship can be derived which predicts SO_2 removal efficiency directly:

$$E = 1 - \left(\frac{Tout - Tsat}{Tin - Tsat}\right)^{0.62} \quad (2\text{-}26)$$

However, Tout - Tsat is the approach to the adiabatic saturation temperature at the spray dryer outlet (t_p). Therefore, Equation 2-26 can be written as:

$$E = 1 - \left(\frac{t_p}{Tin - Tsat}\right)^{0.62} \qquad (2\text{-}27)$$

It should be kept in mind that this model was developed from the assumption that most of the SO_2 is removed during the constant rate drying period.

B&W performed a series of tests at their Alliance Research Center (ARC) with their 1500 acfm pilot spray absorber. The diffusion model predictions were compared with data obtained from this pilot plant and are presented in Figure 2-5a. All of the data points fell above the model predictions. Thus, rather than overstating the performance, the model actually underpredicted SO_2 removal to a relatively significant extent. From this, B&W concluded[2] that the constant rate period[5] is not the only stage during which SO_2 absorption occurs.

B&W also plotted data that were obtained from demonstration tests with lime at Pacific Power and Light's Jim Bridger Station. This pilot system is a 120,000 acfm spray absorber. The Jim Bridger data tended to cluster around the line which represents Equation 2-25; however, a linear regression performed on the data[7] yielded a poorly correlated line (correlation coefficient was 0.28).

Buell[2] also collected data in order to test the simple diffusion model developed by B&W. Buell obtained data from their 20,000 acfm spray absorber, which was operated at 8500 acfm during EPA-sponsored tests at Colorado Springs' Martin Drake Station. The results are plotted in Figure 2-5b. The data showed reasonably good agreement with the model.[2]

It is difficult to compare the results obtained from these pilot plants because the conditions under which the tests were run, i.e. stoichiometric ratio, approach to saturation, inlet SO_2 concentration, etc., were not given for all cases. Since Buell and B&W employ different spray dryer designs (Buell uses a top entry spray dryer and B&W uses a horizontal entry spray dryer) and atomization methods (Buell uses a rotary atomizer and B&W uses a two-fluid nozzle), the droplet size and flue gas - slurry contact may differ significantly between the two systems. The size of the droplet affects the drying time and the amount of SO_2 absorbed by the droplets. This may contribute to the difference in the results obtained by Buell at the Martin Drake Station and B&W at their ARC pilot plant. Also, the difference between the results at the ARC pilot plant and the results at the Jim Bridger Station and the Martin Drake Station may be related to the size of the spray dryer. The ARC pilot plant spray dryer is relatively small (1500 acfm) in comparison to the Martin Drake (8500 acfm) and the Jim Bridger (120,000 acfm) spray dryers. The small ARC spray dryer achieved much greater SO_2 removal than was predicted by the model or was achieved in the other two spray

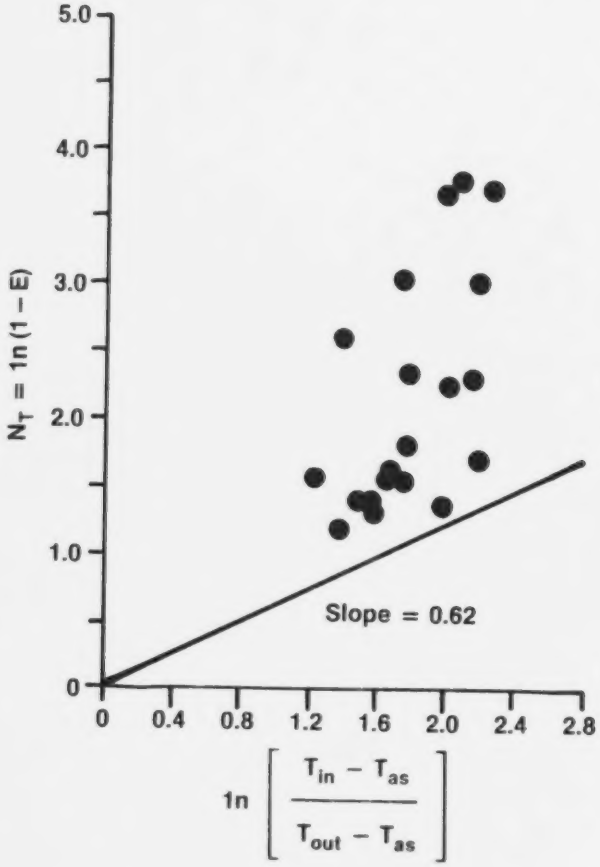

Figure 2-5a. Babcock and Wilcox'x test of the constant rate period absorption model. Data from ARC pilot scrubber with stoichiometric ratio greater than 1.0.[5]

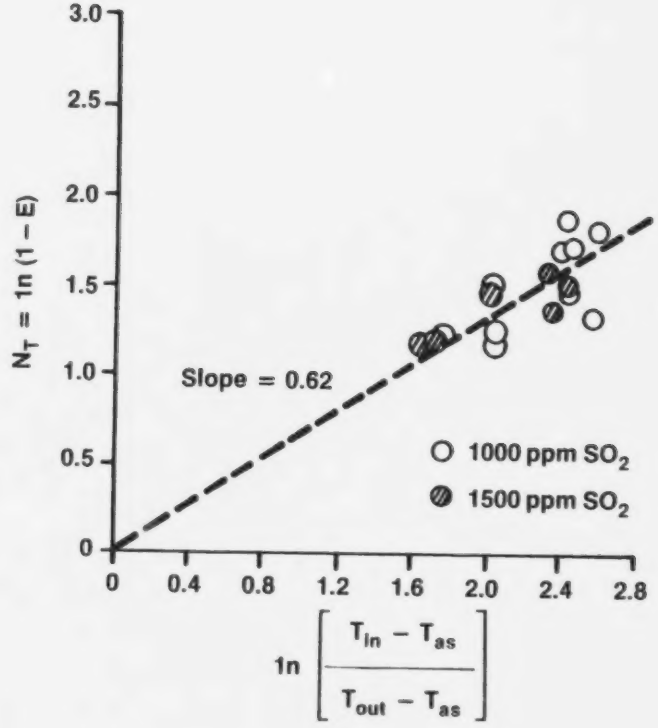

Figure 2-5b. Buell's test of the constant rate period absorption model. Data from the Martin Drake Station with stoichiometric ratio greater than 1.2 and residence time = 10 sec[2].

dryers. A possible explanation for these differences is that in a small spray dryer "wall effects" tend to be more important than in a large spray dryer, and permit greater SO_2 removal.[8] These wall effects involve reactions that occur between the SO_2 and lime reagent which coats the walls of the spray dryer. Since there is more wall surface area per molecule of SO_2 present in a small spray dryer than in a large spray dryer, greater SO_2 removal would be expected in the small dryer.

2.1.2.2.2 Stoichiometric Ratio Correlation (Transfer Area Model). Babcock and Wilcox also developed a general empirical correlation that relates stoichiometric ratio to SO_2 removal efficiency in the spray dryer. The basic premise for this model[5] is that the SO_2 absorption rate is proportional to the lime surface area. The model states that the gas flow rate times the change in SO_2 concentration in the gas with respect to time is proportional to the lime spray rate times the specific surface area of the lime. This relationship is expressed in Equation 2-28:

$$G\, dy/d\theta \propto L\, X'_o\, S_p \qquad (2\text{-}28)$$

This equation can be manipulated to yield an equation which relates SO_2 removal efficiency to the stoichiometric ratio. The variables that will be used in the following derivation are:

y = SO_2 concentration, moles SO_2/mole dry gas

L = Slurry spray rate, lb slurry/sec

X'_o = Lime concentration, moles/lb of slurry

S_p = Specific surface of lime, ft^2/lb of lime

G = Dry gas flow rate, moles/sec

SR = LX'_o/Gy = moles lime/mole SO_2 = Stoichiometric ratio

θ = Gas residence time, sec

E = SO_2 removal efficiency

$-K'$ = $K\, S_p\, \theta$

K = Proportionality constant

First, a proportionality constant K is introduced, which allows both sides of Equation 2-28 to be equated. Thus, Equation 2-28 becomes:

$$G\, dy/d\theta = KLX'_o\, S_p \qquad (2\text{-}29)$$

Separating variables, Equation 2-29 becomes

$$dy = \frac{KLX'_o}{G}\, S_p\, d\theta \qquad (2\text{-}30)$$

Noting that LX'_o/Gy has the units of stoichiometric ratio (SR), the above equation can be modified to

$$\frac{dy}{y} = K \frac{LX'_o}{Gy} S_p \, d\theta = K \, SR \, S_p \, d\theta \qquad (2\text{-}31)$$

Both sides of Equation 2-31 are then integrated between initial and final conditions of SO_2 concentration.

$$\int_{y_i}^{y_f} \frac{dy}{y} = K \, SR \, S_p \int_{\theta=0}^{\theta_f = \theta} d\theta \qquad (2\text{-}32)$$

This integration yields:

$$\ln y_f - \ln y_i = K \, SR \, S_p \theta \qquad (2\text{-}33)$$

The left hand side of Equation 2-33 can be mathematically manipulated to express SO_2 removal efficiency (see Equation 2-20 and 2-21). By assigning another constant $-K' = KS_p\theta$, Equation 2-33 becomes:

$$\ln (1-E) = -K' \, SR \qquad (2\text{-}34)$$

A plot of -ln (1-E) versus SR should be linear as long as all other variables are held constant (i.e. inlet temperature, approach to saturation, atomization quality, moisture content of the solids, etc).[5]

Equation 2-34 can be further manipulated to describe SO_2 removal efficiency directly:

$$E = 1 - e^{-K'SR} \qquad (2\text{-}35)$$

This equation cannot be used to predict SO_2 removal efficiency from the stoichiometric ratio (SR) until the value of K' has been determined for the particular spray drying system. K' can be determined from the slope of a plot of -ln(1-E) versus SR for a set of constant operating conditions.

This model was tested by B&W with data collected at the ARC pilot unit. The results of the test are plotted in Figure 2-6a. The results suggest that if adequate moisture remains in the solids (i.e., if a close approach temperature is used) the stoichiometric ratio correlation may be valid.[5]

Buell also compared the removal predicted by the model with data gathered at the Martin Drake Station. The -ln (1-E) was plotted against the stoichiometric ratio in Figure 2-6b, and a linear regression was performed on the points. This gave a well-correlated line with a slope of 1.3, which is equivalent to K'. Figure 2-6b indicates that the model

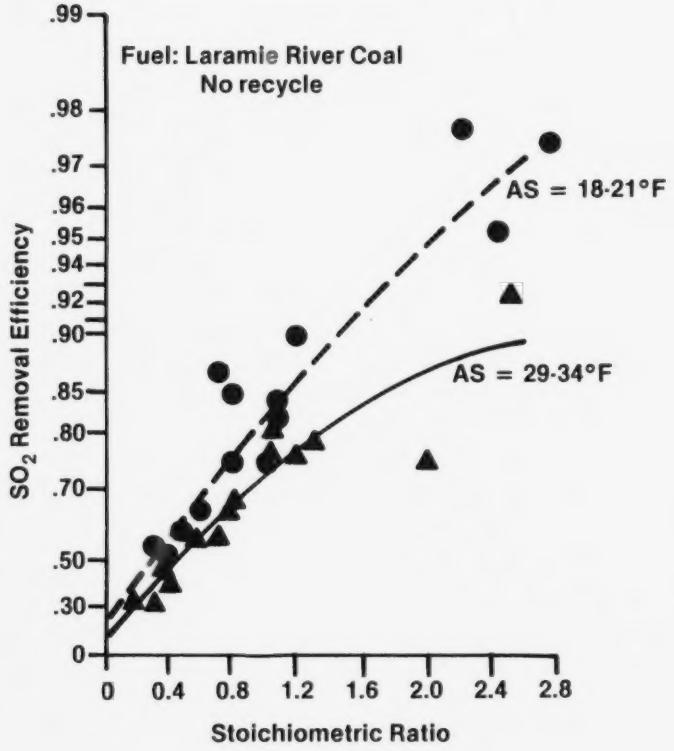

Figure 2-6a. Babcock and Wilcox's test of stoichiometry correlation model. Test data from ARC pilot plant. [AS = Approach to saturation temperature][5]

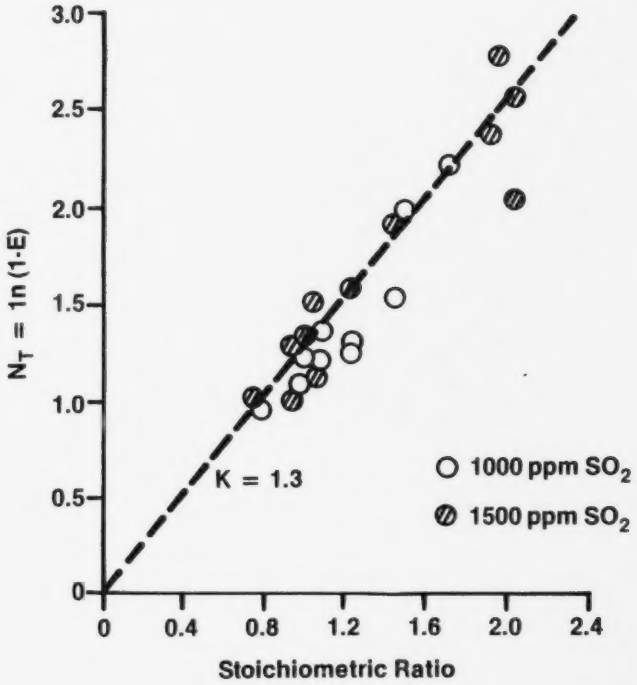

Figure 2-6b. Buell's test of stoichiometry correlation model. Test data from the Martin Drake Station. [With approach to saturation (AS) of 18° to 24° F and a residence time of 10 sec.][2]

agrees with the data. Therefore, this general correlation seems to predict SO_2 removal efficiency fairly well within the operating conditions used.

2.2 PROCESS PARAMETERS AFFECTING THE SPRAY DRYING PROCESS

From the discussion presented in Section 2.1, it is evident that many important parameters affect SO_2 removal efficiencies in the dry scrubbing processes. In general, the variables that have the strongest effect on the reactions between SO_2 and lime in the spray dryer are those that affect the rates of heat and mass transfer. The approach to saturation temperature of the dryer outlet gas affects mass transfer in all phases of the spray drying process, because it affects the moisture content of the drying droplets and the dried solids and the humidity of the flue gas.

In Section 2.1, it was postulated that the spray drying reaction rate is controlled first by the diffusion of SO_2 to the surface of the droplet and second, by the dissolution of $Ca(OH)_2$ into ions. The rate of dissolution of $Ca(OH)_2$ changes as the slurry droplet dries. Initially, $Ca(OH)_2$ ions saturate the slurry droplet and are easily dissoluted, but as the droplet dries dissolution becomes limited by the amount of moisture left in the droplet. Therefore, three major processes can be characterized:

1) Gas phase SO_2 absorption into the slurry droplet
2) $Ca(OH)_2$ dissolution in the slurry droplet
3) $Ca(OH)_2$ dissolution in the spray-dried solids

The parameters that affect these processes are presented below.

Both the approach to saturation temperature and the size of the initial slurry droplet affect mass transfer during these three processes, and are therefore crucial process variables. The process variables can be categorized as follows:

1) Variables affecting SO_2 mass transfer to the slurry droplet
   - Approach to saturation temperature
   - Size of the slurry droplet - method of atomization
   - Mixing of the gas and droplets
   - Residence time of the flue gas in the dryer
   - Inlet SO_2 concentration
   - Inlet flue gas temperature

2) Variables affecting Ca^{++} mass transfer in the slurry droplet

   Stoichiometric ratio

   Approach to saturation temperature

   Size of the slurry droplet

   Residence time of the flue gas in the dryer

3) Variables affecting Ca^{++} mass transfer in the spray-dried solids

   Approach to saturation temperature

   Size of the initial slurry droplet

   Slaking

   Stoichiometric ratio

   Off-product recycle

   Method of particulate collection

These variables and their effects are discussed in the following sections. Reported test results that indicate the effect these variables have on SO_2 removal efficiency will also be discussed.

2.2.1 Approach to Saturation

Operating the spray dryer outlet at a close approach to saturation temperature increases the residual moisture level in the spray-dried solids and affects all three mass transfer processes. The closer the approach to saturation temperature, the cooler and more humid the flue gas becomes. High humidity lengthens the evaporation period and also increases the amount of moisture retained by the solids. By reducing the outlet temperature from the spray dryer by 10°F (from a 30°F approach to a 20°F approach), SO_2 removal efficiency can be increased by approximately 10 percent when lime is the absorbent.[9]

As the temperature of the flue gas gets closer to the adiabatic saturation temperature, the moisture content of the spray-dried solids increases and the outlet temperature of the flue gas decreases. However, there is a practical limit to the amount of moisture that can be retained by the solids without causing difficulties in discharging the solids from the spray dryer. Wet solids can have particularly severe effects with single-point discharge spray dryers, which may be susceptible to plugging. Also, the reduction in the spray dryer outlet temperature may cause problems in the downstream collection device, particularly if a fabric filter is used. Therefore, the minimum recommended approach to saturation is 20°F[2]; any closer approach may create equipment operation and maintenance problems with both the spray dryer and fabric filter. Problems that may occur in the fabric filter are often alleviated by reheating the flue gas exiting the spray dryer, but there are also

problems involved with reheating. Gas downstream of the air heater can be used for reheat, but the amount of untreated gas involved in reheating begins to limit overall SO_2 removal efficiencies. Gas upstream of the air heater can be used, but there is an energy penalty because less energy will be available for air preheat.[1]

The effect of changes in approach temperature on SO_2 removal efficiency is presented in Figures 2-7a and 2-7b. No inlet SO_2 concentration was specified for the data presented in Figure 2-7a.

2.2.2 Slurry Droplet Size - Method of Atomization

The size of the slurry droplets also affects all three mass transfer processes. The spray of slurry droplets must be finely atomized to provide the large surface area required for rapid SO_2 absorption. However, the droplets must be large enough so that they do not dry out before a satisfactory degree of reaction has occurred, the reaction being highly dependent on the presence of water. (The drying time varies with the square of the initial droplet diameter.)[3] Typically, one cubic foot of reagent properly atomized will have a surface area of 18,000 square feet.[4] Proper atomization is extremely important for mass transfer during the pseudo-equilibrium period, where the spray-dried solids exit the spray dryer with an equilibrium moisture content, because the size of the final agglomerate is directly related to the initial droplet size.

The dispersion of the slurry droplets in the flue gas also depends upon good atomization. The spray must become and remain dispersed in the reactor so that intimate contact between the drying agglomerates of lime and the flue gas can be maintained throughout the reactor.

Atomization is normally accomplished with a nozzle or a rotary atomizer. Rotary atomizers are the most common devices used for droplet production in commercial spray drying systems sold to date. Rotary atomizers appear to have the following potential advantages over nozzles.[4]

1) Droplet size is accomplished simply by atomizer wheel speed adjustment; therefore, droplet size is independent of flow volume.
2) Spray pattern is independent of flow volume.
3) They are less likely to block or clog.
4) There is no high pressure associated with the reagent or atomizing fluid.

The first two items are particularly important because relatively quick changes can be made in slurry flow rates to compensate for changes in boiler load or inlet SO_2. These changes can be made without altering

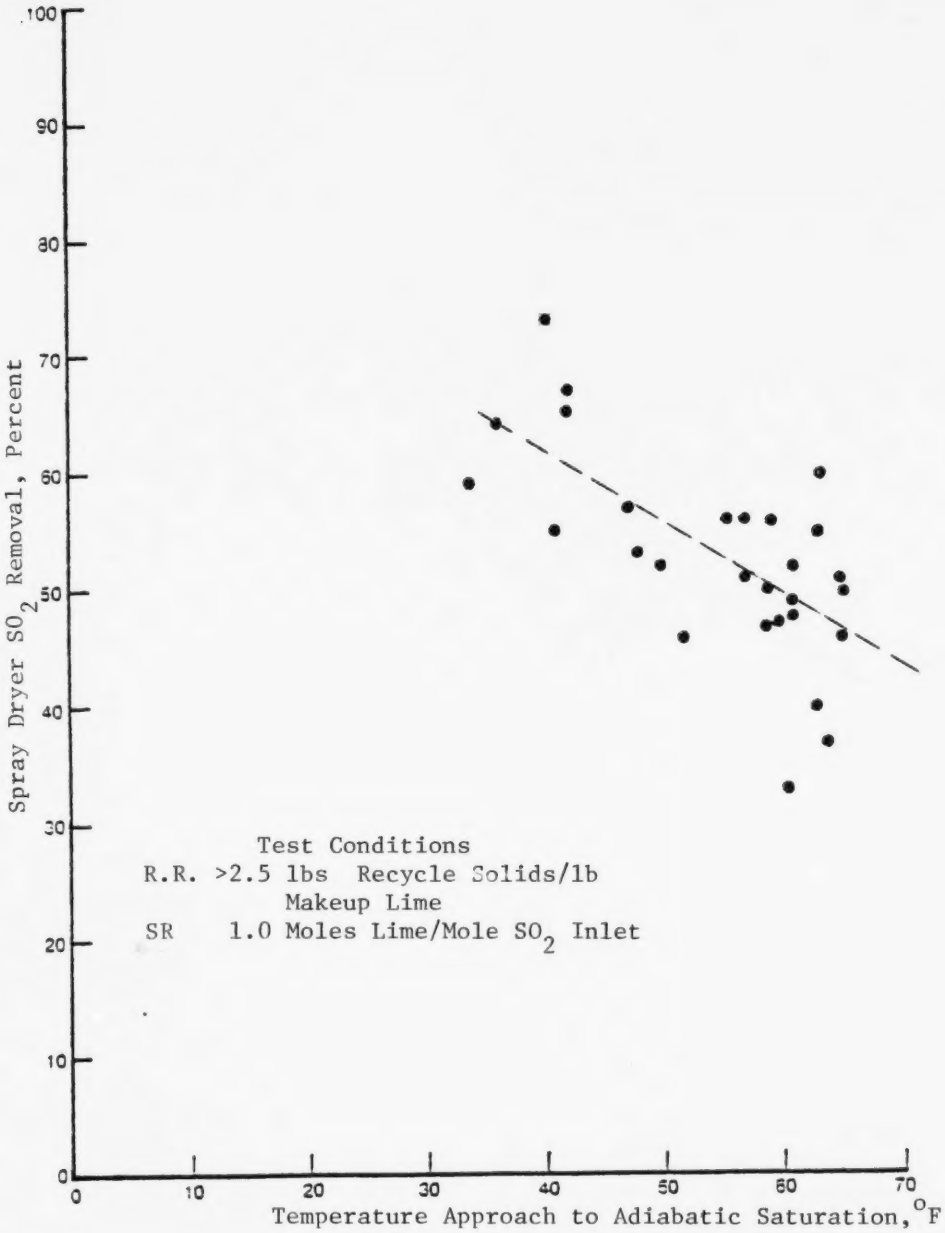

Figure 2-7a. Effect of approach to adiabatic saturation temperature on spray dryer SO_2 removal.[3]

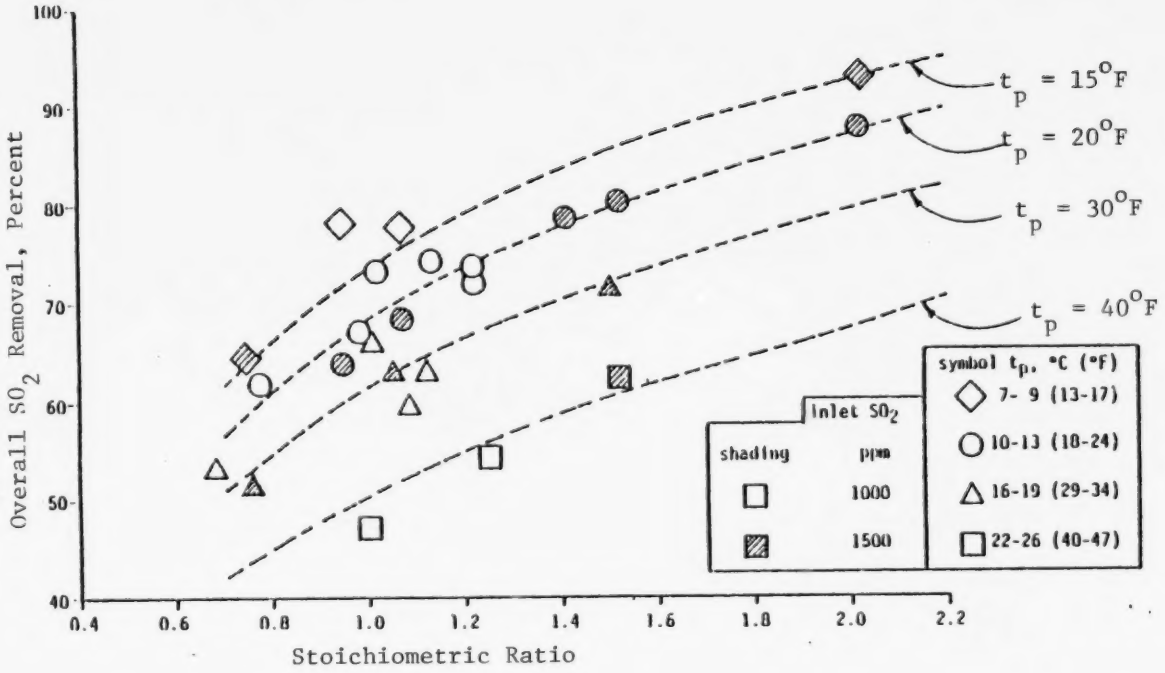

Figure 2-7b. Effect of approach to adiabatic saturation temperature (t_p) on spray dryer SO_2 removal.[2]

droplet size or spray pattern, two important variables influencing SO_2 removal reactions in the spray dryer.

The size of the slurry droplets is a strong function of the rotary atomizer's wheel tip speed, because the diameter of the droplet is inversely proportional to rotational speed for a given wheel. Thus, there is an optimum atomizer wheel speed that will give the best SO_2 removal efficiency. Tests by Buell to determine this optimum speed[2] indicated that for their particular system the best results were obtained at a wheel speed of 12,500 rpm, which corresponds to a tip speed of 537 ft/sec.[2] This test was performed on a 10-inch diameter wheel with an inlet gas flow rate of 8,500 acfm and a gas disperser vane angle of 45°. The inlet temperature and SO_2 concentration were 350°F and 1000 ppm SO_2, respectively. A stoichiometric ratio of 1.0 was used, and the approach to saturation temperature at the spray dryer outlet was 30°F.

2.2.3 Residence Time of the Flue Gas in the Dryer

The effect of residence time is most important during the first two mass transfer processes, SO_2 mass transfer to the slurry droplet and Ca^{++} mass transfer in the slurry droplet, because it determines the amount of time the flue gas and slurry droplets will be in contact in the spray dryer. The flow rate of gas through the absorber must be high enough for efficient mixing of the gas and spray, but not so high that a proper degree of drying cannot occur in the chamber. The residence time, defined as the chamber volume divided by the absorber outlet gas flow volume, must be controlled to an optimum value so that high SO_2 removal rates are obtained. The slower the drying process, the longer surface moisture will exist on the droplet, allowing for more reaction. Also, problems with chamber wall deposits and wet off-products can be minimized by sizing the spray dryer properly.[2]

A test was performed by Buell to determine the optimum spray dryer residence time as the flue gas inlet volume was varied from 6000 to 11,000 acfm while all other parameters were held constant. For this particular system, the optimum residence time was found to be 10 seconds for a 12.5-foot diameter spray dryer with an atomizer wheel speed of 12,500 rpm and a gas disperser vane angle of 15°. The inlet temperature and SO_2 concentration were 350°F and 1000 ppm SO_2, respectively. The stoichiometric ratio was 1.0, and the approach to saturation temperature was 30°F.[2]

2.2.4 Stoichiometric Ratio

The stoichiometric ratio is most important during the last two mass transfer processes, those that involve Ca^{++} mass transfer. The stoichiometry determines the amount of lime that will be present to react with the

SO_2 and significantly affects SO_2 removal in spray drying (see Section 2.1.2.2.2). The relationship between SO_2 removal efficiency and the stoichiometric ratio (SR) is expressed by the proposed mathematical model[3]:

$$E = 1 - e^{-K'SR} \qquad (2\text{-}35)$$

This model proposes that SO_2 removal is a function of the stoichiometric ratio. Figures 2-6a and 2-6b showed that the pilot spray dryer test data is well correlated to the mathematical model. Thus, it would appear that the model is valid for the operating conditions used in these tests.

The obvious method for increasing SO_2 removal would be to increase the lime stoichiometry, but there are several factors which limit the amount of lime which can be added. First of all, the amount of slurry that can be added to the flue gas is set by heat balance considerations to ensure the solids will be properly dried. Secondly, the amount of lime that can be added to the slurry is limited, because an upper limit is reached on the weight percent of lime in the slurry. Finally, the effect of the stoichiometric ratio on SO_2 removal efficiency begins to level off at SR values greater than 3.0.

2.2.5 Droplet - Gas Mixing

Mixing of the slurry droplets and the flue gas affects the mass transfer of SO_2 to the droplet. In order to provide for good contact between the flue gas and the slurry droplets, intimate mixing must be achieved. This requires fine atomization of the slurry droplets, as well as proper gas flow patterns. Some designs rely on gas dispersers placed around the atomizer that impart a swirling downward motion to the gas. These gas dispersers cause the slurry droplets and spray-dried solids to be carried along in the helical pattern of the entering flue gas. This helps to assure more complete mixing of the slurry droplets and flue gas as it passes through the chamber.[4] Another design also includes a "central gas disperser" that ducts part of the flue gas flow up toward the atomizer.

Buell performed tests to determine the optimum gas disperser vane angle to maximize SO_2 removal efficiency while all other parameters were held constant. This particular spray dryer was operated at a stoichiometric ratio of 1.0 and an atomizer speed of 12,500 rpm. The flue gas entered the spray dryer at 8,500 acfm, with a temperature of 350°F, and contained 1,000 ppm SO_2. The approach to saturation temperature at the dryer outlet was 30°F. The results of the tests on this dryer indicated that a gas disperser angle between 15 and 20 degrees from the vertical resulted in optimum performance.[2]

2.2.6 Lime Slaking

The quality of the slaking process determines how large, porous and reactive the lime particles are. The amount of pore surface area is important for reaction to proceed in the spray-dried solids. Therefore, slaking has the greatest effect on the mass transfer of Ca^{++} in the spray-dried solids. The techniques used in the slaking of lime can significantly affect its reactivity and surface area. Thus, slaking methods are among the first important design considerations in a dry scrubbing system. Slaking involves hydrating the lime to form calcium hydroxide in the presence of excess water, as described by Equation 2-36.[2]

$$CaO_{(s)} + H_2O_{(l)} \longrightarrow Ca(OH)_{2(s)} + 27{,}500 \text{ Btu/lb-mole} \quad (2\text{-}36)$$

When high calcium, soft-burned pebble lime is slaked with clean water at a water-to-lime ratio of 3:1 or 4:1, the lime pebbles rapidly disintegrate in an explosive, chain-slaking reaction. This produces a slurry of extremely fine (0.5 to 4.0 μm), porous slaked lime particles suspended in water with a large total surface area, which is ideal for use in the spray absorption process.[2] The water used for slaking must be of good quality. The water should not only be softened to prevent scaling problems, but it must be low in sulfates and other chemicals which can cause a reduction in the reactivity of the lime. For best results, slaking should take place at a relatively constant temperature of 190-200°F.[4]

Slaking under non-optimum conditions, using hard-burned or dolomitic lime with too high a water-to-lime ratio, or using poor quality slaking water containing excessive dissolved solids, will result in a less reactive slaked lime slurry. Such a slurry is characterized by larger and less porous slaked lime particles. The lime particles must be porous to provide a large surface area for good chemical reaction.[2] However, it appears that low quality cooling tower water can be used for dilution purposes.[2] As can be seen from Table 2-2, the degree of SO_2 removal was reduced when cooling tower water was used to slake the lime, but the cooling tower water did not reduce SO_2 removal when it was used to dilute the slaked lime slurry.

TABLE 2-2[2]

SPRAY DRYER FGD PERFORMANCE USING
COOLING TOWER BLOWDOWN WATER

Stoichiometric Ratio mol CaO/mole SO_2	Approach to Saturation (°F)	Use of Cooling Tower Water	Percent SO_2 Removal
1.04	30	slaking	45.9
1.03	20	slaking	53.9
1.46	30	dilution	78.2
0.99	20	dilution	61.0
1.08	30	slaking and dilution	50.1

2.2.7 Inlet SO_2 Concentration

The concentration of SO_2 in the flue gas that enters the spray dryer affects the mass transfer of SO_2 to the slurry droplet. The inlet SO_2 concentration has only a moderate affect on SO_2 removal over the range of concentrations which have been investigated and for which data are available. Figure 2-8a shows that SO_2 removal in the spray dryer decreases gradually with increasing flue gas inlet SO_2 concentration from 400 to 2000 ppm SO_2. Figure 2-8b shows that relatively constant SO_2 removal is obtained at 1000 and 1500 ppm SO_2, but a considerable decline in performance is experienced at 2000 to 2500 ppm. The reasons for this decline are unclear but seem to involve the precipitation of reaction product on the entire lime surface, which plugs the sorbent pores and limits diffusion. It is possible to utilize some of the lime that does not react by using a partial recycle of the off-product from the spray dryer.[2]

2.2.8 Flue Gas Inlet Temperature

The inlet temperature of the flue gas affects SO_2 diffusion and therefore, influences the mass transfer of SO_2 to the slurry droplet. Contradicting results have been obtained regarding the effect of flue gas inlet temperature on SO_2 removal efficiency. In a test performed by Babcock and Wilcox, the inlet temperature was reduced from 280°F to 230°F at a constant approach to saturation of 20°F.[9] The decrease in temperature resulted in a 10-percent decrease in SO_2 removal efficiency. However, a series of tests performed by Buell, which are presented in Figure 2-9, indicate that the inlet gas temperature has a negligible effect on SO_2 removal.[2]

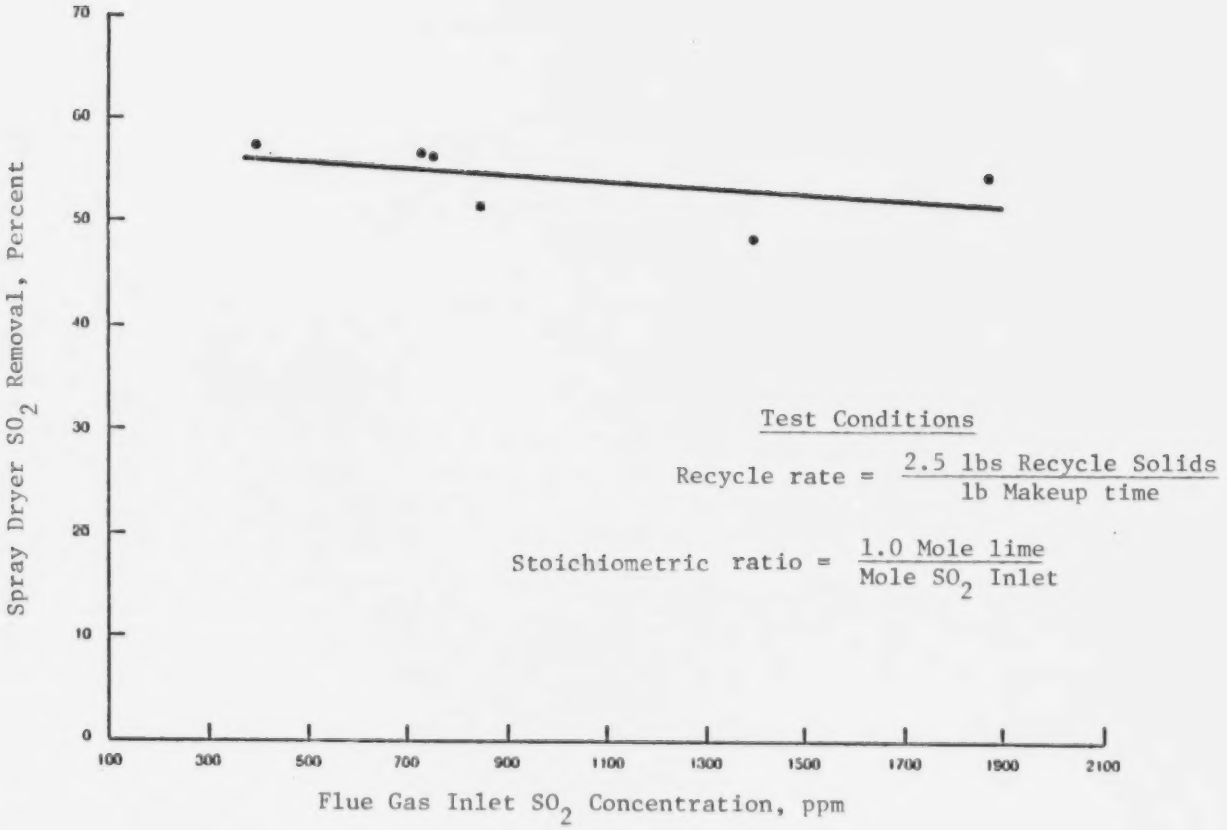

Figure 2-8a. Effect of inlet SO_2 concentration on spray dryer SO_2 removal.[3]

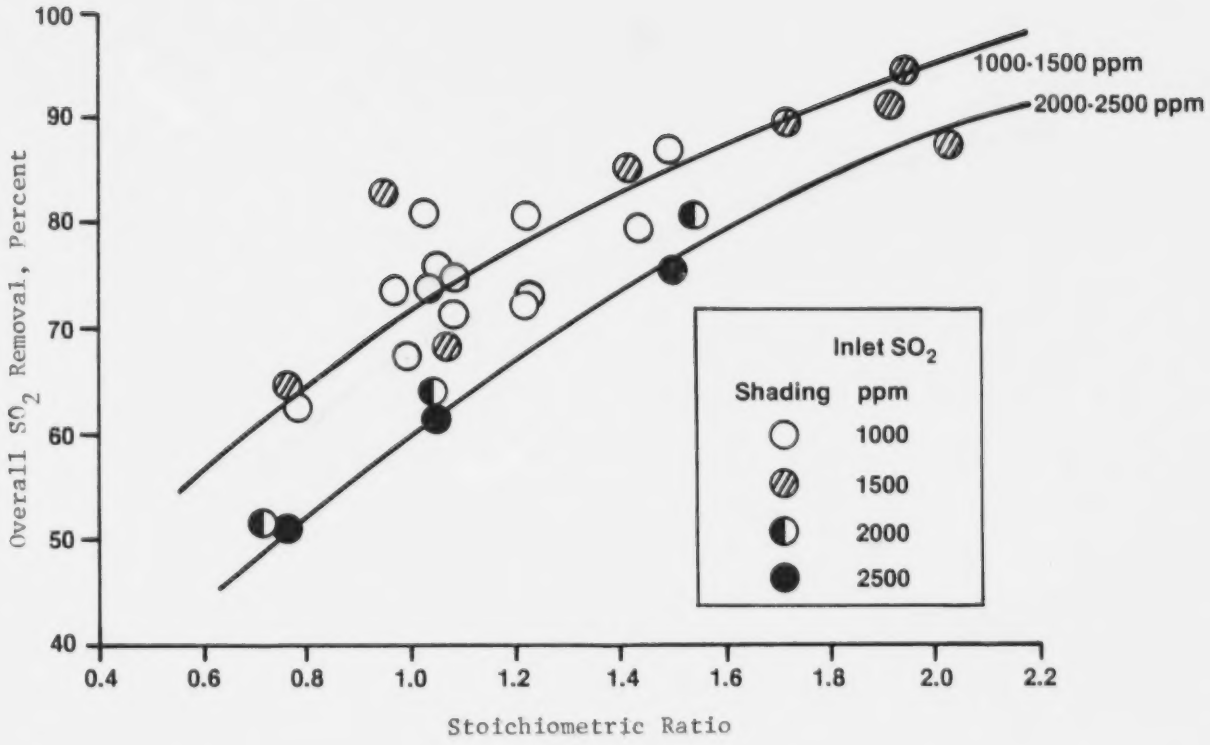

Figure 2-8b. Effect of inlet SO_2 concentration on spray dryer SO_2 removal[2] (test conditions: t_p = 18° to 24° F, inlet gas temp. = 290° to 360°F, residence time = 10 sec).[2]

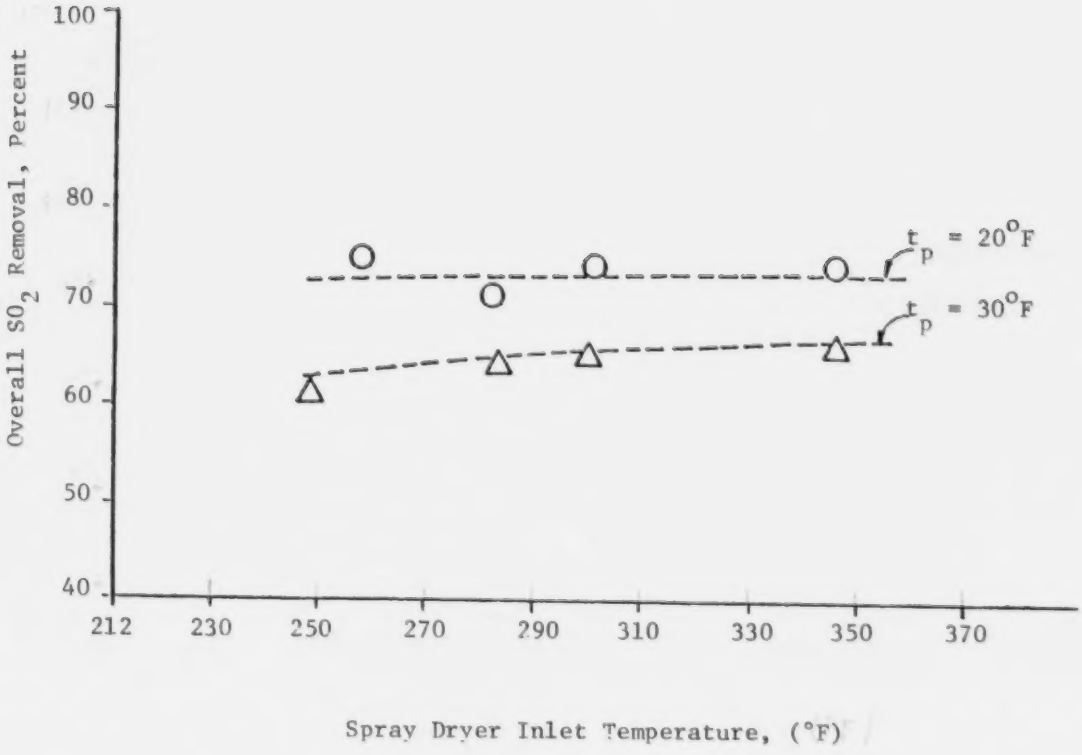

Figure 2- 9. Effect of flue gas inlet temperature on spray dryer SO_2 removal. (Test conditions: inlet SO_2 concentration = 1000 ppm, stoichiometric ratio = 1.0 and residence time = 10 sec.)[2]

The mathematical model developed by B&W, which is presented below,

$$E = 1 - \left(\frac{t_p}{Tin-Tsat}\right)^{0.62} \qquad (2\text{-}27)$$

predicts that higher flue gas inlet temperature will result in higher SO_2 removal efficiency. An attempt was made to numerically evaluate the effect of changing the inlet flue gas temperature, by using this mathematical model. Since it is difficult to assess the adiabatic saturation temperature without knowing the flue gas humidity, this temperature was assumed to be 125°F. A reduction in the flue gas inlet temperature from 280°F to 230°F, at a constant approach of 20°F, results in a decrease in SO_2 removal efficiency of 8 percent. This seems to support the results of the test performed by B&W. Further testing may be required to clarify the effect of inlet flue gas temperature on SO_2 collection efficiency.

2.2.9 Spray-Dried Off-Product Recycle

The use of off-product (reacted and unreacted sorbent and fly ash) recycle may provide more available lime surface which allows for increased mass transfer of Ca^{++} in the spray-dried solids. Recycling of the spray dryer off-product permits the reuse of unreacted lime reagent, and if the fly ash is high in available alkalinity, it may reduce the amount of required lime by substituting fly ash alkalinity for lime.[4] Fly ash recycle may improve spray dryer performance in two ways: (1) by providing available alkalinity and (2) by acting as a surface catalyst to enhance the lime-SO_2 reaction. The fly ash acts as a surface catalyst by providing an alternate site for $CaSO_3$ to precipitate, thus decreasing the solid deposits on the lime particles which cause increased resistance to mass transfer.

Fly ashes have been known to contribute significantly to the absorption of SO_2 in wet scrubbers; in fact, some wet scrubbers have relied principally upon fly ash alkalinity. It appears that water is the key to activating alkaline fly ashes. Initially, it was thought that fly ash could not become significantly wetted in a dry scrubber; therefore, fly ash was not expected to play a significant role in dry scrubber performance. When SO_2 removals as high as 70 percent were experienced in early dry scrubbing ventures, it appeared that the alkaline fly ash was somehow becoming wet.[5]

It is believed that the fly ash becomes wet by absorbing and condensing water vapor from the humid flue gas in the spray dryer.[5] Surface resistivity tests support this assertion. It has been shown that surface condensation can occur well above the water vapor dew point.[5]

Two methods of characterizing fly ash alkalinity have been developed: the available alkalinity and reactive alkalinity. The available alkalinity is determined from elemental ash analyses and is defined as:[5]

$$AA = \frac{\text{moles}(Na_2O + K_2O + MgO + CaO - SO_3) \text{ entering scrubber as ash}}{\text{moles of } SO_2 \text{ entering scrubber}} \quad (2\text{-}37)$$

The reactive alkalinity is determined as a function of pH and is defined as:[5]

$$RA = \frac{\text{milliequivalents of acid titrated per gram ash}}{2000} \times \frac{\text{lbs ash to dry scrubber/hr}}{\text{lbs moles } SO_2 \text{ to dry scrubber/hr}} \quad (2\text{-}38)$$

Theoretically, available and reactive alkalinity should be numerically equivalent at a low pH if available alkalinity adequately describes the alkaline chemistry of fly ashes.[5]

Since making additional alkaline material available for reaction with SO_2 is the primary objective of recycling part of the off-product, care must be taken in the design of the recycle system so that the maximum benefit is realized. The pH of the slurry to which the recycle material is added must be sufficiently low so that a reasonable amount of the recycle alkali will go into solution. Tests performed by Buell showed that if off-product was added to the lime slurry, which was saturated with $Ca(OH)_2$ at a pH of 12, no measurable benefit resulted, regardless of the amount of process off-product added. When a separate slurry of process off-product and water alone was prepared in a separate tank and mixed with the lime slurry at the point of injection to the absorber, however, considerable benefit resulted.[2]

Several tests have been performed on the effects of recycling both the spray dryer reaction product and the fly ash on SO_2 removal efficiency.[2,5,9] Tests performed by Babcock and Wilcox indicate that recycling the partially spent reactant and ash can significantly benefit lime utilization. Samples collected from the spray dryer hopper and the baghouse hopper were analyzed for calcium, magnesium, potassium, and sodium. The product analysis is shown in Table 2-3. From these data it appears that the

TABLE 2-3

HOPPER ASH ANALYSES COMPARISON[9]

	Spray Dryer hoppers		Baghouse hoppers		
	A	B	A	B	C
Calcium (Ca)	5.50	4.60	14.90	17.90	19.30
Magnesium (Mg)	0.01	0.56	0.02	0.98	0.80
Potassium (K)	1.50	1.50	1.50	1.50	1.50
Sodium (Na)	0.50	0.50	0.70	0.70	0.70

system has classified the particulates with the high alkalinity fraction in the baghouse hoppers and the low alkalinity fraction in the spray dryer hoppers. The concentrations of magnesium, potassium and sodium are about the same in the spray dryer and baghouse, however, the baghouse calcium concentration is about three or four times greater than the spray dryer calcium concentration. Although a test comparing SO_2 removal using spray dryer solids with baghouse solids was not performed by B&W, the alkalinity results would seem to indicate that recycling material from the baghouse hoppers would be more beneficial than using solids from the spray dryer hoppers.[9] However, these ash analyses do not indicate the amount of sulfite in the ash hoppers, therefore the available alkalinity of the ash cannot be determined. It is the available alkalinity, not the alkalinity, that effects SO_2 removal.

Research-Cottrell has also performed tests to determine the effects of solids recycle on SO_2 removal efficiency. The results of these tests are presented in Figure 2-10a and show that SO_2 removal in the spray dryer increases with increasing recycle ratio up to 2.5 - 3.0 lbs recycle solids/lb makeup lime and then begins to level off. Figure 2-10a also shows that SO_2 removal is not significantly different employing either spray dryer solids or baghouse solids as the recycled material, which contradicts the results of the Babcock and Wilcox analysis.[9] The reason for this contradiction is not clear, but there may have been differences in the available alkalinity of the off-products, or any number of other variables. B&W has shown that the fraction of available alkalinity which actually is utilized during a single passage through the dry scrubber diminishes as the available alkalinity increases. For example, if the ash alkalinity doubles from one coal to another, the beneficial effect on SO_2 removal will not double.[5] This too may explain the differences in results achieved by the two tests.

Buell also tested the effect of off-product recycle. The results are shown in Figure 2-10b and indicate a substantial benefit was gained through the use of recycle. The recycled fly ash had an available

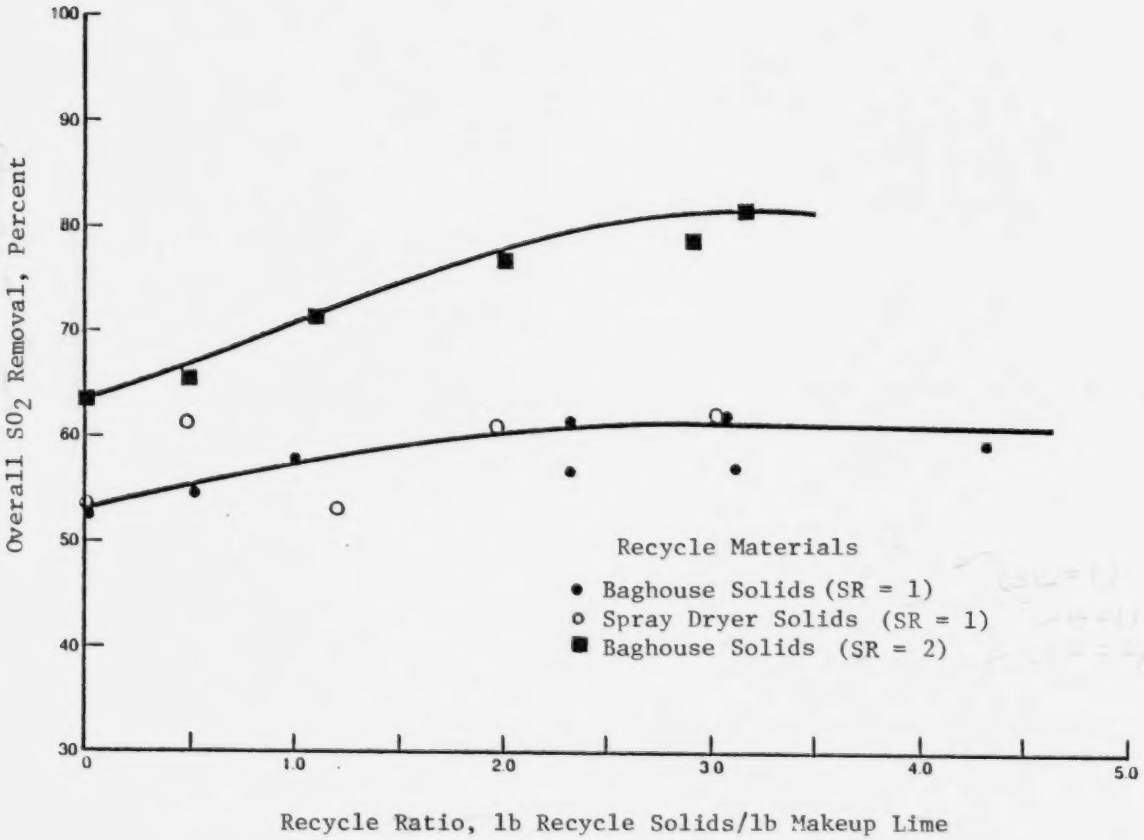

Figure 2-10a. Effect of recycle ratio on overall SO_2 removal.[3]

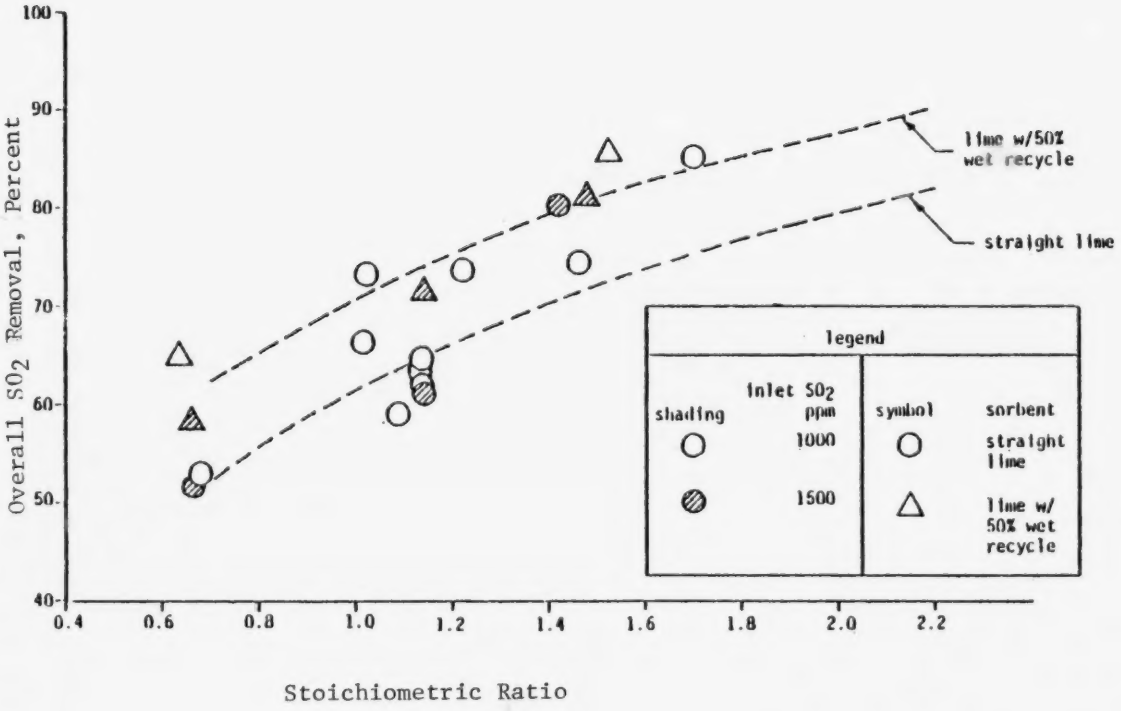

Figure 2-10b. Effect of recycle on spray dryer SO_2 removal.[2]

alkalinity of 0.4 to 0.6 percent, which is relatively low. Therefore, the performance benefit may be due more to re-use of $Ca(OH)_2$ recovered from the off-product and fly ash surface catalyst effects [2] than to fly ash alkalinity.[2]

Even if the fly ash has little available alkalinity, beneficial effects may result from its presence in the atomized slurry droplets by its action as a surface catalyst. The fly ash particles are considerably larger than the elementary particles of slaked lime (approximately 10 times).[2] The presence of large inert bodies in the slurry droplet will increase the ratio of surface area to water volume of the droplet, as well as provide sites for the formation of crystalline reaction products. This will tend to keep the slaked lime particles surfaces "open" to mass transfer for a longer period.[2] Electron micrographs suggest that the lime present is made more available for reaction because of the increased area for dispersion on the recycle solids.[3]

2.2.10 Fabric Filter versus ESP Particulate Collection

For the spray drying system either an ESP or a fabric filter can be used to remove particulates from the spray dryer exhaust to meet environmental emission requirements. The type of particulate collection device used will influence mass transfer in the spray-dried solids. Some tests have shown that the downstream collection device can increase the total system SO_2 removal by approximately 10 percent.[3]

Initially, it was felt that a fabric filter would provide better SO_2 removal than an ESP, and only one commercial system purchased to date uses an ESP, the rest employ fabric filters.[4] As the fabric filter operates a cake of the spray-dried solids builds up on the filter. If this cake contains unreacted sorbent it can act to remove SO_2 as the flue gas passes through the filter. However, test results obtained by B&W at the Jim Bridger Station have shown that both ESPs and fabric filters provide about the same degree of SO_2 removal.[9] Figure 2-11a shows SO_2 removal with the spray dryer only, and Figure 2-11b shows SO_2 removal with the addition of a particulate collection device. From these figures it can be seen that the particulate collection device increases SO_2 removal by approximately 8 percent. It can also be seen that the ESP provides slightly better SO_2 removal than the fabric filter under the same test conditions.[9]

One of the advantages of using an ESP instead of a fabric filter is that the ESP allows the spray dryer to be operated at a closer approach to the saturation temperature without causing maintenance problems in the collection device. A closer approach to the saturation temperature will provide greater SO_2 removal in the spray dryer. ESPs have been found to perform very well in collecting the particulates from the spray dryer exhaust. The spray-dried product does not build up on the discharge

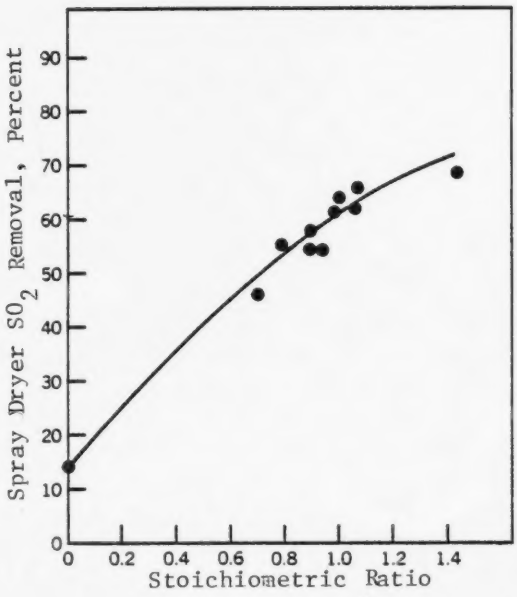

Figure 2-11a. Spray dryer only SO_2 removal.[9] [Inlet temperature = 270°-290°F; Approach to saturation = 20°F.]

Figure 2-11b. Overall SO_2 removal.[9] [Inlet temperature = 280-290°F; Approach to saturation = 20°F]

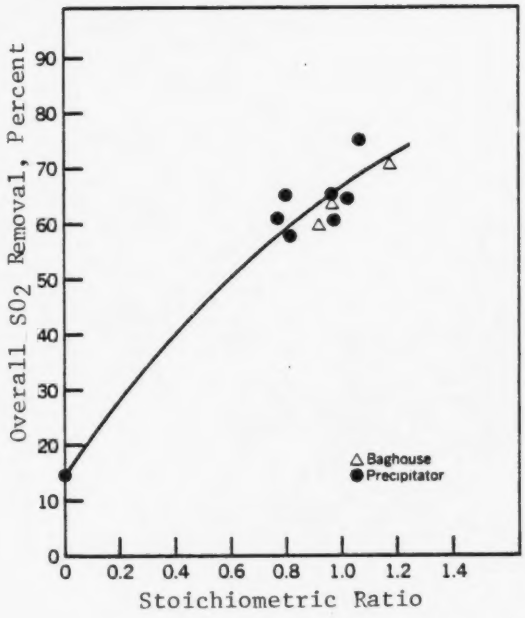

and collecting electrodes. Due to the humidity of the flue gas the fly ash becomes conditioned, which results in higher particulate migration velocities than would be expected. Also, the low outlet temperature from the spray dryer reduces the resistivity of the fly ash. In addition, ESPs can be operated at lower system pressure drops than fabric filters.[4]

Fabric filters have also been found to collect the spray-dried solids very well. The main advantage of a baghouse is that it is a bulk collection device whereas a precipitator is a percentage collector. Tests on recirculation have at times produced a dust loading as high as 25 gr/ft^3 as an extreme condition. If environmental restrictions were to call for a maximum outlet loading of 0.01 gr/ft^3 the precipitation efficiency would have to be 99.96 percent - a number that may be difficult to achieve consistently with a precipitator in a power plant. Properly designed baghouses, on the other hand, should be able to meet a .01 grain outlet emission regardless of inlet loading. In addition, the cost of a precipitator for the above duty could be far more than the comparable baghouse, and the baghouse will generally be more reliable in producing low opacity.[4]

2.3 DATA GAPS IN LITERATURE

This paper has identified several areas that may require further clarification. These are:

1) Spray dryer performance when inlet SO_2 exceeds 2500 ppm
2) Additional evaluation of the applicability of the mathematical models
3) Effect of recycling spray dryer solids versus baghouse solids
4) Effect of inlet flue gas temperature on SO_2 removal efficiency
5) Characterization of spray dryer wall effects
6) Further analyses of the competition between SO_2 and CO_2 for available lime

The most prominent data gap is lack of information on spray dryer performance when inlet SO_2 concentration exceeds 2500 or 3000 ppm. These data will be important not only in evaluating the validity of the proposed reaction models, but in determining the applicability limits of lime spray drying for utility and industrial units firing coals containing greater than 3 percent sulfur, an area of considerable current interest.

Evaluation of the simple diffusion model proposed by B&W,

$$- \ln (1-E) = 0.62 \ln\left(\frac{Tin - Tsat}{Tout - Tsat}\right), \qquad (2\text{-}25)$$

requires data on SO_2 removal efficiency (E), the inlet gas temperature (Tin), spray dryer outlet temperature (Tout), and the inlet gas moisture content (which is required for the determination of Tsat). This type of information is not readily available in technical papers and articles published to date.

Many of the published test results lack detailed and complete information on the test conditions. It is acknowledged that this information will not be readily available from privately funded test work. However, additional raw data from EPA-sponsored research may prove helpful in many respects.

Additional work may also be needed to clear up conflicting results from tests measuring the effect of SO_2 removal using recycled baghouse solids versus spray dryer solids and the effect of varying the inlet flue gas temperature. An attempt to characterize "wall effects", which may cause differences in SO_2 removal in different size spray dryers might also prove worthwhile, since pilot-scale test results are typically used to predict full-scale system performance. It would also be helpful to characterize the competition between SO_2 and CO_2 for reaction sites.

2.4 LITERATURE CITED FOR SPRAY DRYING

1. Kelly, M.E. and S. A. Shareef. "Second Survey of Dry SO_2 Control Systems." EPA Report 600/7-81-018. (NTIS No. PB 81-157919) February 1981.

2. Parsons, E. L., et al. "SO_2 Removal by Dry FGD," In: Proceedings of Sixth Symposium on Flue Gas Desulfurization, Houston, Texas. EPA-600/9-81-0196, Vol. 2, pp. 801-852. April 1981.

3. Stevens, N. J. "Dry SO_2 Scrubbing Pilot Test Results." In: Proceedings of Sixth Symposium on Flue Gas Desulfurization. Houston, Texas. EPA-600/9-81-0196, Vol. 2, pp. 777-800. April 1981.

4. Meyler, J. A. "Dry Flue Gas Scrubbing: A Technique for the 1980's." (Presented at 1980 Joint Power Conference. Phoenix, Arizona. September 1980.)

5. Downs, W., W. J. Sanders and C. E. Miller. "Control of SO_2 Emissions by Dry Scrubbing." (Presented at the American Power Conference. Chicago, Illinois. April 21-23, 1980.)

6. Getler, J. L. et al. "Modeling the Spray Absorption Process for SO_2 Removal." Journal of the Air Pollution Control Association 29:12. December 1979. p. 1270-1274.

7. Downs, W., Babcock and Wilcox, letter to Apple, C. A., Radian Corporation. March 17, 1981.

8. Downs, W., Babcock and Wilcox, Telephone conversation with Apple, C. A., Radian Corporation. November 18, 1980.

9. Hurst, T. B. and G. T. Bielawski. Dry Scrubber Demonstration Plant - Operating Results. In: Proceedings of Sixth Symposium on Flue Gas Desulfurization. Houston, Texas. EPA-600/9-81-0196, Vol. 2, pp. 853-860. April 1981.

10. Brna, T. G., S. J. Lutz and J. A. Kezerle. "Performance Evaluation of an Industrial Spray Dryer for SO_2 Control. (Prepared for Presentation at EPA's Sixth FGD Symposium. Houston, Texas. October 1980.)

11. Stevens, N. J., G. B. Manavizadeh, G. W. Taylor and M. J. Widico. Dry Scrubbing SO_2 and Particulate Control. (Presented at EPA's Third Symposium on the Transfer and Utilization of Particulate Control Technology. Orlando, Florida. March 1981.)

12. Parsons, E. L., V. Boscak, T. G. Brna and R. L. Ostop. SO_2 Removal by Dry Injection and Spray Absorption Techniques. (Presented at EPA's Third Symposium on the Transfer and Utilization of Particulate Control Technology. Orlando, Florida. March 1981.)

SECTION 3

DRY INJECTION OF SODIUM COMPOUNDS

The commercial application of dry injection to coal-fired boilers is still in the developmental stage. Bench-scale and pilot-scale tests are presently being conducted to characterize the performance of dry injection systems. Tests have been conducted with flue gas containing up to 3000 ppm sulfur.[1] A generalized flow diagram of this process with nahcolite as the sorbent is presented in Figure 3-1.

Dry injection involves two steps: injection of the dry sorbent into the flue gas and particulate collection to remove the unreacted and reacted solids and fly ash from the gas stream. The point of sorbent injection has been varied from the boiler furnace all the way to the flue gas entrance to the particulate collection device, either an ESP or baghouse fabric filter. Solids collection with a fabric filter seems to be more advantageous than collection with an ESP because a filter cake of the dry sorbent collects in the baghouse. Typically, this filter cake contains unreacted sorbent, which reacts with SO_2 in the flue gas to further increase SO_2 removal. Therefore, this analysis concentrates on a dry injection system in which the sorbent is injected into the flue gas after it exits the air preheater, and which uses a baghouse filter for solids collection. An analysis of the final baghouse solids has shown that the principal reaction product is usually sodium sulfate (Na_2SO_4).

For a typical dry injection system, the flue gas exits the air preheater at temperatures between 275° and 350°F and is contacted with an alkaline sorbent. This sorbent is finely ground to provide a large surface area for chemical reaction. A variety of alkaline sorbents have been tested including: limestones, dolomites, quicklime, hydrated lime, magnesium dioxide, sodium bicarbonate, sodium carbonate, nahcolite, and various trona grades. Investigations have shown that only sodium compounds have good capability for reducing the SO_2 content of the flue gas.[2] Nahcolite and trona ores, which are natural sodium-based compounds, appear to be the most reactive sorbents. Furthermore, it has been shown that nahcolite, which contains 70 to 90 percent sodium bicarbonate ($NaHCO_3$), provides greater SO_2 removal than trona ore ($Na_2CO_3 \cdot NaHCO_3 \cdot 2H_2O$).[2]

High SO_2 removal efficiencies have been obtained with the injection of dry nahcolite, ground to minus 200 mesh (less than 74 microns), into the SO_2-laden flue gas. Past studies have shown that dry injection of nahcolite into flue gas containing less than 2000 ppm SO_2 followed by a

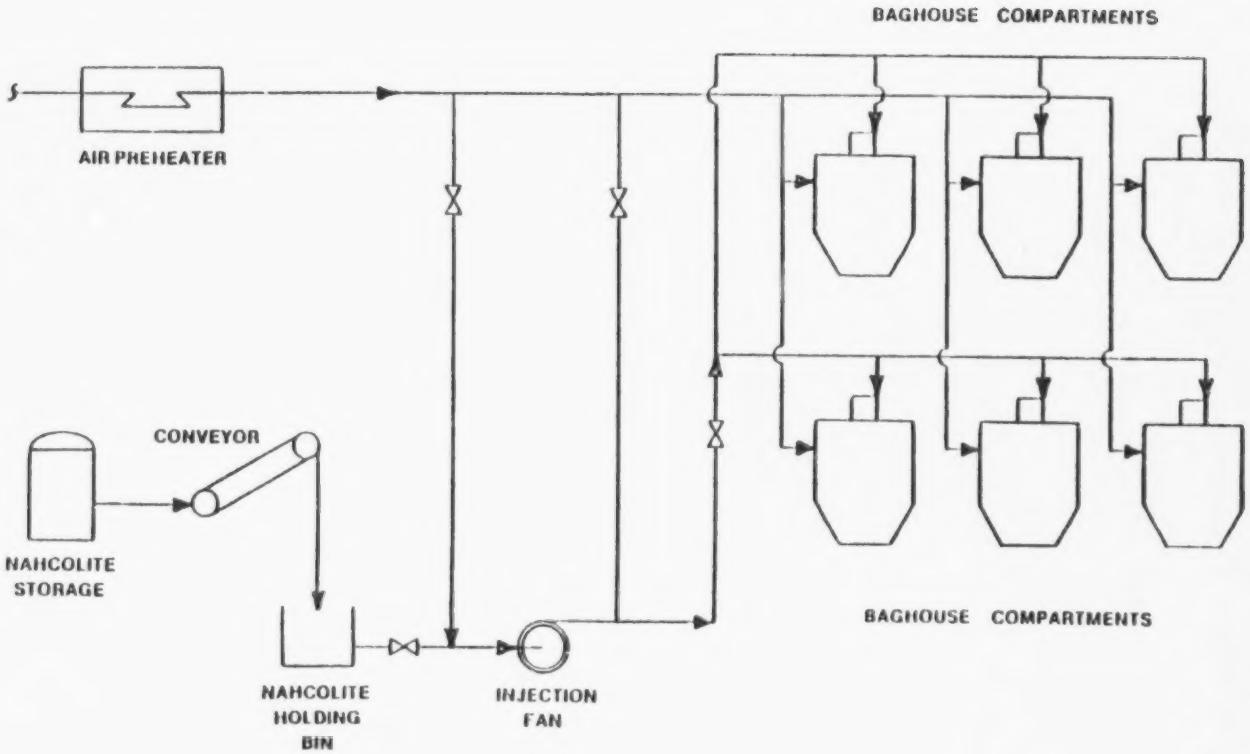

Figure 3-1. Nahcolite dry injection flow diagram.

fabric filter resulted in total SO_2 removal efficiencies of 60 to 80 percent at flue gas temperatures between 300° and 350°F and stoichiometric ratios of Na_2O to inlet SO_2 of 0.7 to 1.8. A recently completed study by the Department of Energy (DOE) at their Pittsburgh Energy Technology Center (PETC) has shown up to 95 percent SO_2 removal with the dry injection of nahcolite. Tests were performed with coals containing 1.1, 1.6 and 3.5 percent sulfur, at an average temperature of 400°F. Ninety-five percent removal of SO_2 was obtained with the 1.1 and 1.6 percent sulfur coals at a stoichiometric ratio (SR) of 1.5. It was found that SO_2 removal decreased somewhat as the inlet SO_2 concentration increased, however, 90 percent removal was obtained at a SR of 1.5 for the 3.5 percent sulfur coal.[1]

Several modes of sorbent injection have been or are being investigated:

1) Continuous. After the bag is cleaned, sorbent entrained in the flue gas is continuously supplied to the bag surface from injection points located upstream of the baghouse.

2) Batch. After the bag is cleaned, all sorbent is added to the bag as a precoat before flue gas flow is resumed.

3) Semi-batch. After the bag is cleaned some sorbent is precoated onto the bags and the remainder is added continuously at an upstream injection point.

The best injection method appears to be the semi-batch method, because it allows for SO_2 removal in the duct leading to the fabric filter and also provides an initial unreacted filter cake to remove SO_2.[2]

One system design uses 20 percent of the feed sorbent to precoat the bag filters, while the remainder of the material is fed into the duct leading to the baghouse over a 40-minute period. Once the remainder of the sorbent has accumulated on the filter bags, the system is operated for another 30 minutes without further sorbent addition. Thus, the baghouse is operated for approximately 70 minutes between cleanings. Once the bags are cleaned, they are precoated again.[3] It takes approximately 6 minutes for the cleaning and precoating operation.[3] In this system the ground nahcolite sorbent was fed into the duct at less than 10 gr/ft^3 of flue gas to prevent particle settling in the duct.[3] Typical flue gas residence times in the duct are between 1 and 4 seconds.[4] Air-to-cloth ratios used in the design of the baghouse system are in the range of 2 to 3 ft/min.

3.1 REACTIONS AND REACTION MODELS FOR SODIUM DRY INJECTION

This section presents the current theories on the reactions that occur during dry injection of sodium-based alkalis into SO_2-laden flue gas. The chemical reactions between the gaseous SO_2 and the finely

ground sodium-based sorbent and the physical changes in the sorbent that occur during these reactions are discussed. Current theories on the mechanisms and rate controlling steps involved in the dry injection reactions, including both qualitative and quantitative models, are also presented.

3.1.1 Chemical Reactions and Physical Changes

This section analyzes the chemical reactions and physical changes that occur when flue gas is desulfurized by contact with a powdered dry sodium-based sorbent, such as nahcolite or trona. The chemical reactions involve the adsorption of SO_2 by the sorbent particles with the subsequent formation of sodium sulfate or sulfite. Several changes in the physical structure of the sorbent particles accompany these chemical reactions.

The chemical adsorption of SO_2 by the solid sorbent particles can involve reaction at two places in the dry injection system:

1) Reaction between the gaseous SO_2 and entrained sorbent particles in the flue gas duct
2) Reaction between the gaseous SO_2 and a packed bed of sorbent particles in the baghouse filter cake

These reactions are strictly gas-solid reactions. Changes in the molar volume and porosity of the sorbent particles accompany these reactions. These physical changes influence the reactivity of the sorbent particles.

3.1.1.1 Chemical Reactions. This section presents the chemical reactions that occur when gaseous SO_2 is reacted with solid sodium-based compounds. The behavior of two sorbents, nahcolite and trona, will be characterized. The chemical reactions that are presented for nahcolite also hold for pure sodium bicarbonate. The reaction mechanisms and rate controlling steps are not analyzed here but will be identified in Section 3.1.2, Reaction Models.

The overall chemical reactions that occur during dry injection of nahcolite and trona are shown in Equations 3-1 and 3-2, respectively.

$$2NaHCO_{3(s)} + SO_{2(g)} + \tfrac{1}{2}O_{2(g)} \longrightarrow Na_2SO_{4(s)} + 2CO_{2(g)} + H_2O_{(g)} \qquad (3\text{-}1)$$

$$2(Na_2CO_3 \bullet NaHCO_3 \bullet 2H_2O)_{(s)} + 3SO_{2(g)} + 3/2\ O_{2(g)} \longrightarrow 3Na_2SO_{4(s)} + 4CO_{2(g)} + 5H_2O_{(g)} \qquad (3\text{-}2)$$

These reactions do not occur in a single step but instead proceed by a series of three reaction steps: (1) thermal decomposition of sodium bicarbonate ($NaHCO_3$), (2) uptake of gaseous SO_2 by the sorbent, and (3) oxidation of sodium sulfite (Na_2SO_3) to sodium sulfate (Na_2SO_4). These reactions are described below.

1. In the first step sodium bicarbonate is thermally decomposed into a very active form of sodium carbonate. This reaction is shown in Equations 3-3 and 3-4 for nahcolite and trona, respectively.

$$2NaHCO_{3(s)} + \text{heat} \longrightarrow Na_2CO_{3(s)} + H_2O_{(g)} + CO_{2(g)} \qquad (3\text{-}3)$$

$$2(Na_2CO_3 \cdot NaHCO_3 \cdot 2H_2O)_{(s)} + \text{heat} \longrightarrow 3Na_2CO_{3(s)} + CO_{2(g)} + 5H_2O_{(g)} \qquad (3\text{-}4)$$

Both CO_2 and H_2O are volatilized during this reaction, thus reducing the molar volume of the sorbent. The decomposition of pure sodium bicarbonate begins at 100°F at a very slow rate. The decomposition rate becomes very rapid at temperatures greater than 250°F, and is instantaneous at temperatures of 518°F or greater. Therefore, typical air preheater outlet temperatures between 275°F and 350°F should provide for rapid decomposition of the bicarbonate. Once the nahcolite and trona ores have both been decomposed to sodium carbonate they follow the same reaction steps.

2. The second step is the reaction between the gaseous SO_2 and the solid sodium carbonate, as is characterized by Equation 3-5.

$$Na_2CO_{3(s)} + SO_{2(g)} \longrightarrow Na_2SO_{3(s)} + CO_{2(g)} \qquad (3\text{-}5)$$

This reaction causes the molar volume of the solids to increase. Presumably,[4] this reaction can take place with direct replacement of CO_2 by SO_2.[4] However, this reaction may be somewhat dependent upon the presence of moisture.[2] Research by Rivers and Doyle for the American Air Filter Co.[2] and Stern[2] has shown that SO_2 removal with nahcolite drops off considerably when the flue gas moisture content is less than 5 percent. However, increasing the moisture content from 5 to 15 percent had little effect upon the degree of SO_2 removal.[2]

3. The final reaction step is the oxidation of sodium sulfite (Na_2SO_3) to sodium sulfate (Na_2SO_4).

$$Na_2SO_{3(s)} + \tfrac{1}{2}O_{2(g)} \longrightarrow Na_2SO_{4(s)} \qquad (3\text{-}6)$$

The oxidation of sodium sulfite to sodium sulfate causes the molar volume of the solids to increase even more. Analyses of the product solids collected in the fabric filter have shown that the final reaction product is predominantly sodium sulfate (Na_2SO_4).[4,6,8] Also, thermodynamic equilibrium calculations utilizing the principle of minimization of free energy show that at temperatures below 1500°F Na_2SO_4 is the thermodynamically favored product.[4] Contrary to the work of others, Genco et al.[3] found that the reaction product was predominantly sodium sulfite, with some sodium sulfate present.

These chemical reactions generate a number of physical changes in the molar volume and porosity of the sorbent particles. These physical changes in turn affect the reactivity of the sorbent.

3.1.1.2 Physical Changes. The physical changes that have the greatest effect on the reactivity of the sorbent are changes in the pore structure and molar volume of the particles. These physical changes are caused by the chemical reactions which were discussed in the previous section. Initially, the molar volume of the sorbent is decreased by the decomposition of sodium bicarbonate ($NaHCO_3$) to sodium carbonate (Na_2CO_3), thereby increasing the reactivity of the sorbent. The thermal decomposition of $NaHCO_3$ releases CO_2 gas and H_2O vapor and causes pores to develop in the sorbent particles.[2] These pores provide a greater surface area for chemical reaction and a greater volume for SO_2 diffusion. The reactivity of the sorbent particles has been found to increase by up to a factor of 60 because of thermal decomposition.[4]

Naturally occurring nahcolite is relatively nonporous. However, Howatson et al.[5] investigated the pore development of nahcolite, which was thermally decomposed at 300°F, with a scanning electron microscope (SEM). The study found scattered development of 0.1 to 0.7μm pores after 10 minutes. After 20 minutes the surface was completely covered with pores averaging about 0.3μm in diameter.[5] The Na_2CO_3 particles which are formed have a much larger void space than the parent $NaHCO_3$ particle.[6] It should be noted that these changes in the pore volume of the particle do not cause a change in the diameter of the particle.

With the flue gas exiting the air preheater at a temperature of approximately 300°F and with the bag filter operating for 70 minutes between cleanings, the sorbent particles should have sufficient time for full development of a pore system. Tests with nahcolite at gas temperatures of 270°F have shown that it takes about 40 minutes for the reaction to achieve maximum steady state SO_2 removal which seems to indicate that this time is required for full pore development.[7] Decomposition at temperatures higher than 300°F also produces pores averaging 0.3μm in diameter, but pore formation is more rapid than at lower temperatures. Superior Oil Company reported that the greatest internal surface area is

generated by decomposing $NaHCO_3$ at temperatures between 250°F and 300°F for minus 200-mesh (74μm) particles.[8] Stern, however, found that the maximum specific surface area for particles between 90 and 500μm was generated by decomposing nahcolite at 600°F in a forced draft oven.[9]

In addition to temperature, another factor influencing the rate of decomposition of the $NaHCO_3$ is the size of the sorbent particle. Laboratory-scale fixed-bed data from Superior Oil Company testing indicated that 85 percent of the $NaHCO_3$ particles between 400 and 200 mesh (37 and 74μm) were converted to Na_2CO_3 in approximately 20 minutes.[10] In contrast, approximately 70 minutes were required for $NaHCO_3$ particles between 4 and 3½ mesh (4760 and 5660μm) to reach the same degree of conversion. This particle size effect can be explained by heat transfer principles. In order for the $NaHCO_3$ particles to decompose fully the temperature at the center of the sorbent particles must be raised to approximately 250°F. According to Fourier's law of heat conduction the rate of heat transfer per unit area is inversely proportional to the distance across which heat must be transferred. Therefore, heat transfer across a large radius is slower than heat transfer across a small radius, and it will take longer for the center of a large particle to reach the decomposition temperature than the center of a small particle.

Trona[2] has been found to be less reactive than nahcolite in dry injection.[2] It is postulated that trona is less reactive because it already contains one mole of Na_2CO_3 for every mole of $NaHCO_3$ present. Thus the decomposition of trona does not generate as much pore volume as the decomposition of nahcolite. This results in less pore surface area available for reaction and a lower reactivity relative to nahcolite. However, trona achieves maximum steady state SO_2 removal immediately, which seems to indicate that the pores are developed more rapidly in trona than in nahcolite.

Once the $NaHCO_3$ has been decomposed to Na_2CO_3, it reacts with the gaseous SO_2 to form Na_2SO_3. A slight increase in molar volume results from this reaction. The molar volume of Na_2CO_3 is about 42 cm^3/gm-mole, while the molar volume of Na_2SO_3 is about 48 cm^3/gm-mole. Increases in molar volume tend to reduce the size of the pores, thus reducing the reactivity of the sorbent.

The final reaction is the oxidation of Na_2SO_3 to Na_2SO_4, which requires half a mole of oxygen for each mole of Na_2SO_3.[2] A molar volume increase also accompanies this oxidation reaction.[2] The molar volume of Na_2SO_4 is about 53 cm^3/gm-mole. Overall, the reaction of Na_2CO_3 to Na_2SO_4 results in a 25.8 percent increase in molar volume.

The chemical reaction of gaseous SO_2 with solid Na_2CO_3 proceeds from the exterior of the sorbent particle inward, causing an ash of Na_2SO_4 to form on the surface of the particle. Scanning electron micrograph's (SEM's) of halved particles indicated that there is a surface product zone, an intermediate reaction zone, and a central unreacted core.[6] Relatively high sulfate concentrations were found in the outer ash layer which surrounded the porous unreacted core.[4] This outer layer of Na_2SO_4 ash has a greater molar volume than the Na_2CO_3 in the core and apparently causes the pores to plug which limits the diffusion of SO_2 to the unreacted Na_2CO_3 core.

3.1.2 Reaction Models

The reaction mechanisms that govern the sodium-based dry injection process are not well defined. Investigators have studied a wide range of parameters while evaluating the dry injection system, but the test conditions were so varied that in almost all cases it was difficult to draw conclusions about the rate controlling mechanisms. However, analyses of the reacted sorbent revealed characteristics which have enabled the postulation of qualitative models. These qualitative models provide a basis for developing quantitative (mathematical) models to predict SO_2 removal under given reaction conditions. The available information on both qualitative and quantitative models is summarized in the following sections. The mathematical models which are developed for the dry injection reactions in this report were not evaluated against test data to determine their validity, because the published data to date do not provide many of the variables required for the evaluation of the models.

3.1.2.1 Qualitative Models. The reaction mechanisms governing the gas-solid reactions that take place during dry injection are quite complex. The reactions involve mass transfer, heat transfer, structural changes, and product formation. However, based on classical mass transfer theory three possible rate controlling steps can be postulated:

1) External Diffusion - Diffusion of gaseous SO_2 from the flue gas to the particle surface through a stagnant gas film around the particle.

2) Internal Diffusion - Diffusion of gaseous SO_2 from the surface of the particles through pores in the particle to the site of the chemical reaction. (This is most important when the outer surface of the particle has reacted to form an inert shell of ash (Na_2SO_4).)

3) Chemical Reaction - As discussed in Section 3.1.1.1, there are two chemical reactions involved in the formation of Na_2SO_3, either one may control the rate of reaction. Thus, the rate of decomposition of $NaHCO_3$ to Na_2CO_3 and the rate of reaction of Na_2CO_3 with SO_2 to form Na_2SO_3 must be evaluated to establish a chemical rate controlling step.

External diffusion is controlled by aerodynamics, while internal diffusion and chemical reaction are functions of the physical characteristics of the sorbent particle and the affinity of the SO_2 for the sorbent. The adsorption of gaseous SO_2 by the sorbent particle is influenced by the particle surface area available for reaction, by internal pore volume, and by the mean diameter of the pores in the sorbent particle.

An analysis of which chemical reaction controls the rate of reaction is presented below. It has been reported that for particles smaller than 841μm the decomposition of $NaHCO_3$ to Na_2CO_3 is much faster than the reaction between Na_2CO_3 and SO_2 to form Na_2CO_3.[4] Since the oxidation of Na_2SO_3 to Na_2SO_4 occurs rapidly, it has been postulated that the rate of chemical reaction is controlled by the formation of Na_2SO_3. However, another analysis of reaction rates for particles between 250 and 330μm showed that the rate of reaction of Na_2CO_3 to Na_2SO_4 increased up to the point of 25 percent conversion and then decreased.[4] A possible explanation for the initial increase in reaction rate is that the thermal decomposition of $NaHCO_3$ produces a better pore system as time proceeds, providing a large surface for reaction. From these results, then, it appears that decomposition of $NaHCO_3$ to Na_2CO_3 may actually be the rate limiting chemical reaction.

The decline in reaction rate after 25 percent conversion of Na_2CO_3 to Na_2SO_3 is attributed to the buildup of an ash layer, which tends to plug the pores and limit gaseous diffusion to the unreacted Na_2CO_3.[4] When the pores begin to plug up, internal diffusion of SO_2 through the pores begins to limit the rate of reaction.

Several analyses of the bag filter product produced interesting results. Scanning electron micrographs (SEM's) of halved sorbent particles showed that a reacted layer of Na_2SO_4 ash surrounded an unreacted core of Na_2CO_3.[6] Analysis by X-ray flourescence also showed the same result.[6] These physical characteristics warrant the application of the classical unreacted-core model. Applying this model to the test data resulted in the theory that initially the rate of SO_2 removal was controlled by chemical reaction, but that diffusion of gaseous SO_2 through the Na_2SO_4 ash layer soon became the rate controlling step.[6] Bench-scale studies by Stearns Rogers, Inc. for the Superior Oil Company also showed that the diffusion of SO_2 through the surface layer of Na_2SO_4 ash was the rate determining step for particles between 2000 and 11,000μm.[4]

These qualitative descriptions of the dry injection reactions provide the basis for developing mathematical relationships describing SO_2 removal.

3.1.2.2 Quantitative Models. As discussed previously, an analysis of the reacted sorbent particles showed an unreacted Na_2CO_3 core surrounded by a reacted Na_2SO_4 ash layer. These characteristics seem to warrant the application of the unreacted-core model. This model was first developed in 1955 by Yagi and Kunii[11] and appears to be applicable to the dry injection system. Work by two other investigators (Superior Oil[4] and Erdos et al.) has led to the development of two mathematical relationships, both based upon empirical data correlation instead of reaction theory. These empirical models and the unreacted core model are discussed below.

3.1.2.2.1 Unreacted-Core Model. The unreacted core model is based on the theory that five steps occur in succession during the overall reaction. The first three steps are:

1) Diffusion of gaseous SO_2 to the surface of the sorbent particle through the stagnant gas film surrounding the particle

2) Penetration and diffusion of gaseous SO_2 to the surface of the unreacted core through a layer of ash product

3) Chemical reaction of gaseous SO_2 with the sorbent at the reaction surface

The last two steps involve the diffusion of the CO_2 generated during reaction from the sorbent particles through the ash layer and into the flue gas. Each of these steps has a different resistance to reaction, but the step with the highest resistance is considered to be rate controlling. Yagi and Kunii[11] developed mathematical relationships for three cases. In each case one of the three steps described above was assumed to control the rate of reaction. The derivations of these relationships are presented in Appendix B. The final form of these derivations is presented below.

Gas Film Diffusion Controls

The case where diffusion through the gas film controls the reaction rate is represented by the concentration profile presented in Figure 3-2a. This model assumes that the resistance through the ash is small and that the chemical reaction is instantaneous; therefore no gaseous SO_2 is present at the surface of the sorbent particle. An expression describing the conversion of sorbent as a function of time was developed from mass transfer theory,[11] and is presented below.

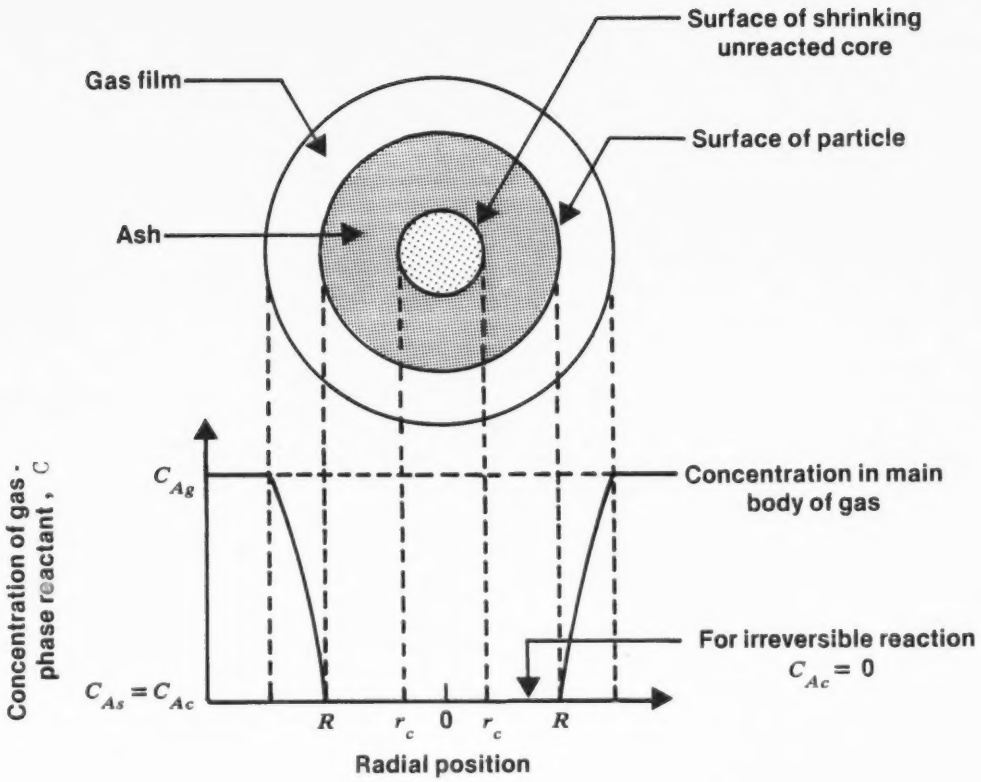

Figure 3-2a. Representation of a reacting particle when gas-film diffusion is the rate controlling step.[11] (Where A represents SO_2 and the subscripts g, s, and c represent the gas, particle surface, and particle core, respectively.)

$$\frac{t}{\tau} = 1 - \left(\frac{r}{R}\right)^3 = X \qquad (3\text{-}7)$$

and

$$\tau = \frac{R\ \rho}{3\ k_g C_{SO_2\text{-}g}\ (MW)}$$

where:

t = Time, sec

τ = The time needed for complete conversion of the sorbent, sec

r = Radius of the unreacted core, ft

R = Initial particle radius, ft

X = Fractional conversion of the sorbent, $\frac{\text{mole } Na_2SO_3 \text{ final}}{\text{mole } Na_2CO_3 \text{ initial}}$

ρ = Density of the sorbent, lb/ft^3

k_g = Mass transfer coefficient for SO_2 to the particle, ft/sec

$C_{SO_2\text{-}g}$ = Concentration of SO_2 in the gas phase, $lb\text{-}mole/ft^3$

MW = Molecular weight of sorbent lb/lb-mole

Equation 3-7 can be rewritten to express SO_2 removal efficiency directly:

$$E = \left(\frac{t}{\tau}\right)SR \qquad (3\text{-}8)$$

Ash Layer Diffusion Controls

Figure 3-2b presents a concentration profile for the case where diffusion of SO_2 through the layer of Na_2SO_4 ash controls the rate of reaction. The SO_2 reacts immediately upon reaching the unreacted core; therefore, there is no SO_2 present at the surface of the core. The derivation of a mathematical expression for this case requires a two-step analysis and is detailed in Appendix B. The expression that was developed is presented in Equations 3-9 and 3-10.

$$\frac{t}{\tau} = 1 - 3\left(\frac{r}{R}\right)^2 + 2\left(\frac{r}{R}\right)^3 \qquad (3\text{-}9)$$

By using Equation B-11 in Appendix B, Equation 3-9 can be reduced to the following relationship:

$$\frac{t}{\tau} = 1\text{-}3(1 - X)^{2/3} + 2(1 - X) \qquad (3\text{-}10)$$

where:

$$= \frac{R^2\ \rho}{6\ D_v\ C_{SO_2\text{-}g}\ (MW)}$$

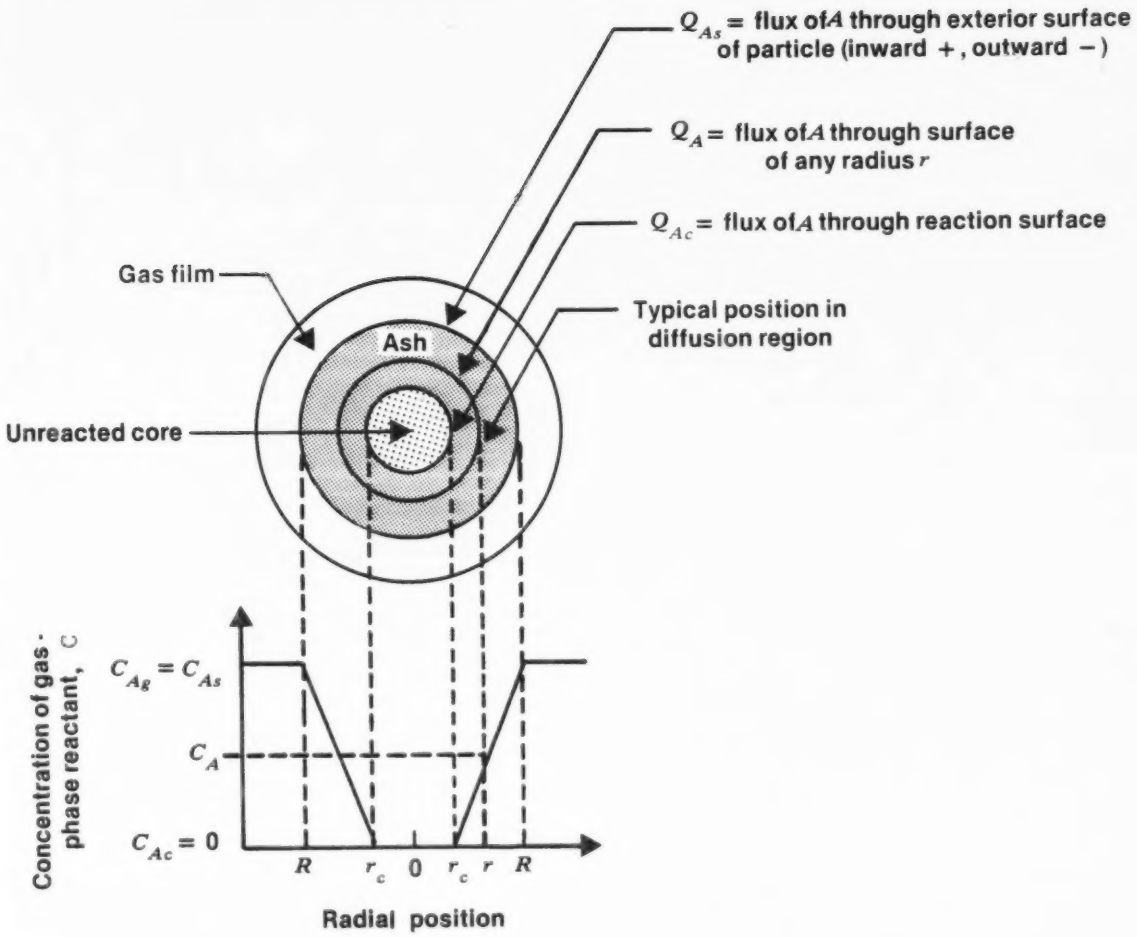

Figure 3-2b. Representation of a reacting particle when ash diffusion is the rate controlling step.[11] See notation key on Figure 3-2a.

All the variables have the same meaning as those used to describe Equation 3-7 and the value D_v is equal to the mass diffusivity of SO_2 to the sorbent in ft^2/sec. Due to the form of Equation 3-10 it cannot be solved to express SO_2 removal efficiency directly. However, the SO_2 removal efficiency can be introduced into Equation 3-10 because SO_2 removal efficiency (E) is equal to the sorbent conversion (X) times the stoichiometric ratio (SR). Therefore, sorbent conversion (X) can be expressed as

$$X = \frac{E}{SR} \qquad (3\text{-}11)$$

Chemical Reaction Controls

Finally, an expression was developed to describe the case where chemical reaction controls the rate of reaction.[11] A concentration profile for this case is presented in Figure 3-2c. Since the progress of the reaction is unaffected by the presence of the ash layer, the quantity of material reacting is proportional to the available surface of the unreacted core.[11] The mathematical relationship that was developed is given in Equation 3-12.

$$\frac{t}{\tau} = 1 - \frac{r}{R} = 1 - (1 - X)^{1/3} \qquad (3\text{-}12)$$

where:

$$\tau = \frac{R\rho}{k_s C_{SO_2\text{-}g}\ (MW)}$$

The value k_s is the first order rate constant for the surface reaction (units of ft/sec), and all other variables are the same as those that have been defined previously under Equation 3-7. Equation 3-12 can be rearranged to express SO_2 removal efficiency directly:

$$E = 1 - \left[1 - \left(\frac{t}{\tau}\right)^3\right] SR \qquad (3\text{-}13)$$

The mathematical models which have been derived in this section can be used in conjunction with experimental data to determine which model best describes the actual performance of a dry injection system. The kinetics and rate controlling steps of the gas-solid reaction are deduced by noting how the progressive reaction of sorbent particles is influenced by particle size and operating temperature. The following observations are a guide to experimentation and to the interpretation of experimental data.

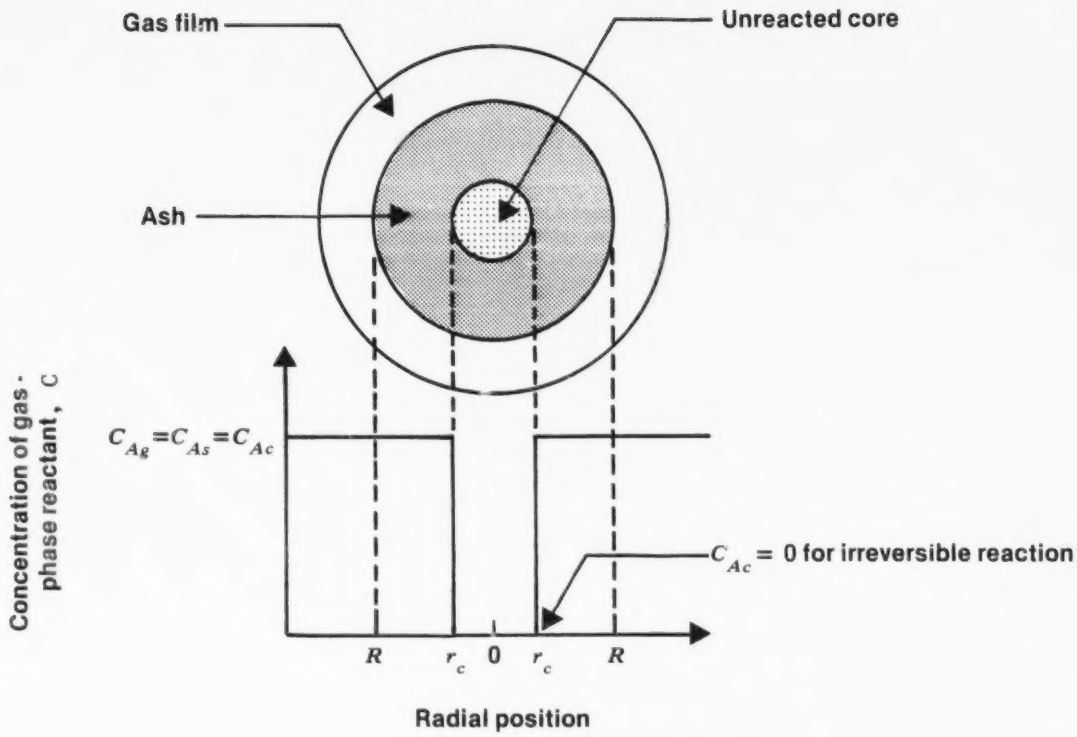

Figure 3-2c. Representation of a reacting particle when chemical reaction is the rate controlling step.[11] See notation key in Figure 3-2a.

Temperature usually affects chemical reaction much more than external and internal diffusion. Therefore, experiments at different temperatures should easily distinguish between ash and film diffusion on one hand and chemical reaction on the other hand as the rate controlling step.

Sorbent particles of different sizes can also help to reveal the rate controlling step. The time needed for reaction can be related to the size of the particle by using Equations 3-7, 3-9 and 3-12. The time required for a sorbent particle to achieve a given level of fractional conversion can be related to particle size by the following relationships.

$t \propto R^{1.5 \text{ to } 2.0}$ for gas film diffusion controlling (the exponent drops as the gas velocity rises) (3-14)

$t \propto R^2$ for ash diffusion controlling (3-15)

$t \propto R$ for chemical reaction controlling (3-16)

Thus, kinetic test runs with different sizes of particles can be used to distinguish between reactions in which the chemical and physical steps control.

A plot of time versus sorbent conversion can also help to establish a rate controlling step. Figure 3-3 shows plots of Equations 3-7, 3-10, and 3-12 for the cases where gas diffusion, ash diffusion and chemical reaction control the reaction rate, respectively. A comparison of kinetic runs with these predicted curves should indicate which step is rate-controlling. Unfortunately, the difference between ash diffusion and chemical reaction as the controlling step is not easily distinguished and may not be detectable because of scatter in experimental data.

Typically, if a hard solid ash forms during reaction, the resistance to gaseous SO_2 diffusion through the ash is usually much greater than the resistance through the gas film that surrounds the sorbent particle. Also, ash layer resistance is unaffected by changes in the velocity of the gas. This fact can be used to distinguish whether diffusion through the ash layer or through the gas film is rate controlling.

If the unreacted-core model adequately describes the reaction kinetics in dry injection systems, then trends in kinetic data, as described above, should allow a rate controlling step to be established. However, experimental results to date have shown a great deal of inconsistency. Experiments have been carried out with varying particle sizes, temperatures,

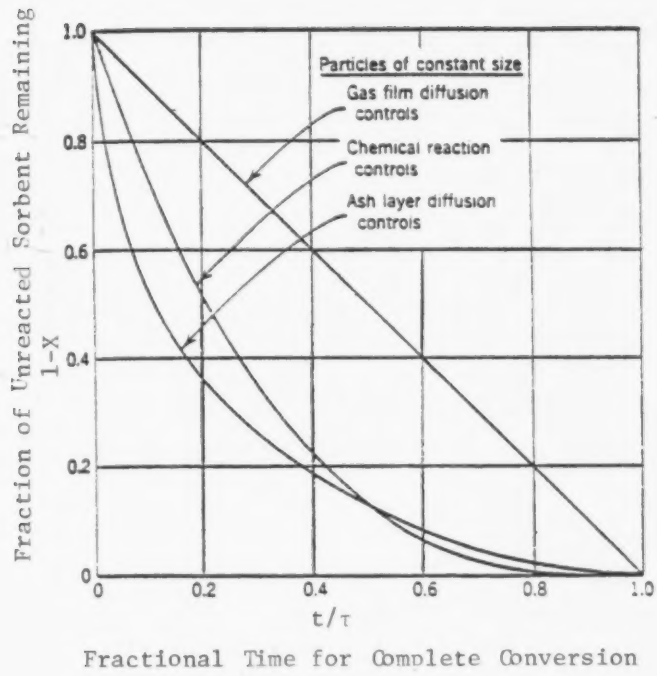

Figure 3-3. Progress of reaction of a single spherical particle with surrounding gas measured in terms of time for complete conversion.[11]

and operating conditions, which make it difficult to directly compare data and to determine a rate controlling step. However, the experimental data do reveal some valuable information.

The Superior Oil Company attempted to evaluate the diffusivity of SO_2 through the ash layer and the gas film surrounding the sorbent particles. From diffusivity relationships, it was estimated that the diffusivity of the gaseous SO_2 through the ash layer ranged from 0.001 to 0.007 cm^2/sec for 2000μm particles at 300°F, while the diffusivity of SO_2 through air at 300°F is approximately 0.27 cm^2/sec.[6] Therefore, the resistance of gas film diffusion is negligible compared with the resistance of the ash layer. Also, it was observed that the velocity of the flue gas has a negligible effect upon SO_2 removal. These facts seem to eliminate gas film diffusion as the rate controlling step.

3.1.2.2.2 Empirical Models. Experimental studies by both Superior Oil Company and Erdos et al.[4] have resulted in mathematical expressions that relate the rate of reaction to the fractional conversion of the sorbent. The relationships developed by these two sources were based on the correlation of experimental data. These two models however, are quite different.

Superior Oil Company performed experiments using a thin bed reactor with nahcolite particles between 2000 and 11,000μm in diameter, the nahcolite having been predecomposed at approximately 300°F. These experiments created an ash layer of Na_2SO_4 that was 100 to 200μm thick. The relationship developed from these experiments to express the rate of reaction is given in Equation 3-17.

$$r = \frac{k\ (1 - X)^{1/3}}{1 - (1 - X)^{1/3}} \qquad (3\text{-}17)$$

where:

r = Reaction rate, cm^3/sec

k = Rate constant, cm^3/sec

X = Fractional sorbent conversion, $\frac{\text{mole } Na_2SO_3 \text{ final}}{\text{mole } Na_2CO_3 \text{ initial}}$

The rate constant, k, for this expression was determined to be 1×10^{-3} to 14×10^{-3} cm^3/sec by employing the unreacted-core model for diffusion of SO_2 through the ash layer. The variability in the rate constant was caused by changes in the diffusivity of SO_2 through the ash layer as the experimental conditions were varied. The diffusivity was found to increase with increasing temperature and particle size.[2] The diffusivity was also found to decrease with increasing inlet SO_2 concentration. An increase in the inlet SO_2 content of the flue gas will cause a thicker ash

layer to be produced, which may cause the diffusivity of SO_2 through the ash to be reduced.

Erdos et al.[4] also performed thin bed reactor experiments with nahcolite. Sorbent particles with diameters of 250 to 330μm that had been predecomposed at 482°F were used. The thin bed reactor was operated at 302°F during the experiments. Correlation of the experimental data led to the development of the following expression, which describes the rate of reaction as a function of the sorbent conversion.

$$r = k\, P_{SO_2}\, X^{1/2}(1 - X)^{3/2} \qquad (3\text{-}18)$$

where:

r = Overall rate of reaction, cm^3/sec

k = Rate constant, $cm^3/(atm\text{-}sec)$

P_{SO_2} = Partial pressure of SO_2 in flue gas, atmosphere

X = Fractional solids conversion, $\frac{\text{mole } Na_2SO_3 \text{ final}}{\text{mole } Na_2CO_3 \text{ initial}}$

The results of the work by Superior Oil Company and Erdos et al. are difficult to compare because of differences in their experimental set-up. Although both used a thin bed reactor in the experiments, the size of the sorbent particles and the decomposition temperature of the sorbent were different. The greatest difference was in the sorbent particle size; Superior Oil Company used particles that were 10 to 50 times larger than the particles used by Erdos. Although there were experimental differences, some comparisons between the two models can be made.

Plots of the equations developed by Superior Oil Company and Erdos et al. are presented in Figures 3-4a and 3-4b. The data from Superior Oil Company were extrapolated to small particle sizes for these plots. These figures show that the two expressions are quite different up to approximately 25 percent sorbent conversion (see Figure 3-4a). The Superior Oil Company relationship predicts an infinite initial reaction rate which declines rapidly as reaction proceeds. This equation also predicts that significant reaction will occur in the first few seconds of SO_2-sorbent particle contact in the duct (see Figure 3-4b). On the other hand, Erdos et al. predict that the initial reaction rate is low and that no significant reaction will occur in the ductwork. These differences may be due to the large difference in sorbent particle size used by Erdos et al. and the Superior Oil Company.

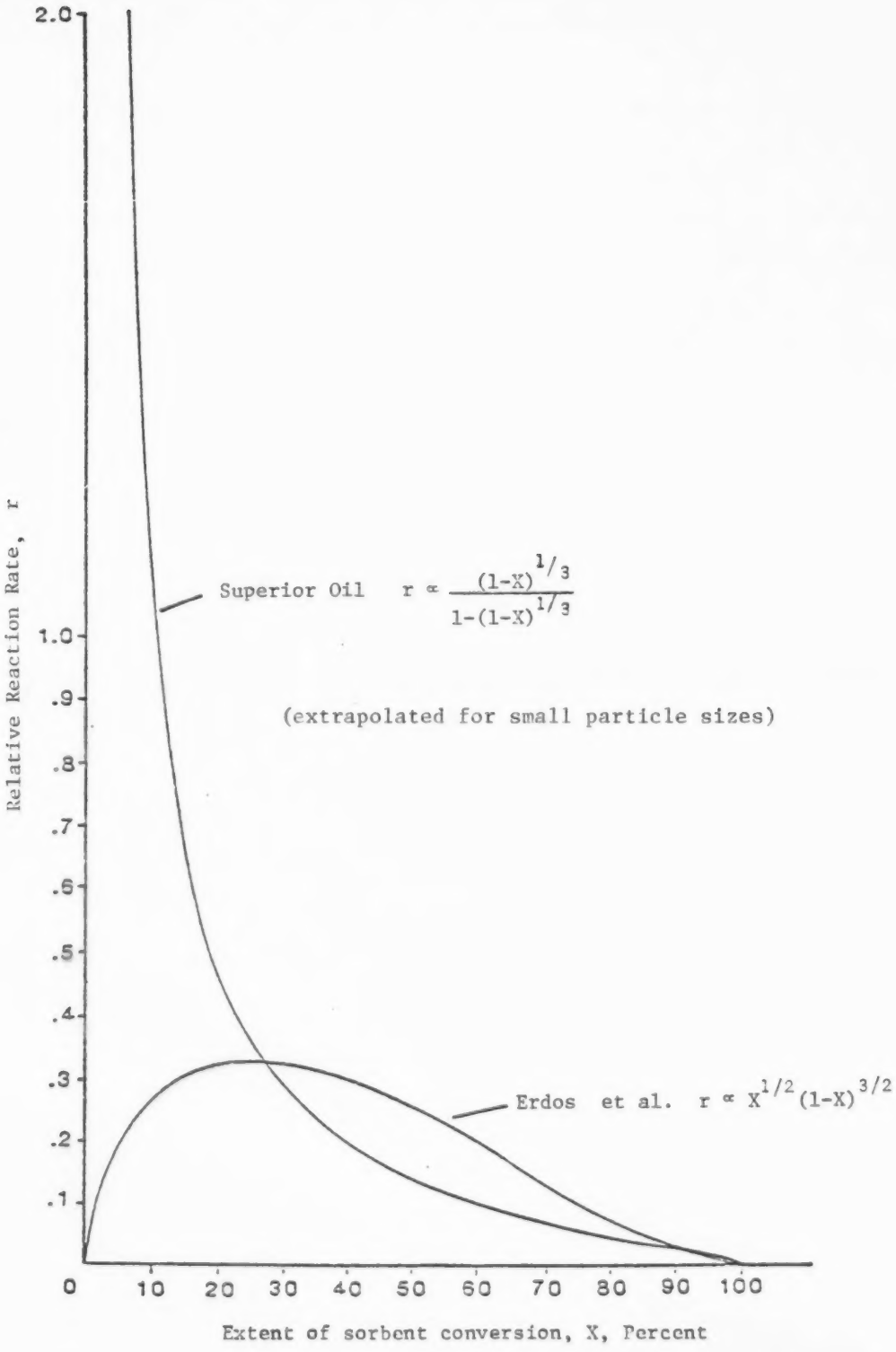

Figure 3-4a. Reaction rate as a function of extent of sorbent conversion.[4]

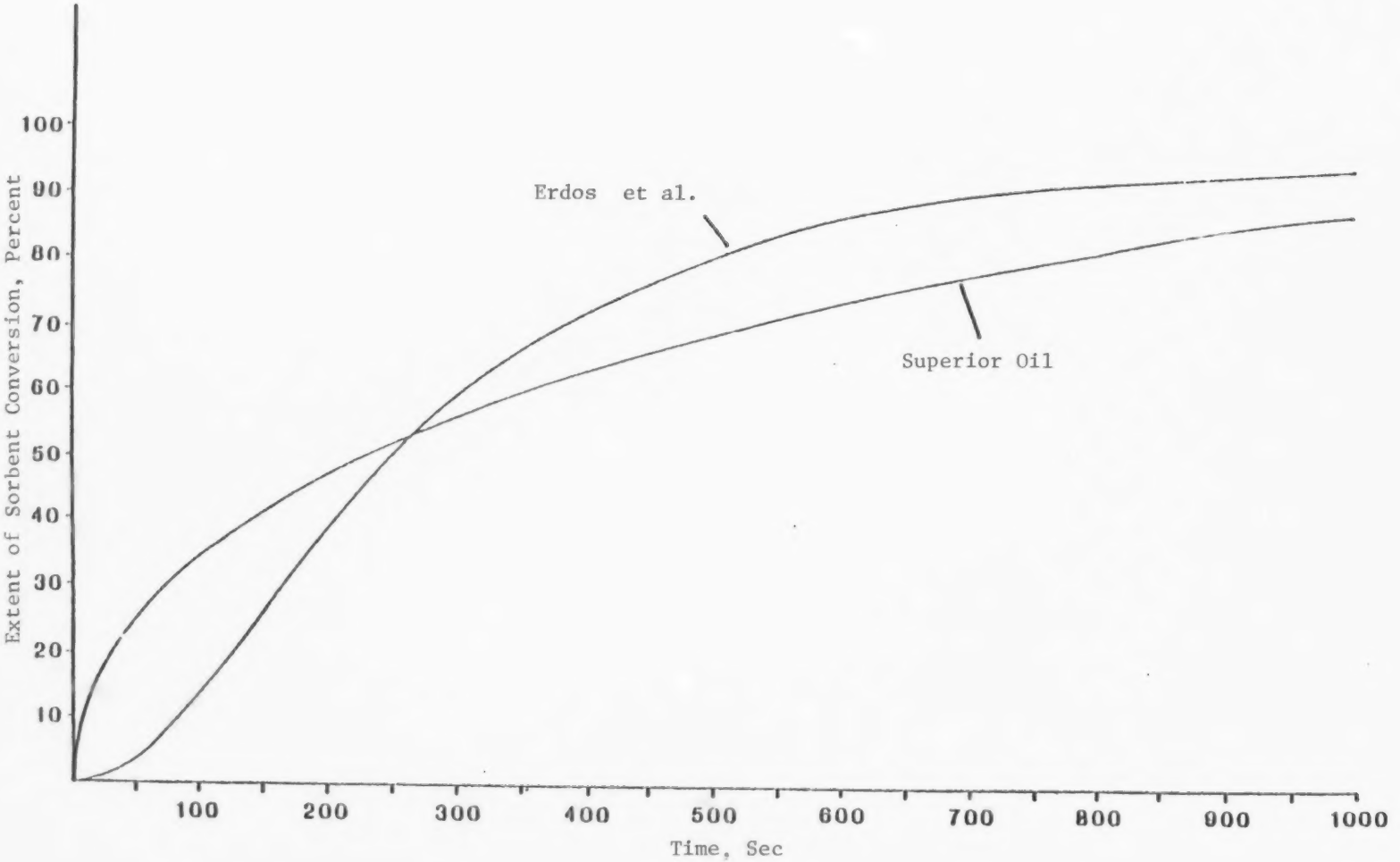

Figure 3-4b. Extent of solid conversion with time for reaction of SO_2 with sodium bicarbonate.[4]

Experiments have been performed to characterize SO_2 removal in the ductwork.[4,5,7,12] The results of these experiments, which are presented in Sections 3.2.6 and 3.2.7, show that over 50 percent of the total removal can occur in the first two seconds and that the extent of SO_2 removal is extremely temperature dependent. This contradicts the relationship developed by Erdos et al. and supports Superior Oil's relationship. However, neither the relationship developed by Erdos et al. nor Superior Oil account for the effect of temperature and particle size on SO_2 removal. Both relationships are empirical and are generally only applicable to the test conditions under which they were developed.

3.2 PROCESS PARAMETERS AFFECTING THE DRY INJECTION PROCESS

There are many process parameters which affect SO_2 removal efficiency in the dry injection processes. In general, the parameters that have the greatest effect on SO_2 removal in dry injection are those that affect the rates of mass transfer and chemical reaction. As discussed in Sections 3.1.2.1 and 3.1.2.2, the rate of reaction may be controlled by the diffusion of SO_2 through the gas film surrounding the sorbent particle, diffusion through the inert ash layer on the particle surface, or chemical reaction. Parameters that influence these three reaction steps are characterized below.

1) Variables affecting SO_2 mass transfer to the sorbent particles
   - Particle size
   - Residence time of the reactants in the duct
   - Inlet SO_2 concentration
   - Gas velocity and air-to-cloth ratio
   - Mode of sorbent injection
   - Gas temperature

2) Variables affecting SO_2 mass transfer through the inert ash layer
   - Sorbent preparation
   - Particle size
   - Residence time
   - Filter cleaning intervals
   - Stoichiometric ratio

3) Variables affecting chemical reaction
   - Sorbent type
   - Sorbent preparation
   - Temperature
   - Stoichiometric ratio

These parameters and their effects are discussed in the following sections. Test results that indicate the effect these parameters have on SO_2 removal efficiency will also be discussed. These test results are often quite conflicting, making it difficult to draw general conclusions about the dry injection process. Tables 3-1a and 3-1b provide a list of completed laboratory-scale and pilot plant dry injection studies. These tables present the process parameters and test conditions which were examined by the various investigators. This information can be used as a guide to interpreting the results presented in the following sections.

3.2.1 Sorbent Type

The type of sorbent used for dry injection will directly affect the chemical reactions that occur. Tests with a wide variety of sorbents have shown that only sodium compounds produce significant SO_2 removal at typical air preheater outlet temperatures (approximately 300°F). Lime and limestone have been demonstrated to achieve SO_2 removal only at much higher gas temperatures (600°F+)[1]. Sorbents that have been shown to have good potential for SO_2 removal are sodium bicarbonate, nahcolite ore, and trona ore. Nahcolite ore is a naturally occurring mineral which typically contains 70 to 90 percent sodium bicarbonate. Trona ore is also a naturally occurring mineral which contains approximately 40 to 50 percent sodium carbonate (Na_2CO_3), and 20 to 30 percent sodium bicarbonate ($NaHCO_3$).

Experimental results from tests using sodium carbonates and sodium bicarbonates indicate that the bicarbonate form is much more reactive than the carbonate form. The increased reactivity of $NaHCO_3$ is thought to result from the pores that develop when $NaHCO_3$ particles are thermally decomposed to Na_2CO_3. In general, the sorbent with the highest percentage of "bicarbonate parts" for "total sodium parts" present would be expected to perform the best.[2]

Buell performed a series of tests comparing SO_2 removal efficiency with the type of sorbent used.[2] Three sorbents were evaluated: nahcolite, trona, and refined trona ores. The nahcolite ore was obtained from Horse Draw, Colorado; the trona ore was obtained from Owens Lake, California; and the refined trona ore was Owens Lake ore that was upgraded by a carbonation and crystallization process. The chemical compositions of these sorbents are shown in Table 3-2. The experimental results, which are presented in Figures 3-5a through 3-5c, show that nahcolite provides much better SO_2 removal than trona, and that refined trona out performs raw trona. The dependence of SO_2 removal on the sodium bicarbonate content is evident from these results.

Tests performed by several other sources (American Air Filter,[4] Electric Power Research Institute,[10] DOE/Pittsburgh,[1] Stern[9], and Shah and Teixeira[12]) also indicate that nahcolite is much more reactive than trona. Therefore, much higher stoichiometries of trona are required to

TABLE 3-1a. LABORATORY STUDIES OF FGD BY INJECTION OF DRY ADSORBENT[2]

Adsorbent	Mean Particle Size (micron)	Temperature °F	Flow Rate acfm	Air-To-Cloth Ratio ft/min	Inlet SO_2 Concentration ppm	Stoichiometric Ratio	Injection Mode		Reference[a]
							Continuous	Batch	
Nahcolite	--	200 - 250	0.7 - 1.6	3.9	1000	1 - 4	X	X	R.T. Pring (59)
Nahcolite	--	200 - 250	---	2 - 3	---	1 - 4	X	X	D.J. Doyle (17)
Nahcolite	45 - 75	300	---	---	2500 - 3000	---		X	J.M. Genco (27)
	500 - 666	300	---	---	34,000	---		X	
Nahcolite, Sodium Bicarbonate	2000 - 11,000	300	---	Plug Flow Reactor	450 - 10,000	---		X	Superior Oil (70)
Activated nahcolite, trona	90 - 500	300 - 750	10.5	Plug Flow Reactor	500 - 2500	---		X	F.R. Stern (66)
Nahcolite, Sodium Bicarbonate, Trona, Sodium Carbonate	19 - 250	230 - 800	360 - 1440	1 - 4	350 - 750	0 - 4	X	X	Muzio et al (54)
Nahcolite, Trona	37.5 - 75	600 - 2000	---	---	925	0.8 - 2.6	X		Ness and Selle (55)

[a]Numbers refer to reference # in Bibliography (Section 4).

TABLE 3-1b. STUDIES OF FGD BY INJECTION OF DRY ADSORBENT ON PILOT PLANT EQUIPMENT[2]

Adsorbent	Site	Mean Particle Size (micron)	Temperature °F	Flow Rate (10^3 acfm)	Air-To-Cloth Ratio ft/min	Inlet SO_2 Concentration ppm	Stoichiometric Ratio	Injection Mode		Reference[a]
								Continuous	Batch	
Nahcolite	Public Ser. of N.J., Mercer Sta.	37.5	300 - 600	7.5 - 15	3	---	0.7 - 1.8	X	X	Liu et al. (44)
Nahcolite	Owens-Corning	---	300	0.3 - 0.4	6 - 8	---	0.7 - 0.8	X		Veazie et al. (71)
Nahcolite	So. Calif. Edison Los Alamitos Pl.	---	240	0.7 - 1.5	3 - 6.5	---	0.5 - 1	X		Bagwell et al. (1)
Nahcolite	Colorado Ute Nucla Sta.	---	---	---	---	---	---			Wheelabrator-Frye (72)
Nahcolite	Basin Electric Coop	1 - 10	500 - 2500	---	3	800 - 3000	0 - 2	X		Superior Oil (70)

[a]Numbers refer to reference # in Bibliography (Section 4).

TABLE 3-2. CHEMICAL COMPOSITION OF SODIUM COMPOUNDS USED IN DRY INJECTION[2]

	Nahcolite		Refined Trona	Trona
Test Run	N-5A	N-5B	B-1	T-1
Constituent				
$NaHCO_3$	52.76	54.01	59.32	26.43
Na_2CO_3	3.64	3.13	14.22	41.39
NaCl	0.49	0.46	1.27	4.14
Na_2SO_4	0.40	0.32	1.19	5.19
Na_2SO_3	0.001	0.002	< 0.001	< 0.001
$NaNO_3$	0.02	0.03	< 0.01	< 0.01
Insolubles	40.86	40.01	15.34	9.72
Water	1.83	2.04	8.65	13.12

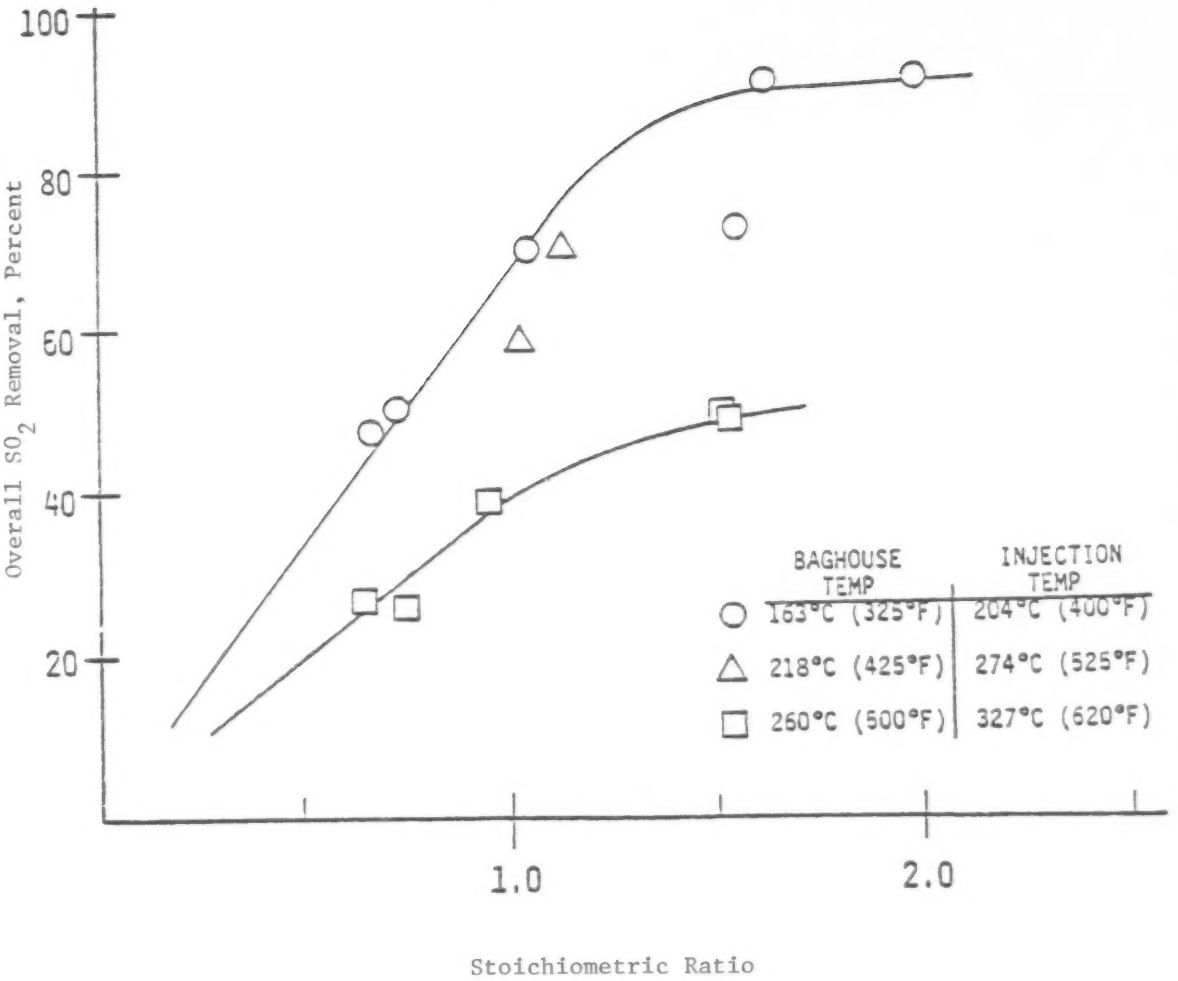

Figure 3-5a. SO_2 removal with dry injection of nahcolite into duct of pilot system.[2]

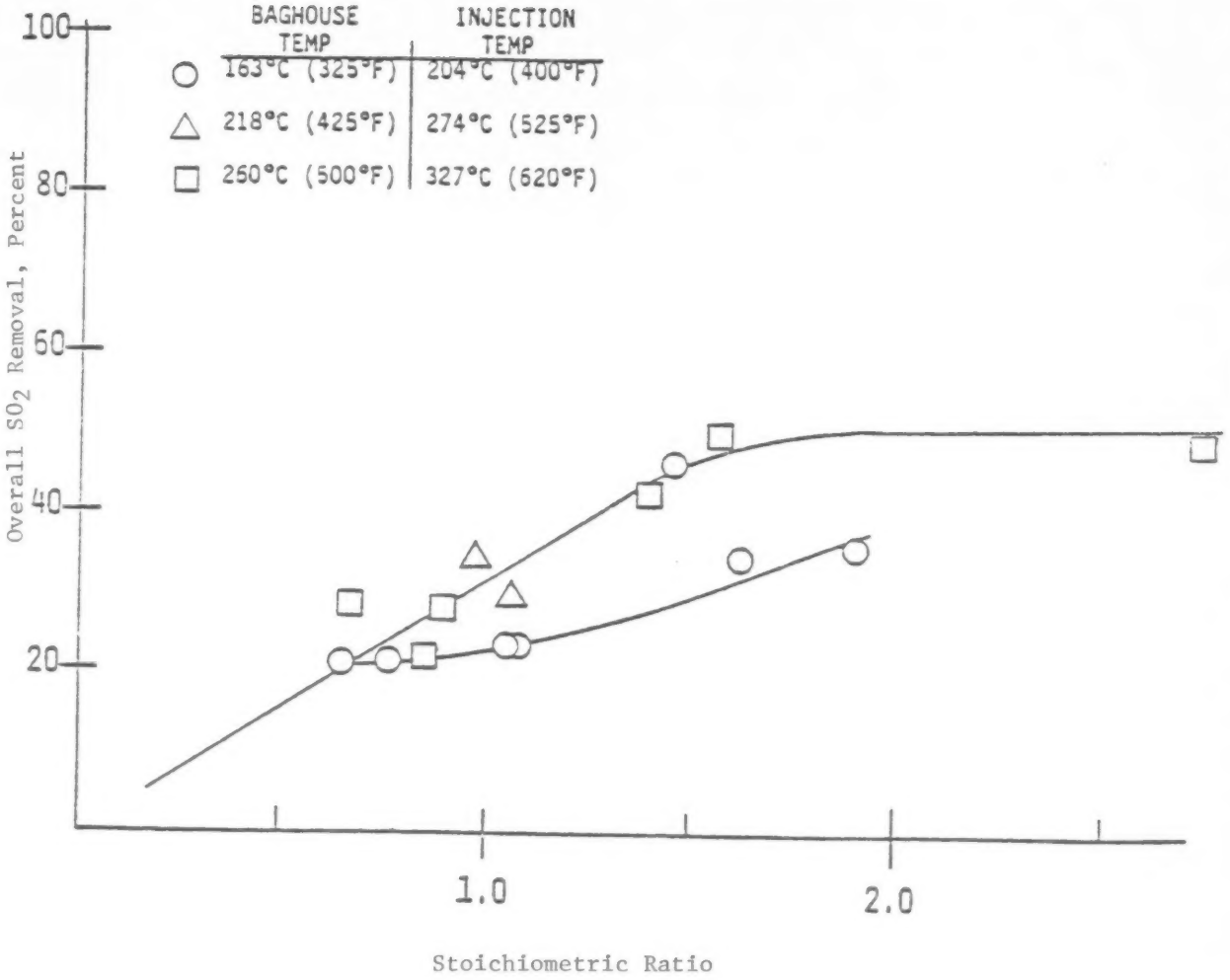

Figure 3-5b. SO_2 removal with dry injection of trona into the duct of the pilot system.[2]

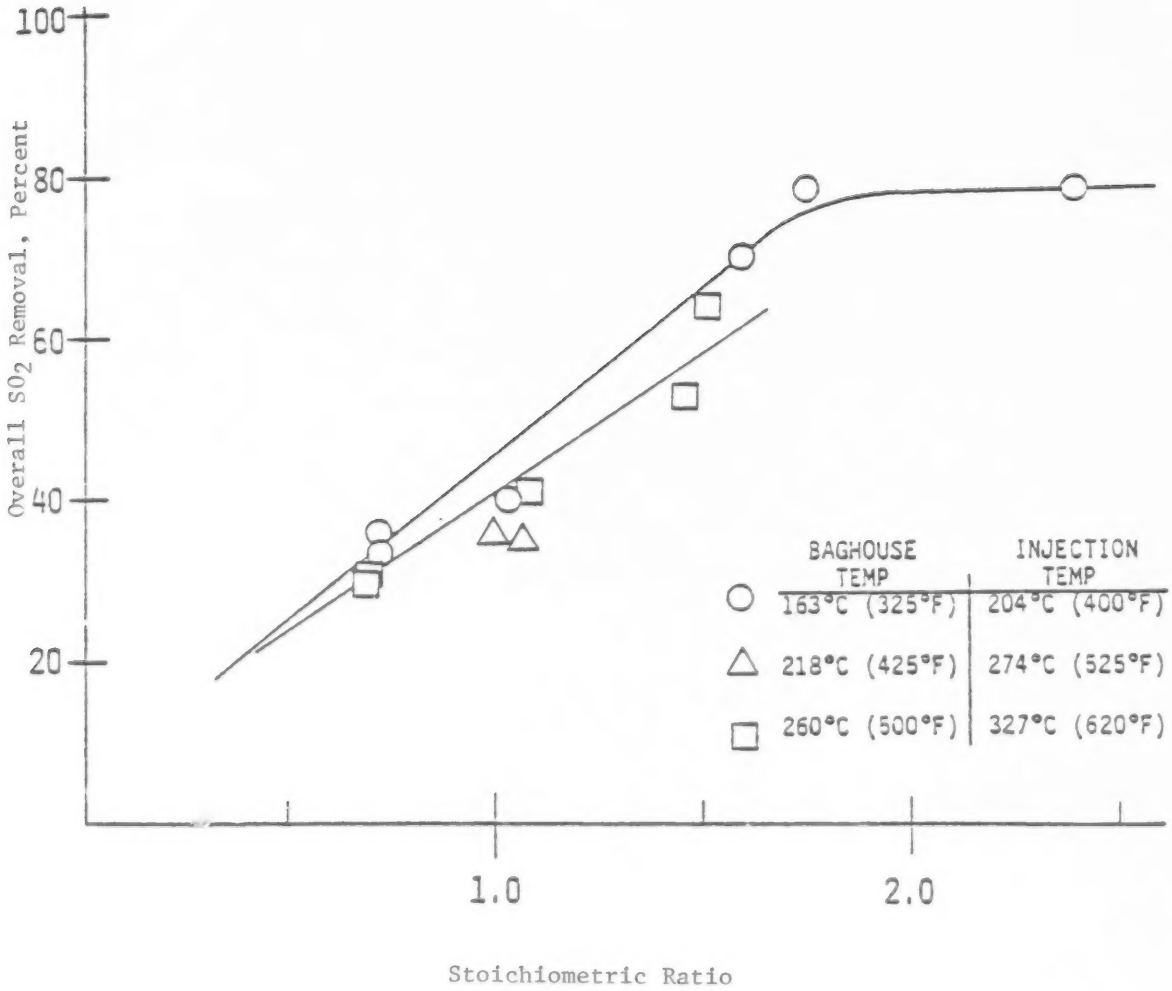

Figure 3-5c. SO_2 removal with dry injection of refined trona into duct of pilot system.[2]

achieve the same SO_2 removal obtained with nahcolite and there is a reported upper limit of 50 percent SO_2 removal at stoichiometries greater than 2.0 (see Figure 3-5b). Experiments with trona produced several interesting results. Tests performed by DOE's Pittsburgh Energy Technology Center showed that two batches of trona of identical composition, tested under identical conditions, resulted in different SO_2 removal.[7] The reason for this inconsistency may be due to differences in the ages and storage methods of the batches. Also, tests conducted for EPRI by KVB Inc., indicated that trona reacts rapidly with SO_2 upon injection and that SO_2 removal was essentially independent of the fabric filter cleaning cycle time.[7] In comparison, KVB found that about 40 minutes were required to achieve maximum steady state SO_2 removal with nahcolite.

The SO_2 removal performance of nahcolite has also been compared to that of pure sodium bicarbonate. The results from these experiments are often conflicting. Tests by Superior in a counter-current reactor showed 84 percent SO_2 removal with commercial sodium bicarbonate and 67 percent with nahcolite. However, these results are not directly comparable because there were differences in the test conditions, as shown in Table 3-3. Tests performed by Air Preheater at the Mercer Generating Station showed that better SO_2 removal was obtained with nahcolite than with $NaHCO_3$ (see Table 3-3). However, these results are not directly comparable because the $NaHCO_3$ and nahcolite particles used were not the same size. Also, since nahcolite is composed of approximately 70 percent $NaHCO_3$, it has to be injected at a higher mass rate than pure $NaHCO_3$ to attain the same stoichiometric ratio. This extra mass loading may enhance SO_2 removal with nahcolite. In addition, the entire surface of a pure sodium bicarbonate particle is reactive, and the entire particle surface can react, blocking the pores and inhibiting SO_2 diffusion. Since nahcolite contains impurities which will not react with the SO_2, this tends to keep the pores in the particles more open to SO_2 diffusion. The Electric Power Research Institute (EPRI) also performed tests comparing SO_2 removal with nahcolite and sodium bicarbonate. Under identical test conditions the nahcolite achieved 80 percent removal, while the $NaHCO_3$ achieved 68 percent removal. These results are also presented in Table 3-3.

3.2.2 Sorbent Preparation

Treatment of the sorbent prior to injection influences both the chemical composition and porosity of the sorbent. Any changes in porosity will influence the ability of SO_2 to diffuse through the ash layer that surrounds the sorbent particles, and changes in chemical composition will affect the rate of chemical reaction. Sorbent preparation generally involves grinding the particles to increase the surface area available for reaction and heating to thermally decompose the $NaHCO_3$ to Na_2CO_3, causing an increase in the pore volume of the particles. The effects of thermal decomposition will be discussed in this section; particle size effects are discussed in the following section.

TABLE 3-3. SO_2 REMOVAL WITH $NaHCO_3$ AND NAHCOLITE

Test Location	Sorbent	Particle Size, μm	Stoichiometric Ratio Mole Na_2O/Mole SO_2	Flue Gas Temperature °F	SO_2 Removal Efficiency, %
Superior Counter Current Reactor[a]	$NaHCO_3$	4300	0.86	300	84
	Nahcolite	3700	0.89	270	67
Mercer Generator Station[b]	$NaHCO_3$	60	1.0	600	90
	$NaHCO_3$	60	1.0	350	48
	Nahcolite	10	1.0	600	94
	Nahcolite	10	1.0	350	65
Electric Power Research Institute (EPRI)[c]	$NaHCO_3$	74	1.0	270	68
	Nahcolite	74	1.0	270	80

[a] This test was performed by batch injection into a plug flow reactor.

[b] This test was performed by continuous injection into the ductwork leading to a top-entry baghouse.

[c] This test was performed by continuous injection into the ductwork leading to a bottom-entry baghouse.

The thermal decomposition of $NaHCO_3$ to Na_2CO_3 increases the porosity of the sorbent, which increases the surface area available for contact with SO_2. Howatson[5] investigated the pore development of nahcolite at 300°F with a scanning electron microscope (SEM) and found scattered development of 0.1 to 0.7μm pores after 10 minutes. After 20 minutes the surface was completely covered with pores averaging about 0.3μm. The Na_2CO_3 particles produced in this manner have a much larger void space than the parent $NaHCO_3$ particle.[6] These pores provide a greater surface area for chemical reaction and a greater volume for SO_2 diffusion. The reactivity of the sorbent particles has been found to increase by up to a factor of 60 because of thermal decomposition.[7]

Investigations have been conducted[3,13] to determine if decomposition of the sorbent prior to injection enhances SO_2 removal and to determine the optimum decomposition temperature. These experiments have often produced conflicting results. However, a majority of the tests shows that predecomposition of the sorbent at high temperatures reduces SO_2 removal efficiency. Carson[13] reported that predecomposition of $NaHCO_3$ to Na_2CO_3 significantly reduced the desulfurization capacity of the sorbent; however, the decomposition temperature was not specified.[3] A bench-scale study by Genco and Rosenberg[3] with a fluidized bed reactor also showed a reduction in SO_2 removal with nahcolite that had been predecomposed at 600°F.

The rate of decomposition and the surface area generated during decomposition are influenced by the sorbent injection temperature, i.e. the temperature of the flue gas at the point of sorbent injection. Stern[9] found that the maximum specific surface area for particles between 90 and 500μm is generated by decomposing nahcolite at 600°F in a forced draft oven.[8] However, a study by the Superior Oil Company[8] with 74μm sorbent particles showed that decomposition of nahcolite and $NaHCO_3$ at 300°F produced material with higher reactivity than did sorbent that was untreated or treated at higher temperatures. These differences may be due to the different sizes of the sorbent particles used or differences in the method of decomposition, or may be due to differences in the $NaHCO_3$ content of the nahcolite samples used.

3.2.3 Particle Size

The size of the sorbent particles affects the mass transfer of SO_2 through the gas film that surrounds the particle, because it determines the surface area through which the SO_2 must diffuse. Particle size also influences diffusion through the inert ash layer because the rate of decomposition of $NaHCO_3$ to Na_2CO_3 is somewhat dependent upon particle size, and the decomposition rate influences the porosity of the sorbent particle. Results characterizing the role of particle size in SO_2 removal efficiency are often conflicting. However, the general concensus is that better removal is obtained with smaller particles.

Work by Carson[13] showed an inverse relationship between particle size and SO_2 removal. As can be seen from Figure 3-6, SO_2 removal increased as the particle size was reduced from 193μm to 32μm.[8] Stern[9] also conducted tests with nahcolite particles with diameters of 90, 190, and 500μm, which had been predecomposed in a forced draft oven at 600°F. It was found that the maximum utilization of sorbent for SO_2 removal occurred with the smaller particles. Trona was also used in experiments by Ness and Selle at the Grand Forks Energy Technology Center (GFETC). Results with 74 and 149μm trona particles showed that the 74μm trona exhibited an increased capacity for SO_2 removal over that of the 149μm trona[6]. The increased SO_2 removal with smaller particles is probably due to the increased surface area and faster decomposition rate obtained with smaller particles. Fixed-bed experiments with sodium bicarbonate performed by the Superior Oil Company indicated that 85 percent of the $NaHCO_3$ particles between 37 and 74μm were converted to Na_2CO_3 in approximately 20 minutes[10]. In contrast, approximately 70 minutes were required for $NaHCO_3$ particles between 4760 and 5660μm to reach the same degree of conversion.

Several reports, however, have indicated that particle size has little or no effect on SO_2 removal for certain size ranges. Ness and Selle[6] from GFETC found that decreasing the particle size below 149μm did not affect the amount of SO_2 removed by nahcolite. Shah and Teixeira[12] tested two sizes of sodium bicarbonate, 37 and 74μm, at a pilot scale dry injection system and found that the smaller particles did not provide greater overall SO_2 removal. However, the smaller particles exhibited increased removal in the ductwork prior to entering the baghouse.

Tests by Genco and Rosenberg[3] conflict with all other test results. They found greater conversion to sulfate with 420 to 595μm nahcolite particles than with 44 to 74μm particles.[4] Using a fluidized bed reactor and 300°F flue gas they found 85 percent utilization of the small particles after 6.6 hours, and 99 percent utilization of the large particles after only 4.5 hours. They attempted to explain these results by pointing out that the raw nahcolite exhibited self-classification during grinding. That is, the smaller particles contained 84.7 percent $NaHCO_3$ compared with 77.7 percent $NaHCO_3$ in the larger particles. Since the unreacted portion of the smaller particles will have a higher concentration of Na_2CO_3 per unit volume than the large particles, the increased $NaHCO_3$ content in the small particles causes utilization to look worse.[4] However, this difference in $NaHCO_3$ content does not account for a 14 percent variation in utilization. However, the poorer utilization obtained with the smaller particles may be due to their higher $NaHCO_3$ content. Since the small particles do not contain as many unreactive impurities as the large particles, the surface of the small particles will tend to be more highly reacted, blocking the pores and restricting SO_2 diffusion. Since the nahcolite particles were reacted for such a long time (up to 6.6 hours), these surface effects become noticeable.

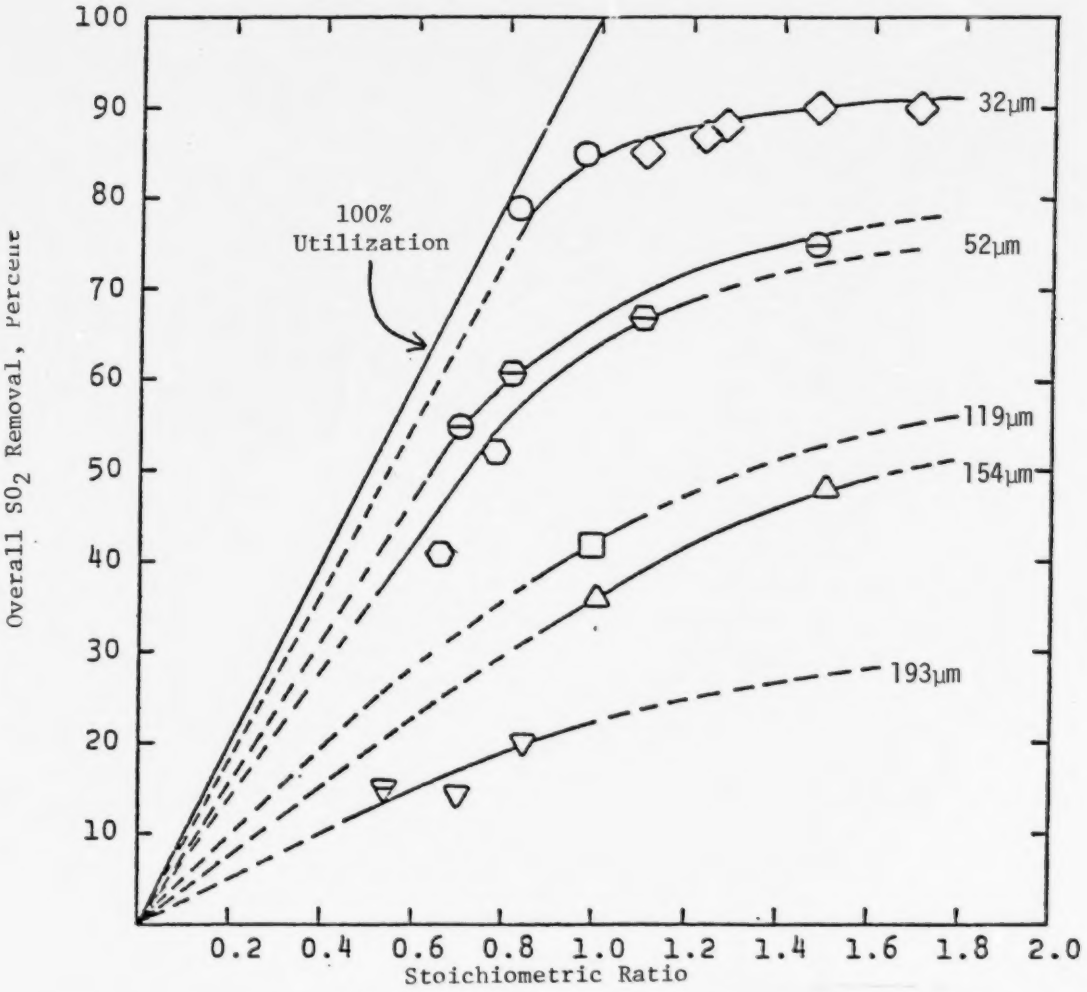

Mass Mean Diameter (μm)		Baghouse Temperature (°F)
○	32	300
⊖	32	250
◇	32	(1978 data)
⬡	52	300
⊖	52	250
□	119	300
△	154	300
▽	193	300
⩛	193	250

Figure 3-6. SO_2 removal as a function of $NaHCO_3$ stoichiometric ratio for different particle sizes.[13]

3.2.4 Temperature

The temperature of the flue gas influences the diffusivity of the SO_2 molecules and the mass transfer of SO_2 to the sorbent particles. However, SO_2 mass transfer properties will vary only slightly in the typical flue gas temperature range (300°F to 400°F). As discussed in Section 3.2.2, the temperature at which the sorbent is injected into the flue gas affects the thermal decomposition of $NaHCO_3$ to Na_2CO_3. This in turn influences the reactivity of the sorbent. Many tests have been performed trying to characterize the effect of temperature on SO_2 removal. Again, these tests have yielded conflicting results. However, it appears that the best SO_2 removal occurs when the nahcolite is injected into the duct at approximately 600°F, and the baghouse is operated at approximately 300°F. The high injection temperature allows for rapid decomposition of $NaHCO_3$ to Na_2CO_3, and a temperature of 300°F is optimum for the reaction between Na_2CO_3 and SO_2 to form Na_2SO_3.

Two methods of elevating the flue gas temperature above air preheater outlet temperatures have been employed in pilot-scale systems. One method involves using a stream of hot flue gas which bypasses the air preheater; the other method utilizes heaters or heat exchangers at the air preheater outlet duct.

Available test data on the effect of temperature on SO_2 removal are presented in Table 3-4. These data show SO_2 removal to generally increase with increasing temperature. Temperature changes seem to affect the decomposition reaction but appear to have little affect on the other chemical reactions that occur. These conclusions are supported by fixed-bed experiments performed by Superior Oil Company on predecomposed nahcolite which indicated that changes in temperature from 200° to 600°F had no effect on the rate of reaction of Na_2CO_3 to Na_2SO_3.[6] However, Hartman[14] found that the optimum temperature for the desulfurization reaction

$$Na_2CO_{3(s)} + SO_{2(g)} \longrightarrow Na_2SO_{3(s)} + CO_{2(g)} \qquad (3\text{-}5)$$

was approximately 250° to 300°F.

Results of tests conducted by KVB, Inc. for EPRI indicate that the optimum temperature for SO_2 removal is 550°F, and at 800°F SO_2 removal drops off considerably.[1] Work by Nesse and Selle[6] at GFETC showed that the optimum temperature for SO_2 removal in suspension in the ductwork is 650°F,[6] and work by Liu and Chaffee[16] for Air Preheater seem to support these results. Nahcolite and sodium bicarbonate were tested, and both exhibited similar behavior in suspension. Approximately 13 percent of the total removal took place in the duct at temperatures between 270° and 350°F, while 63 percent of the total removal occurred in the duct at 600°F.[6] Work by Liu and Chaffee,[16] which is presented in Figure 3-7, shows that SO_2 removal efficiency with nahcolite increases steadily from 300° to 600°F.

TABLE 3-4. EFFECT OF TEMPERATURE ON DRY INJECTION SO_2 REMOVAL

Test Location	Sorbent Type	Stoichiometric Ratio Mole Na_2O/Mole SO_2	Flue Gas Temperature °F	SO_2 Removal Efficiency, %
Buell[a,c]	Nahcolite	1.0	325	67
Martin Drake Station	Nahcolite	1.0	500	38
	Trona	1.0	325	23
	Trona	1.0	500	32
	Refined Trona	1.0	325	45
	Refined Trona	1.0	500	41
Air Preheater Mercer Station[b]	Nahcolite	1.0	350	66
	Nahcolite	1.0	512-604	94
	$NaHCO_3$	1.0	271-312	40
	$NaHCO_3$	1.0	349-356	49
	$NaHCO_3$	1.0	532	86
EPRI/KVB[b]	Nahcolite	1.0	270	50
	Nahcolite	1.0	550	80
	Nahcolite	1.0	800	60
University of Tennessee[a]	Nahcolite	0.95	185	17
	Nahcolite	0.95	350-385	86

[a] Baghouse temperature

[b] Injection temperature

[c] Injection temperatures are given in Figures 3-5a through 3-5c.

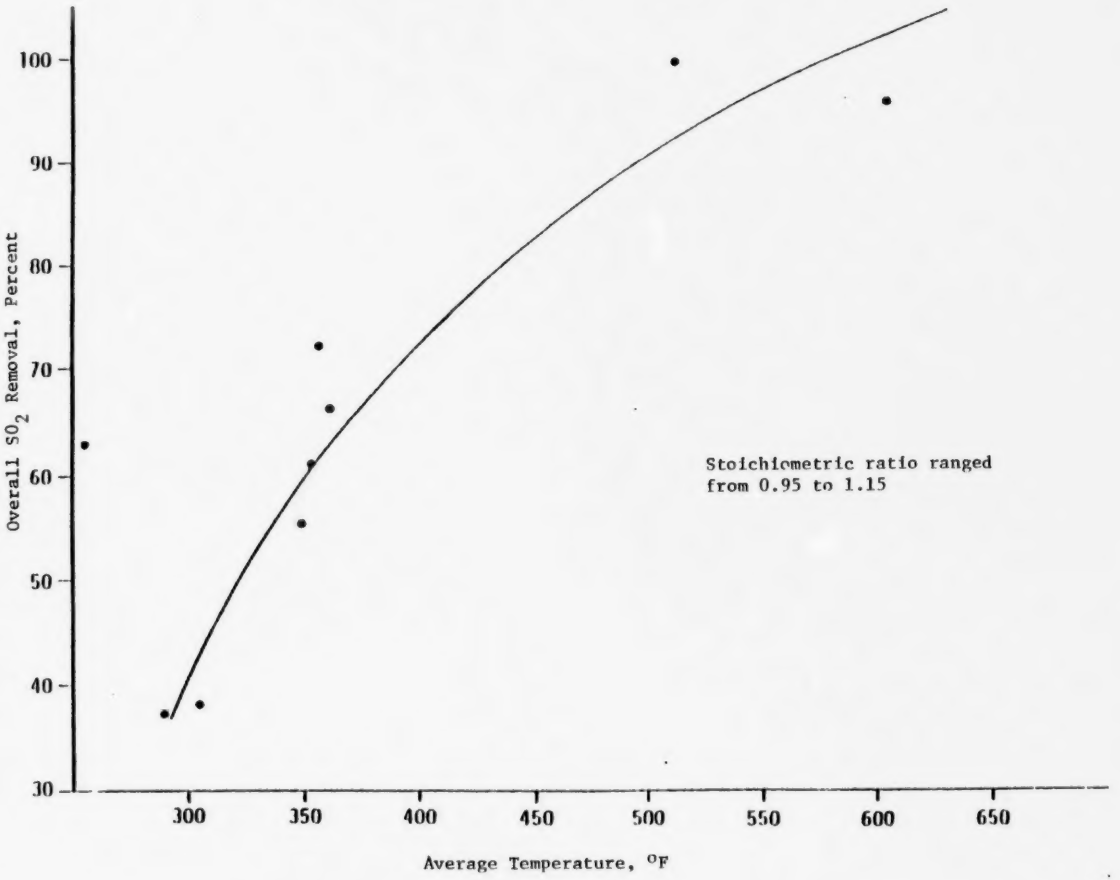

Figure 3-7. Effect of temperature on SO_2 removal efficiency with nahcolite.[16]

Results of tests conducted by Buell contradict the results of other investigators. Sulfur dioxide removal decreased with increasing fabric filter temperature from 325° to 500°F, for both nahcolite and refined trona. However, removal with trona increased as the temperature increased[2] (see Table 3-4).

A discussion of the influence of temperature upon sorbent decomposition was presented in Section 3.2.2 of this report. The apparent increase in SO_2 removal at higher temperatures seems to indicate that sorbent injection at high temperatures may be desirable. However, it should be kept in mind that Na_2CO_3 will begin to sinter and the pores will begin to fuse at temperatures greater than 650°F.[9]

3.2.5 Stoichiometric Ratio

Since the stoichiometric ratio determines the quantity of sodium available to react with a given quantity of SO_2, it affects the chemical utilization of the sorbent particles and the degree of completion of the chemical reaction. Also, at lower stoichiometries the utilization of the sorbent should be greater than at higher stoichiometries. That is the individual sorbent particles will be more highly reacted at lower stoichiometries because fewer particles are available to react with SO_2 in the gas. Therefore, at low stoichiometries the ash layer surrounding the particles should be thicker, and tend to limit SO_2 mass transfer.

The stoichiometric ratio in dry injection is defined as:

$$SR = Me/MSO_2 \qquad (3\text{-}16)$$

where: Me = mole equivalent of Na_2O in the sorbent

MSO_2 = moles of SO_2 in the inlet flue gas

Work by several organizations (EPRI, University of Tennessee, Battelle-Columbus, Air Preheater, American Air Filter, Wheelabrator-Frye, and Buell) has shown an increase in SO_2 removal with increased stoichiometric ratio. SO_2 removal results at different stoichiometries are presented in Figure 3-8 (Air Preheater test).[16]

Buell performed tests using nahcolite, trona, and refined trona. These results were presented earlier in Figures 3-5a through 3-5c and showed increased SO_2 removal with increasing sorbent stoichiometry. Work by Liu and Chaffee for A r Preheater also showed that a decrease in sorbent utilization accompanied the increased SO_2 removal with increasing SR.

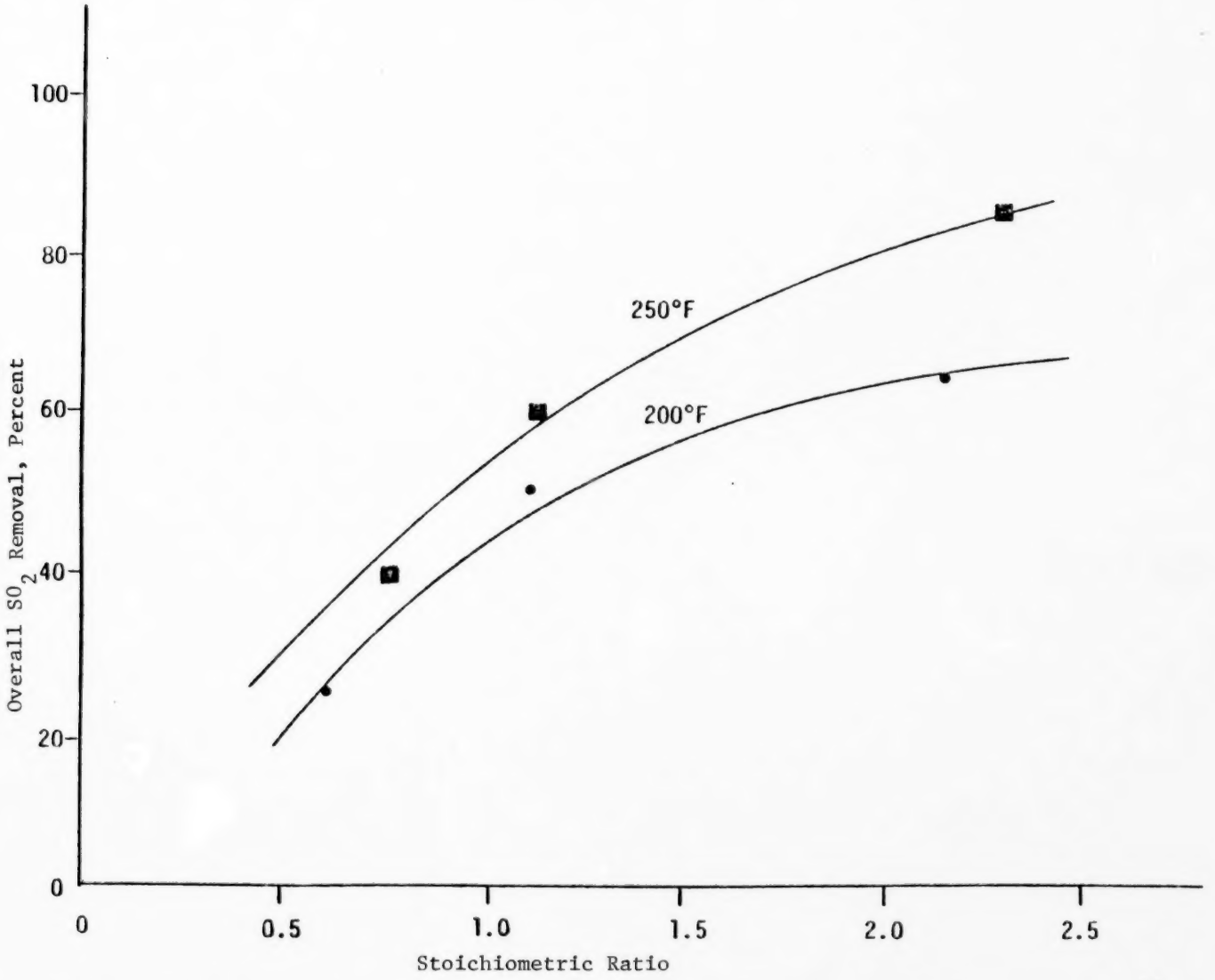

Figure 3-8. Effect of stoichiometric ratio on SO_2 removal efficiency with nahcolite.[16]

3.2.6 Mode of Injection

The mode of sorbent injection affects the external mass transfer of SO_2 to the entrained sorbent particles in the ductwork, and through the filter cake in the fabric filter. The sorbent can be injected into the system in three ways.

1) Continuous. After the bag is cleaned, sorbent is continuously supplied to the flue gas from injection points in the ductwork located upstream of the baghouse. The sorbent then accumulates on the bags to produce a filter cake.

2) Batch. After the bag is cleaned, all sorbent is added to the bag as precoat before flue gas flow is resumed.

3) Semi-batch. This feeding method is a combination of methods 1 and 2. After bag cleaning some sorbent is precoated onto the bags and the remainder is added continuously at an upstream injection point.

In a typical semi-batch system, 20 percent of the ground ore is used to precoat the filter bags. The additional sorbent is added continuously in the duct. A maximum grain loading of 10 gr/acf for continuous injection was used by Genco and Rosenberg to prevent particle settling in the duct.[3]

The effects of precoat on SO_2 removal have been analyzed by KVB for EPRI. They found that precoating the bags with nahcolite increased SO_2 removal from 42 to 66 percent, with all other conditions held constant.[7]

Tests have also been conducted in an attempt to characterize where SO_2 removal occurs, in the ductwork or in the filter. The results of these tests indicated that SO_2 removal in the ductwork is variable, and is a strong function of the flue gas temperature in the duct. Shah and Teixeira[12] found that approximately half of the overall SO_2 removal effected by injecting the $NaHCO_3$ into the ductwork at 530°F occurred in suspension, the balance taking place as the gas stream passed through the filter cake. The baghouse temperature during these experiments ranged from 255° to 290°F. American Air Filter performed experiments without a filter, at temperatures of 200° to 225°F, to characterize SO_2 removal in the duct. They found that essentially no removal occurred[4] when the nahcolite was in suspension in the duct. EPRI[7] also conducted tests at an injection temperature of 550°F and a baghouse temperature of 270°F. At a stoichiometric ratio of 1.0, these tests gave 80 percent total SO_2 removal when the sorbent was injected into the duct and 67 percent with injection at the baghouse inlet. Therefore, 13 percent of the overall SO_2 removal occurred in the duct at 550°F.[7] Finally, Liu and Chaffee from Air Preheater[16] found that the difference in removal using batch or continuous injection was slight. However, they showed that the injection temperature affects the location of SO_2 removal. They found 13 percent of the total removal occurred in the duct at injection

temperatures of 270° to 350°F, while 63 percent of the total removal occurred in the duct at 600°F.[16]

3.2.7 Residence Time of the Reactants in the Duct

The residence time determines the amount of time that the flue gas and sorbent will be in contact in the duct. Therefore, it affects the extent of mass transfer through both the gas film and the ash layer that surround the sorbent particles. Residence time is defined as the volume of the duct containing sorbent divided by the volumetric flow of gas through the duct and is normally expressed in seconds. In general, SO_2 removal in the duct increases with increased residence time.[13]

Figure 3-9 shows that SO_2 removal in the duct increases with increasing residence time. The removal varies exponentially with residence time and is about 70 percent after 1.75 seconds for the displayed curve.

3.2.8 Filter Cleaning Intervals

The longer the baghouse operates between cleanings, the greater the sorbent utilization. An increase in sorbent utilization causes the ash layer surrounding the particles to become thicker. This increase in ash layer thickness decreases the mass transfer of SO_2 through the ash. When the sorbent being used is nahcolite, the filter cells should be operated for at least 40 minutes between cleanings because it takes 40 minutes to achieve maximum steady state SO_2 removal with nahcolite.[1] However, maximum steady state removal with trona is achieved very rapidly.[1] Genco and Rosenberg operated the filter cells for approximately 70 minutes between cleanings for a nahcolite sorbent.[3] The filter cleaning interval must be balanced against the rate of SO_2 removal. After a certain amount of sorbent has been utilized, the rate of SO_2 removal begins to level off, and a longer filter cleaning interval will result in very little additional SO_2 removal.

3.2.9 Inlet SO_2 Concentration

The inlet SO_2 concentration affects the mass transfer of SO_2 to the sorbent particles because it determines the driving force for SO_2 mass transfer to the particle surface. The results of several studies measuring the effect of SO_2 concentration on removal efficiency showed that the inlet SO_2 concentration had only a small effect on removal for a given stoichiometric ratio. Work by Wheelabrator-Frye, with a nahcolite sorbent and inlet SO_2 concentrations of 800 to 2800 ppm, showed that removal was slightly higher for higher inlet SO_2 levels. It was felt that the slight increase in removal resulted from a higher driving force for the diffusion of SO_2 from the bulk gas to the solid particle.

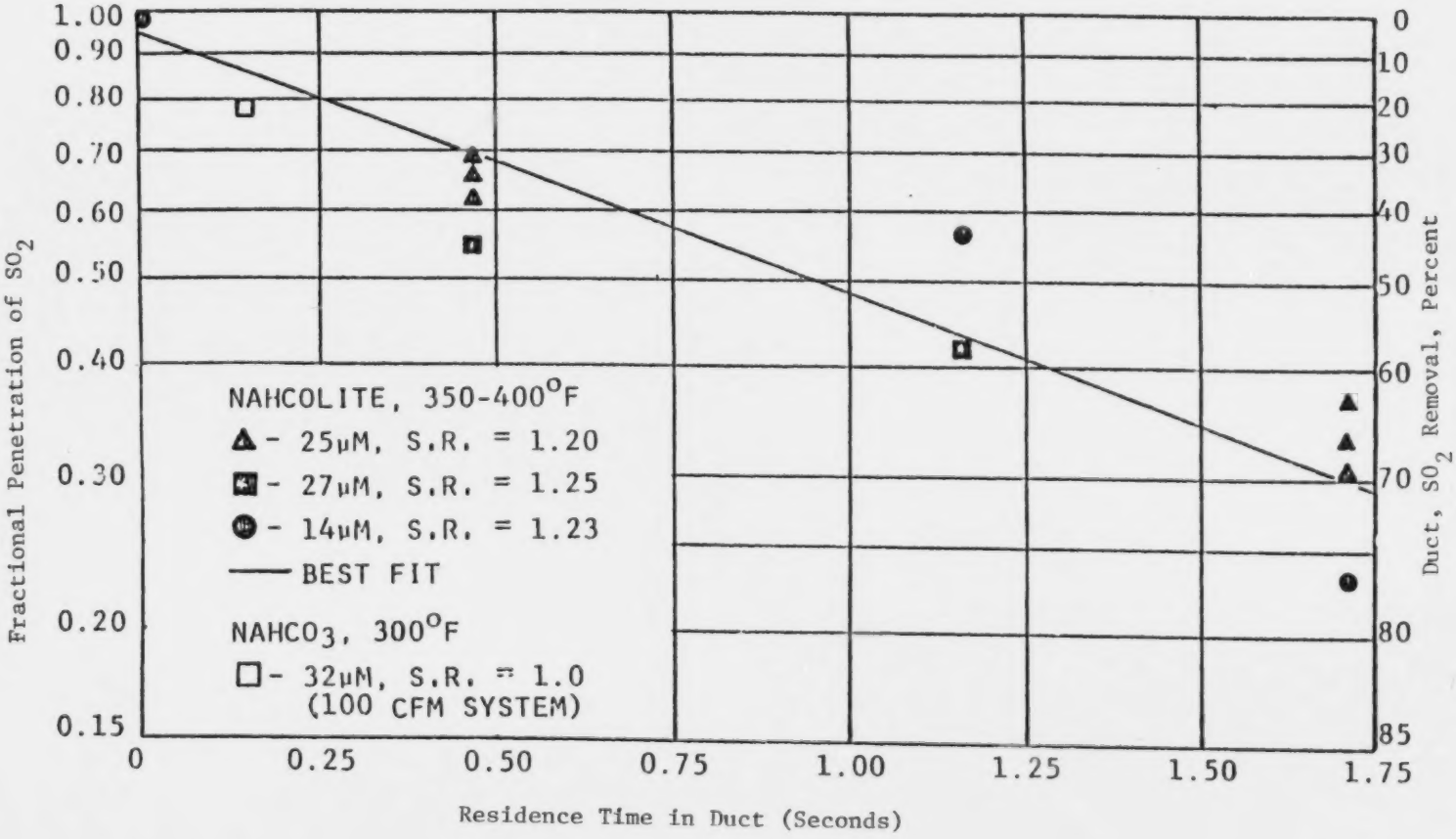

Figure 3-9. SO_2 removal efficiency versus residence time in the duct.[13]

However, the increase in removal was somewhat offset because at higher inlet SO_2 concentrations more nahcolite had to be fed to maintain stoichiometric ratios, which necessitated more frequent bag cleaning and resulted in lower nahcolite residence time in the system.[4] It should be noted that Wheelabrator-Frye's reasoning is not consistent with the reaction models developed in this report because the diffusion of SO_2 from the gas to the particle was not considered to be a rate controlling step.

The dry injection system has not been tested with SO_2 concentrations greater than approximately 3500 ppm in other than laboratory situations. Therefore the applicability of dry injection to use with coals containing greater than 3.5 percent sulfur is not known.

3.2.10 Gas Velocity and Air-to-Cloth Ratio.

The velocity of the flue gas relative to the sorbent particles affects the mass transfer of SO_2 through the stagnant gas film to the surface of the sorbent particle. Gas velocity affects the diffusional properties of the SO_2 and the time the sorbent and flue gas are in contact. The lower the velocity of the flue gas, the longer it remains in the dry injection system to react with the sorbent. However, the results of studies by several sources (Buell, EPRI, American Air Filter, University of Tennessee, and Wheelabrator-Frye) showed that the velocity of the gas had no significant effect on SO_2 removal. The air-to-cloth ratio, which represents the velocity of the gas through the filter cloth and is described as the volumetric flow of the gas through a specified filter area, was varied from 1.4 to 5.0 ft/min with no observable effect on SO_2 removal.[2,7,15]

3.3 DATA GAPS IN LITERATURE

Several areas that require further work include:

1) The degree of SO_2 removal obtained when the inlet SO_2 concentration exceeds 3000 ppm

2) Evaluation of data against the unreacted-core model relationships to establish a rate controlling step

3) Development of equations or rate constants which account for temperature and particle size effects

4) Further clarification of the mechanism involved in the chemical reaction of Na_2CO_3 with SO_2 to form Na_2SO_3

5) The influence of flue gas moisture content on SO_2 removal

6) The effect of the injection and baghouse temperature on SO_2 removal

7) Particle size effects

8) The effect of predecomposition of sorbent on SO_2 removal

It would be extremely useful to perform a more detailed analysis of SO_2 removal at higher inlet SO_2 concentrations than 3000 ppm. This information would be useful in determining the applicability of dry injection to systems that burn medium and high sulfur coals. However, problems with the disposal of dry sodium-wastes may preclude further investigation. Since sodium-wastes are highly leachable careful disposal may be required to prevent the contamination of groundwater, and an economically attractive method for disposal of sodium-waste solids in an environmentally acceptable manner has yet to be developed.

It is also necessary to clarify the mechanism by which the following chemical reaction proceeds.

$$Na_2CO_{3(s)} + SO_{2(g)} \longrightarrow Na_2SO_{3(s)} + CO_{2(g)} \qquad (3\text{-}5)$$

In addition, the importance of the flue gas moisture content on SO_2 removal should be characterized.

The effects of temperature, particle size, and sorbent predecomposition have been characterized, but test results from different sources often conflict. It would be useful to evaluate these parameters in well controlled tests in order to establish which results are applicable to the dry injection system.

Plots of time versus conversion data in conjunction with the unreacted core model could be used to establish a rate controlling step. In order to perform this evaluation, it would be necessary to evaluate the value of τ, the time needed for complete conversion of the sorbent as described by Equations 3-7, 3-10, and 3-12. The mathematical models for dry injection proposed in this paper only take into account reaction time, conversion, and reaction depth. Equations or rate constants which account for the effects of temperature and particle size on SO_2 removal are also needed.

In addition, it may be beneficial to test dry injection on a flue gas produced from combustion under low excess air conditions. It seems that minimizing the oxygen content of the flue gas would reduce the oxidation of Na_2SO_3 to Na_2SO_4. If in fact, the oxidation of Na_2SO_3 causes the pores in the sorbent particle to plug, then a reduction in the amount of Na_2SO_4 generated should reduce plugging and allow for better SO_2 removal.

In order to evaluate the parameters that have been described above, it would be best to use full-scale dry injection equipment. However, if full-scale equipment was not available pilot-scale experiments could still be performed. A fixed-bed, batch reactor, could be used to simulate SO_2 removal in the flue gas duct, and a moving-bed reactor could be used to simulate SO_2 removal in the baghouse filter cake.

3.4 LITERATURE CITED FOR DRY INJECTION

1. Kelly, M.E. and S.A. Shareef. Second Survey of Dry SO_2 Control Systems. EPA Report No. EPA-600/7-81-018. (NTIS No. PB 81-157919.) February 1981.

2. Samuel, E.A. and D.E. Lapp. "Testing and Assessment of a Baghouse for Dry SO_2 Removal, Task 4: SO_2 Removal Using Dry Sodium Compounds". September 1980. Draft report prepared for U.S. EPA, Contract No. 68-02-3119.

3. Genco, J.M. et al. "The Use of Nahcolite Ore and Bag Filters for SO_2 Emission Control." In: Journal of Air Pollution Control Association 25:12. December 1975. p. 1244.

4. Dickerman, J.C. et al. "Evaluation of Dry Alkali FGD Systems." Radian Report No. DCN 78-200-226-03. March 31, 1978.

5. Howatson, J., T.W. Smith, D.A. Outka and H.D. Dewald. "Nahcolite Properties Affecting Stack Gas Pollutant Absorption," Proceedings of 5th National Conference on Energy and the Environment, Cincinnati, Ohio. November 1977.

6. Davis, W.T. and T.C. Keener. "Phase I: Chemical Kinetic Studies on Dry Sorbents, Literature Review." University of Tennessee. August 10, 1980.

7. "SO_2 Control by Dry Sorbent Injection." In: EPRI Journal. June 1980. p. 52.

8. Knight, John H. "The Use of Nahcolite for Removal of Sulfur Dioxide and Nitrogen Oxides from Flue Gas". The Superior Oil Co., 1977.

9. Stern, Frederic R. "Bench-Scale Study of Sulfur and Nitrogen Oxides Adsorption by Nahcolite and Trona." Masters Thesis, University of North Dakota. 1978.

10. "Evaluation of Dry Alkalis for Removing Sulfur Dioxide from Boiler Flue Gases". EPRI Report FP-207. October 1976.

11. Levenspiel, O. Chemical Reaction Engineering, 2nd edition. New York: John Wiley and Sons, Inc., 1972. pp. 357-377.

12. Shah, N.D. and D.P. Teixeira. "Bench-Scale Evaluation of Dry Alkalis for Removing SO_2 from Boiler Flue Gases." (Presented at the Symposium on the Transfer and Utilization of Particulate Control Technology, Denver, Colorado, 1978.)

13. Carson, John R. "Removal of Sulfur Dioxide and Nitric Oxide from a Flue Gas Stream by Two Sodium Alkalis of Various Sizes." Master's Thesis, University of Tennessee, Knoxville. August 1980.

14. Hartman, M. "Comparison of Various Carbonates as Absorbents of Sulfur Dioxide from Combustion Gases." International Chemical Engineering, 18:712. 1978.

15. Davis, W.T. and T.C. Keener. "Research on the Removal of SO_2 by Additive Injection Techniques on a Stoker-Fired Boiler". (Presented at the 71st Annual Meeting of the Air Pollution Control Association, June 25, 1980.)

16. Liu, H. and R. Chaffee. "Evaluation of a Fabric Filter as a Chemical Contactor for Control of Sulfur Dioxide from Flue Gas." Report to NAPCA by the Air Preheater Co. Report No. PB-194-196. December 1961. 159 pp.

SECTION 4

BIBLIOGRAPHY

1. Bagwell, F.A., L.F. Cox, and E.A. Push. "Design and Operating Experience: A Filterhouse Installed on an Oil Fired Boiler." J. Air Pollution Control Association. 19:149. 1969.

2. Banks, R.B. and M.L. Hochhauser. "Desulfurization of Flue Gas with Nahcolite in a Pilot Fabric Filter." (Presented at the 71st Annual Meeting of the Air Pollution Control Association. Houston, Texas. June 25-30, 1978.)

3. Bares, J. et al. "Kinetics of the Reaction Between the Solid Sodium Carbonate and the Gaseous Sulphur Dioxide. III. Study in an Integral Fixed-Bed Reactor." Coll. Czech. Chem. Commun. 35. 1628. 1970.

4. Bechtel Corporation. "Evaluation of Dry Alkalis for Removing SO_2 from Boiler Flue Gases." EPRI Final Report FP-207. Prepared for Electric Power Research Institute, Palo Alto, CA. October 1976. 144 p.

5. Blythe, G.M., J.C. Dickerman, and M.E. Kelly. "Survey of Dry SO_2 Control Systems." EPA-600/7-80-030. (NTIS No. PB 80-166853) February 1980.

6. Brna, T.G., S.J. Lutz, and J.A. Kezerle. "Performance Evaluation of an Industrial Spray Dryer for SO_2 Control." (Prepared for Presentation at EPA's Sixth FGD Symposium. Houston, Texas. October 1980.)

7. Buell-Envirotech. "Research and Development on Test Baghouse at Martin Drake No. 6, City of Colorado Springs: Vol. III - Mathematical Modeling." April 1980.

8. Burnett, J.A. and W.E. O'Brien. "Preliminary Economic Analysis of a Lime Spray Dryer FGD System." Report No. EPA-600/7-80-050; TVA EDT-112. U.S. Environmental Protection Agency. March 1980.

9. Carson, J.R. "Removal of Sulfur Dioxide and Nitric Oxide from a Flue Gas Stream by Two Sodium Alkalis of Various Sizes." Masters Thesis. University of Tennessee, Knoxville. August 1980.

10. Davis, R.A. et al. "Dry SO_2 Scrubbing at Antelope Valley Station." (Presented at the 41st Annual American Power Conference. Chicago, Illinois. April 25, 1979.)

11. Davis, W.T., T.C. Keener, C.S. Means, and R.B. Dooley. "Research on the Simultaneous Removal of SO_x and Particulates from Stoker-Fired Boilers." Paper 77-26.3. Presented at the 70th Annual Meeting of the Air Pollution Control Association. June 1977.)

12. Davis, W.T. and T.C. Keener. "Research on the Removal of SO_2 by Additive Injection Techniques on a Stoker-Fired Boiler." (Presented at the 71st Annual Meeting of the Air Pollution Control Association. June 25, 1980.)

13. Davis, W.T., T.C. Keener, J.R. Carson, and H. Majdeski. "Study of SO_2 Removal in a Fabric Filter Collector by $NaHCO_3$ and Nahcolite Injection." Submitted for publication to JAPCA. April 1980.

14. Davis, W.T. and T.C. Keener. "Phase I: Chemical Kinetic Studies on Dry Sorbents, Literature Review." August 10, 1980.

15. Dickerman, J.C. et al. "Evaluation of Dry Alkali FGD Systems." Radian Corporation Report No. DCN 78-200-226-03. Austin, Texas. March 31, 1978.

16. Downs, W., W.J. Sanders, and C.E. Miller. "Control of SO_2 Emissions by Dry Scrubbing." (Presented at the American Power Conference. Chicago, Illinois. April 21-23, 1980.)

17. Doyle, D.J. "Fabric and Additive Remove SO_2." Electrical World. February 15, 1977.

18. Dulin J.M. "The Use of Nahcolite Ore and Bag Filter for SO_2 Emission Control." Proceedings of ASME National Symposium on "Is Demonstrated Technology Available to Meet Standards." Philadelphia, Pennsylvania. April 24-25, 1973.

19. Dustin, D.F. "Report of Coyote Pilot Plant Test Program." Test Report. Rockwell International (Atomics International Division). Canoga Park, California. November 1977.

20. "SO_2 Control by Dry Sorbent Injection." EPRI Journal. June 1980. p. 52.

21. Erdos, E. "Mathematical Treatment of the Heterogeneous Fixed-Bed Reactor." Coll. Czech. Chem. Commun. 32. 1653. 1967.

22. Erdos, E. "Kinetics of the Reaction Between the Solid Sodium Carbonate and the Gaseous Sulphur Dioxide. II. Interpretation of the Excess Kinetic Function by Means of a Microscopic Model." Coll. Czech. Chem. Commun. 34. 919. 1969.

23. Erdos, E. "Kinetics of the Reaction Between the Solid Sodium Carbonate and the Gaseous Sulphur Dioxide. VI. Statistical Molecular Model of the Excess Kinetic Function." Coll. Czech. Chem. Commun. 36. 485. 1971.

24. Felsvang, Karsten. Results of Pilot Plant Operations for SO_2 Absorption. (Presented at the Joy Western Precipitation Division Seminar. Durango, Colorado. May 21, 1979.)

25. Furlong, Dale A., T.G. Brna, and R.L. Ostop. "SO_2 Removal Using Dry Sodium Compounds." (Presented at the 89th National AIChE Meeting. Portland, Oregon. August 17-21, 1980.)

26. Genco, J.M., H.S. Rosenberg, M.Y. Anastas, E.C. Rosar, and J.M. Dulin. "The Use of Nahcolite Ore and Bag Filters for Sulfur Dioxide Emission Control." J. Air Pollution Control Association. 25(12):1244. December 1975.

27. Genco, J.M. and H.M. Rosenberg. "Sorption of SO_2 on Ground Nahcolite Ore." J. Air Pollution Control Association. 26(10): 989-990. 1976.

28. Getler, J.L., et al. "Modeling the Spray Absorption Process for SO_2 Removal." J. Air Pollution Control Association. 29:12. December 1979. p. 1270-1274.

29. Hartman, M. "Comparison of Various Carbonates as Absorbents of Sulfur Dioxide from Combustion Gases." International Chemical Engineering. 18:712. 1978.

30. Howatson, J., J.W. Smith, D.A. Outka, and H.D. Dewald. "Nahcolite Properties Affecting Stack Gas Pollutant Absorption." Proceedings of 5th National Conference on Energy and the Environment. Cincinnati, Ohio. November 1977.

31. Hurst, T.B., and G.T. Bielawski. "Dry Scrubber Demonstration Plant - Operating Results." In: Proceedings of Sixth Symposium on Flue Gas Desulfurization, Houston, Texas. Volume 2, pp. 853-860. EPA-600/9-81-0196, April 1981.

32. Johnson, O.B. et al. "Coyote Station - First Commercial Dry FGD System." (Presented at the 41st Annual American Power Conference. Chicago, Illinois. April 23-25, 1979.)

33. Kaplan, Steve. "The Niro-Joy Spray Absorber Development Program: Pilot-Plant Description and Test Results." (Presented during Joy/Niro sponsored tour for executives of U.S. Power Industry. Copenhagen, Denmark. September 23-30, 1978.)

34. Kaplan, S.M. and K. Felsvang. "Spray Dryer Absorption of SO_2 from Industrial Boiler Flue Gas." (Presented at the American Institute of Chemical Engineers 86th National Meeting 10th Petro Expo. Houston, Texas. April 1-5, 1979.)

35. Keener, T.C. "Simultaneous Removal of Sulfur Oxides and Particulate Matter From Stoker-Fired Boiler Flue Gas with a Pilot Plant Fabric Filter Collector." Thesis. University of Tennessee. August 1977.

36. Kelly, M.E. and S.A. Shareef. "Second Survey of Dry SO_2 Control Systems." EPA-600/7-81-018. (NTIS No. PB 81-157919) February 1981.

37. Kelly, M.E. and S.A. Shareef. "Third Survey of Dry SO_2 Control Systems." EPA-600/7-81-097. (NTIS PB No. 81-218976) July 1981.

38. Knight, J.H. "The Use of Nahcolite for Removal of Sulfur Dioxide and Nitrogen Oxides from Flue Gas." The Superior Oil Co. 1977.

39. Lakefield Research of Canada, Ltd. "An Investigation of SO_2 Absorption by Nahcolite from Samples of Rio Blanco Oil Shale." Report No. 12. Prepared for the Superior Oil Co. March 1971.

40. Lakefield Research of Canada, Ltd. "An Investigation of SO_2 Absorption by Decomposed $NaHCO_3$." Report No. 15. Prepared for the Superior Oil Co. May 1971.

41. Lakefield Research of Canada, Ltd. "An Investigation of Sulfur Dioxide Absorption by Decomposed Sodium Bicarbonate and Nahcolite." Report No. 20. Prepared for the Superior Oil Co. July 1971.

42. Levenspiel, O. Chemical Reaction Engineering. 2nd edition. New York: John Wiley and Sons, Inc., 1972. pp. 357-377.

43. Liu, H. and R. Chaffee. "Evaluation of a Fabric Filter as a Chemical Contactor for Control of Sulfur Dioxide from Flue Gas." Report to NAPCA by the Air Preheater Co. Report No. PB-194-196. December 1961. 159 p.

44. Liu, H. and R. Chaffee. "Evaluation of Fabric Filters as a Chemical Contactor for Control of SO_2 in Flue Gas." (Presented at the Air Pollution Control Office Fabric Filter Symposium. Charleston, South Carolina. March 1971.)

45. Lutz, S.J., R.C. Christman, B.C. McCoy, S.W. Mulligan, and K.M. Slimak. "Evaluation of Dry Sorbents and Fabric Filtration for FGD." EPA-600/7-79-005. U.S. Environmental Protection Agency, Office of Research and Development. Washington D.C. January 1979. 145 p.

46. Marecek, J. et al. "Kinetics of the Reaction Between the Solid Sodium Carbonate and the Gaseous Sulphur Dioxide. III. Mathematical Treatment of Heterogeneous Countercurrent and Co-current Reactor." Coll. Czech. Chem. Commun. 35. 524. 1970.

47. Marecek, J. et al. "Kinetics of the Reaction Between the Solid Sodium Carbonate and the Gaseous Sulphur Dioxide. IV. Effect of the Gas Phase Composition and of Temperature in an Integral Fixed-Bed Reactor." Coll. Czech. Chem. Comm. 35. 154. 1970.

48. Martin, J.R., W.B. Ferguson, and D. Frabotta. "C-E Dry Scrubber Systems: Application to Western Coals." (Presented at the 1980 American Power Conference. Chicago, Illinois.)

49. Masters, Keith. "The Basis for Spray Dryer Absorption - Spray Drying Technology." (Presented during Joy/Niro sponsored tour for executives of U.S. Power Industry. Copenhagen, Denmark. September 23-30, 1978.)

50. Masters, Keith. Spray Drying Handbook. George Goodwin Limited. London. 1979.

51. McCrea, D.H. et al. "Evaluation of Solid Absorbents for Sulfur Oxides Removal from Stack Gases." Paper EN35A in Second Int'l Clean Air Proceedings. H.M. Englund and W.T. Beery, eds. Academic Press. 1972. p. 922-930.

52. Meyler, J.A. "Flue Gas Desulfurization Utilizing Dry Scrubbing." (Presented at 1978 Joint Power Generation Conference. Dallas, Texas.)

53. Meyler, J.A. "Dry Flue Gas Scrubbing: A Technique for the 1980's." (Presented at 1980 Joint Power Conference. Phoenix, Arizona. September 1980.)

54. Muzio, L.J., J.K. Arand, and N.D. Shah. "Bench-Scale Study of Dry SO_2 Removal with Nahcolite and Trona." In: Proceedings of Second Conference on Air Quality Management in the Electric Power Industry. University of Texas. Austin, Texas. 1980. 33 p.

55. Ness, H.M. and S.J. Selle. "Control of Western Power Plant Sulfur Dioxide Emissions: Development of the Ash-Alkali FGD Process and Dry Adsorption Techniques at the Grand Forks Energy Technology Center." In: Proceedings of DOE Symposium on Environmental Control Activities, Washington, D.C. 1978. 20 p.

56. Parsons, E.L., L.F. Hemenway, O.T. Kragh, T.G. Brna, and R.L. Ostop. "SO_2 Removal by Dry FGD." In: Proceedings of Sixth Symposium on Flue Gas Desulfurization, Houston, Texas. Volume 2, pp. 801-852. EPA-600/9-81-0196, April 1981.

57. Parsons, E.L., V. Boscak, T.G. Brna, and R.L. Ostop. SO_2 Removal by Dry Injection and Spray Absorption Techniques. (Presented at EPA's Third Symposium on the Transfer and Utilization of Particulate Control Technology. Orlando, Florida. March 1981.)

58. Phillips, et al. "Evaluation of Dry Alkalis for Sulfur Dioxide Removal, Both Retrofit and New Construction." Pacific Power and Light Company. March 1977.

59. Pring, R.T. "Fabric Filter: Another Option for Flue Gas Cleanup." Power Eng. 77(1):48. 1973.

60. Reisinger, A.A. and D.C. Gehri. "Two Stage Dry FGD and Particulate Removal." Journal of the APCA. 29:4. April 1979.

61. Rivers, R.D. et al. "The Role of Fabric Collectors in Removing SO_2." (Presented at the First National Fabric Filter Alternatives Forum. Denver, Colorado. July 1976.)

62. Samuel, E.A. and D.E. Lapp, Buell/Envirotech. "Testing and Assessment of a Baghouse for Dry SO_2 Removal, Task 4: SO_2 Removal Using Dry Sodium Compounds." September 1980. Draft Report Prepared for U.S. EPA Contract No. 68-02-3119.

63. Shah, N.D. and D.P. Teixeira. "Bench-Scale Evaluation of Dry Alkalis for Removing SO_2 from Boiler Flue Gases." (Presented at the Symposium on the Transfer and Utilization of Particulate Control Technology. Denver, Colorado. 1978.)

64. Shah, N.D. et al. Application of Dry Sorbent Injection of SO_2 and Particulate Removal. (Presented at the Fourth EPA Symposium on Flue Gas Desulfurization. Hollywood, Florida. November 11, 1979.)

65. Stearns-Roger. "Nahcolite Granule Scrubbing System Feasibility Study." Vol 1. Prepared for Superior Oil Company. Denver, Colorado. November 1974.

66. Stern, F.R. "Bench-Scale Study of Sulfur and Nitrogen Oxides Adsorption by Nahcolite and Trona." Masters Thesis. University of North Dakota. 1978. 81 p.

67. Stern. J.L. "Dry Scrubbing for Industrial Flue Gas Desulfurization: State-of-the-Art, 1980." (Presented at the 89th National Meeting of AIChE. Portland, Oregon. August 17-20, 1980.)

68. Stevens, N.J. "Dry SO_2 Scrubbing Pilot Test Results." In: Proceedings of Sixth Symposium on Flue Gas Desulfurization, Houston, Texas. Volume 2, pp. 777-800. EPA-600/9-81-0196, April 1981.

69. Stevens, N.J., G.B. Manavizadeh, G.W. Taylor, and M.J. Widico. "Dry Scrubbing SO_2 and Particulate Control." (Presented at EPA's Third Symposium on the Transfer and Utilization of Particulate Control Technology. Orlando, Florida. March 1981.)

70. The Superior Oil Co., Oil Shale Dept. "The Use of Nahcolite for Removal of Sulfur Dioxide and Nitrogen Oxides from Flue Gas." Denver, Colorado. 1977. 97 p.

71. Veazie, F.M. and W.H. Kielmeyer. "Feasibility of Fabric Filters as Gas-Solid Contactor to Control Gaseous Pollutants." NTIS Report No. PB 195 884. Owens-Corning Fiberglass Corporation. Granville, Ohio. August 1970.

72. Wheelabrator-Frye. "Non-confidential Test Data from Nahcolite Pilot Baghouse Study." Leland Olds Station. Unpublished. March 1977.

73. Yagi, S. and D. Kunii. In: Proceedings of the 5th International Symposium on Combustion. Reinhold Publishing, New York. 1955.

74. Yang, Ralph T. et al. "A Transient Technique for Measuring Diffusion Coefficients in Porous Solids. Diffusion in Carbonaceous Materials." I&EC, Fund. 16(4). 486. 1977.

APPENDIX A

DERIVATION OF THE DIFFUSION MODEL

A mathematical model describing SO_2 removal in the spray dryer during the constant rate drying period was developed by Downs et al. of Babcock and Wilcox.[1] The equation that was developed is presented below[2]:

$$N_T = \frac{D_v}{\alpha} \frac{N_{Sh}}{N_{Nu}} \ln \left(\frac{Tin - Tsat}{Tout - Tsat} \right)$$

The variables and nomenclature used in this derivation are listed below:

$\underline{a}$ = Interfacial mass or heat transfer surface area, ft^2/ft^3 of reactor

A_D = Droplet surface area, ft^2

A_R = Reactor flow area perpendicular to gas and slurry flow, ft^2

C_p = Flue gas heat capacity, Btu/lb-mole-°F

D = Time dependent droplet diameter, ft

D_i = Initial droplet diameter, ft

D_f = Final droplet diameter, ft

D_v = SO_2 gas diffusivity, ft^2/sec

G = Flue gas flowrate, lb-mole dry gas/sec

h = Convective heat transfer coefficient, Btu/sec-ft^2-°F

kg = Gas film mass transfer coefficient, lb-mole/ft^2-sec

K = Thermal conductivity of flue gas, Btu/sec-ft-°F

L = Water flowrate at atomizer, lb-mole/sec

m = Moisture content of a drop, lb-mole

n_D = Rate of droplet formation, number of drops/sec

N_{Nu} = Nusselt number, dimensionless

N_{Sh} = Sherwood number, dimensionless

N_T = Number of transfer units, dimensionless

ΔT = Instantaneous temperature difference between flue gas and droplet, °F

$\Delta T_{\ell m}$ = Log mean temperature difference between flue gas and droplet, °F

T_i = Inlet flue gas temperature, °F

T_f = Outlet flue gas temperature, °F

T_s = Adiabatic saturation temperature of the flue gas, °F

u_D = Velocity of a droplet, ft/sec

y = SO_2 concentration in the flue gas, mole fraction on dry gas basis

y^* = SO_2 concentration at liquid/gas interface, mole fraction on dry gas basis

Z = Variable distance from the atomizers, ft

α = Thermal diffusivity of flue gas, ft^2/sec

Γ = Droplet spatial concentration, number of droplets/ft^3 of reactor volume

λ = Heat of vaporization of water, Btu/lb-mole

ρ_g = Density of flue gas on a dry gas basis, lb-mole/ft^3

ρ_ℓ = Density of water, lb-mole/ft^3

θ = Time, sec

This derivation requires solving simultaneous mass and energy balances. Although Babcock and Wilcox developed this mathematical model for their ARC pilot plant, which is a horizontal flow spray dryer, it appears to be applicable to top entry spray dryers also.

A.1 Gas Phase Mass Balance and Mass Transfer Equations

The first assumption is that the dispersed slurry droplets are uniformly distributed across the flow area of the reactor. Then if two planes are visualized, one at a distance Z and the other at a distance Z + dZ from the slurry atomizers, a simple material balance for SO_2 can be performed as follows:

$$(Gy)_Z - (Gy)_{Z+dZ} = SO_2 \text{ transferred to the dispersed phase} \quad \text{(A-1)}$$

or

$$(Gy)_Z - [(Gy)_Z + d(Gy)] = SO_2 \text{ transferred to the dispersed phase} \quad \text{(A-2)}$$

Therefore,

$$-d(Gy) = SO_2 \text{ transferred to the dispersed phase} \quad \text{(A-3)}$$

Now, it also follows from film theory that the rate of SO_2 transferred is proportional to the mass transfer surface area times the concentration driving force. Therefore,

$$-d(Gy) = kg\ (\underline{a}\ A_R\ dZ)(y - y^*) \quad \text{(A-4)}$$

A.2 Interfacial Surface Area

The interfacial surface area, $\underline{a}$, is the total surface area of droplets in the control volume $A_R dZ$. To quantify this term requires that the number concentration and the size of drops within the control volume be known. If it is assumed that all drops which are originally formed stay as discrete entities, then the number of droplets per time unit passing through the plane at point Z will equal the rate of drop formation:

$$n_D = \frac{L}{\rho \ell}\left(\frac{6}{\pi D_i^{\,3}}\right) \quad \text{number of droplets/second} \quad \text{(A-5)}$$

From this it follows that the spatial concentration of droplets in the control volume $A_R dZ$ is:

$$\Gamma = n_D/(A_R u_D) \quad \text{number of droplets/ft}^3 \text{ of reaction volume} \quad \text{(A-6)}$$

Since the surface area of a single droplet is πD^2, the total interfacial mass transfer surface area per volume unit of reactor, $\underline{a}$, is:

$$\underline{a} = \pi D^2\ \Gamma \quad \text{(A-7)}$$

or

$$\underline{a} = \frac{n_D}{A_R u_D}\pi D^2 \quad \text{(A-8)}$$

or

$$\underline{a} = \frac{L}{A_R u_D} \frac{6}{\rho_\ell} \frac{D^2}{D_i^3} \tag{A-9}$$

A.3 Number of Transfer Units

Substituting Equation A-9 into Equation A-4 yields:

$$\frac{-d(Gy)}{dZ} = kg \left(\frac{L}{u_D} \frac{6}{\rho_\ell} \frac{D^2}{D_i^3} \right) \left(y - y^* \right) \tag{A-10}$$

Since the SO_2 is an extremely dilute gas, the total dry gas flow rate will change very little even for large changes in y, therefore,

$$\frac{-d(Gy)}{dZ} \simeq -G \frac{dy}{dZ} \tag{A-11}$$

This can be rearranged to give:

$$\frac{-dy}{(y-y^*)} = kg \left(\frac{L}{G} \right) \left(\frac{6}{\rho_\ell} \frac{D^2}{D_i^3} \right) \frac{dZ}{u_D} \tag{A-12}$$

A transfer unit by definition is the integral of a change in a variable divided by a driving force, as expressed in Equation A-13.

$$N_T = \int_{y_i}^{y_f} \frac{dy}{(y-y^*)} \tag{A-13}$$

Therefore,

$$N_T = -\int_0^Z kg \left(\frac{L}{G} \right) \left(\frac{6}{\rho_\ell} \frac{D^2}{D_i^3} \right) \frac{dZ}{u_D} \tag{A-14}$$

Since it was assumed that the gas and dispersed phases move together in plug flow through the reactor, then the velocity of the droplets is equal to the velocity of the gas. Therefore, the independent variable can be changed from position to time via:

$$u_D = \frac{dZ}{d\theta} \tag{A-15}$$

This can be substituted into Equation A-14:

$$N_T = -\int_0^{\theta} kg \frac{L}{G} \left(\frac{6}{\rho_\ell} \frac{D^2}{D_i^3} \right) d\theta \qquad \text{(A-16)}$$

The constants can be pulled out of the integral to give:

$$N_T = \frac{-L}{G} \frac{6}{\rho_\ell D_i^3} \int_0^{\theta} kg\, D^2 d\theta \qquad \text{(A-17)}$$

A.4 Evaporation Equations

Assuming that absorption stops once evaporation stops, the integration limit is the time required to evaporate all of the droplets in the dispersion. Since all droplets were assumed to be initially of the same size, the time it takes to evaporate a single droplet will be the same for all droplets. Thus, the evaporation rate for a single droplet is:

$$-\frac{dm}{d\theta} = \frac{h\, A_D\, \Delta T}{\lambda} \qquad \text{(A-18)}$$

Using the following equations

$$m = \rho_\ell \frac{\pi D^3}{6} \qquad \text{(A-19)}$$

$$A_D = \pi D^2 \qquad \text{(A-20)}$$

$$N_{Nu} = \frac{hD}{K} \quad \text{or} \quad h = \frac{N_{Nu}\, K}{D} \qquad \text{(A-20a)}$$

and the fact that ΔT can be treated as a constant if it is expressed as a log mean temperature difference,

$$\Delta T = \Delta T_{\ell m}, \qquad \text{(A-21)}$$

Equation A-18 becomes:

$$-\frac{d}{d\theta} \left(\pi D^3 \rho_\ell / 6 \right) = \frac{N_{Nu}\, K}{D} \pi D^2 \frac{\Delta T_{\ell m}}{\lambda} \qquad \text{(A-22)}$$

which can be rearranged to give:

$$d\theta = \frac{-\rho_\ell \lambda}{2N_{Nu} K \Delta T_{\ell m}} DdD \qquad \text{(A-23)}$$

Substituting this into Equation A-17 yields:

$$N_T = \frac{L}{G} \frac{6}{\rho_\ell D_i^3} \int_{D_i}^{D_f} kg\, D^2 \left(\frac{\rho_\ell \lambda}{2N_{Nu} K \Delta T_{\ell m}}\right) D\, dD \qquad \text{(A-24)}$$

At this point it would be convenient to put kg into a dimensionless form known as the Sherwood Number:

$$N_{Sh} = \frac{kg\, D}{D_v \rho_g} \quad \text{or} \quad kg = \frac{N_{Sh} D_v \rho_g}{D} \qquad \text{(A-25)}$$

Therefore,

$$N_T = \frac{L}{G} \left(\frac{1}{\Delta T_{\ell m}}\right) \left(\frac{3D_v \rho_g \lambda}{K}\right) \frac{N_{Sh}}{N_{Nu}} \int_{D_i}^{D_f} \frac{D^2}{D_i^3} dD \qquad \text{(A-26)}$$

Equation A-26 can now be integrated to yield:

$$N_T = \frac{L}{G} \left(\frac{1}{\Delta T_{\ell m}}\right) \left(\frac{3D_v \rho_g \lambda}{K}\right) \frac{N_{Sh}}{N_{Nu}} \left(\frac{D_f^3 - D_i^3}{3 D_i^3}\right) \qquad \text{(A-27)}$$

Assuming that liquid film and reactor rate effects are negligible, no generality is lost by assuming that D_f vanishes. Under these conditions:

$$N_T = \frac{-L}{G} \left(\frac{1}{\Delta T_{\ell m}}\right) \left(\frac{D_v \rho_g \lambda}{K}\right) \frac{N_{Sh}}{N_{Nu}} \qquad \text{(A-28)}$$

A.5 Overall Energy Balance

Equation A-28 can be further simplified by recognizing that the ratio of liquid to gas is coupled to the ΔT across the reactor.

Specifically,

$$L \lambda = G C_p (T_i - T_f) \qquad \text{(A-29)}$$

or

$$\frac{L}{G} = \frac{C_p}{\lambda} (T_i - T_f) \tag{A-30}$$

Noting that the $\Delta T_{\ell m}$ is:

$$\Delta T_{\ell m} = \frac{\left(T_i - T_s\right) - \left(T_f - T_s\right)}{\ell n \left(\frac{T_i - T_s}{T_f - T_s}\right)} \quad , \tag{A-31}$$

combining Equations A-30 and A-31 yields:

$$\frac{L}{G} = \frac{C_p}{\lambda} \Delta T_{\ell m} \ \ell n \left(\frac{T_i - T_s}{T_f - T_s}\right) \tag{A-32}$$

Substituting this into Equation A-28 yields:

$$N_T = -\left(\frac{D_v \rho_g C_p}{K}\right) \ell n \left(\frac{T_i - T_s}{T_f - T_s}\right) \frac{N_{Sh}}{N_{Nu}} \tag{A-33}$$

The thermal diffusivity is:

$$\alpha = \frac{K}{\rho_g C_p} \tag{A-34}$$

A.6 The Final Relationship

Equation A-34 can be substituted into Equation A-33 to give the final relationship:

$$N_T = -\left(\frac{D_v}{\alpha}\right) \left(\frac{N_{Sh}}{N_{Nu}}\right) \ \ell n \left(\frac{T_i - T_s}{T_f - T_s}\right) \tag{A-35}$$

REFERENCES FOR APPENDIX A

1. Downs, W., Babcock and Wilcox, letter to Apple, C.A., Radian Corporation. March 17, 1981.

2. Downs, W., W.J. Sanders and C.E. Miller. "Control of SO_2 Emissions by Dry Scrubbing." (Presented at the American Power Conference. Chicago, Illinois. April 21-23, 1980.)

APPENDIX B

DERIVATION OF THE UNREACTED-CORE MODEL[1]

The unreacted-core model can be applied to systems in which a gas reacts with a solid particle. Chemical reaction occurs first at the outer skin of the particle, which is assumed to be spherical, and the zone of reaction moves inward leaving behind a layer of reacted inert ash. The reaction of concern in this analysis is the following desulfurization reaction:

$$Na_2CO_{3(s)} + SO_{2(g)} \longrightarrow Na_2SO_{3(s)} + CO_{2(g)}$$

Five steps are involved in this gas-solid reaction. The first three steps result in the uptake of SO_2 by the sorbent and are listed below.

1) Diffusion of gaseous reactant (SO_2) to the surface of the solid (sorbent) through a stagnant gas film

2) Penetration and diffusion of reactant (SO_2) through the layer of ash to the surface of the unreacted core (Na_2CO_3)

3) Chemical reaction of reactant (SO_2) with the solid (Na_2CO_3) at the reaction surface

The last two steps involve the diffusion of CO_2 from the sorbent particles through the ash layer and into the flue gas. The resistance of these reaction steps usually vary greatly one from the another; therefore the step with the highest resistance is assumed to be rate controlling.

In this development it will be assumed that reaction steps, in the order listed above, control the rate of reaction successively. Equations describing sorbent conversion, X, versus time for each case will then be developed. The fraction of SO_2 removed by the system can be determined by solving for sorbent conversion, X, then multiplying the sorbent conversion by the moles of Na_2CO_3 that were injected into the system, and then dividing by the number of moles of SO_2 originally in the flue gas. The variables used in this analysis are defined below.

S = Surface area of the particle, ft^2

N = Number of moles of Na_2CO_3 or SO_2

t = Time, sec

R = Initial particle radius, ft

C_{SO_2-g} = Concentration of SO_2 in the gas phase, $lb\text{-}mole/ft^3$

C_{SO_2-s} = Concentration of SO_2 at the surface of the particle, $lb\text{-}mole/ft^3$

C_{SO_2-c} = Concentration of SO_2 at the unreacted core surface, $lb\text{-}mole/ft^3$

k_g = Gas phase mass transfer coefficient for SO_2 to the particle, ft/sec

ρ = Density of the sorbent, lb/ft^3

MW = Molecular weight of the sorbent, lb/lb-mole

r = Radius of the unreacted core, ft

τ = The time needed for complete conversion of the sorbent, sec

X = Fractional conversion of the sorbent, $\frac{\text{mole } Na_2SO_3 \text{ final}}{\text{mole } Na_2CO_3 \text{ initial}}$

Q_{SO_2} = Rate of diffussion of SO_2 to particle surface, $\frac{\text{mole } SO_2}{ft^2\text{-sec}}$

D_v = Mass diffusivity of SO_2 to the sorbent, ft^2/sec

k_s = First order rate constant for the surface reaction, ft/sec

v = Volume of sorbent particle, ft^3

Diffusion Through the Gas Film is Rate Controlling

In the first case it is assumed that the rate of reaction is controlled by the diffusion of SO_2 through the stagnant gas film surrounding the sorbent particles. It is further assumed that resistance to diffusion through the ash is negligible and that chemical reaction is instantaneous. The mathematical analysis is based upon an exterior particle surface of unchanging size. Based upon the molar flux of SO_2 to the particle surface, the following relationships are obtained:

$$\frac{-1}{S}\ \frac{dN_{Na_2CO_3}}{dt} = \frac{-1}{4\pi R^2}\ \frac{dN_{Na_2CO_3}}{dt} \qquad \text{(B-1)}$$

Noting from stoichiometry that $dN_{Na_2CO_3} = dN_{SO_2}$ and that the concentration gradient is $(C_{SO_2\text{-}g} - C_{SO_2\text{-}s})$, then

$$\frac{-1}{4\pi R^2}\ \frac{dN_{Na_2CO_3}}{dt} = \frac{-1}{4\pi R^2}\ \frac{dN_{SO_2}}{dt} = k_g\ (C_{SO_2\text{-}g} - C_{SO_2\text{-}s}) \qquad \text{(B-2)}$$

Since the SO_2 reacts instantaneously with the sorbent, $C_{SO_2\text{-}s}$ is zero, and the concentration driving force $C_{SO_2\text{-}g}$ is constant at all times during reaction of the particle. Therefore, Equation B-2 reduces to

$$\frac{-1}{4\pi R^2}\ \frac{dN_{Na_2CO_3}}{dt} = k_g\ C_{SO_2\text{-}g} \qquad \text{(B-3)}$$

The number of moles of sorbent ($N_{Na_2CO_3}$) can be related to the volume of the sorbent in the following way:

$$N_{Na_2CO_3} = \frac{\rho\ V}{MW} \qquad \text{(B-4)}$$

Since a decrease in the volume of unreacted sorbent accompanies the reaction of Na_2CO_3, it follows that

$$dN_{Na_2CO_3} = \frac{\rho\ dV}{MW} = \frac{\rho}{MW}\ d\left(\frac{4}{3}\pi r^3\right) = \frac{4\rho\pi\ r^2}{MW}\ dr \qquad \text{(B-5)}$$

Substitution of Equation B-5 into Equation B-3 gives

$$\frac{-1}{4\pi\ R^2}\left(\frac{4\ \pi\rho\ r^2 dr}{MW\ dt}\right) = k_g\ C_{SO_2\text{-}g} \qquad \text{(B-6)}$$

This can be rearranged to yield

$$\frac{-\rho}{R^2 MW} \int_R^r r^2 dr = k_g C_{SO_2-g} \int_0^t dt \qquad \text{(B-7)}$$

and upon integration and further rearrangement gives

$$t = \frac{\rho \quad R}{3 \; MW \; k_g \; C_{SO_2-g}} \left[1 - \left(\frac{r}{R}\right)^3 \right] \qquad \text{(B-8)}$$

The time needed for complete conversion of the sorbent (τ) can be found by setting r = 0.

$$\tau = \frac{\rho \quad R}{3 \; MW \; k_g \; C_{SO_2-g}} \qquad \text{(B-9)}$$

Therefore the radius of the unreacted core can be expressed in terms of the fractional time needed for complete conversion

$$\frac{t}{\tau} = 1 - \left(\frac{r}{R}\right)^3 \qquad \text{(B-10)}$$

This can also be written in terms of fractional sorbent conversion. Since

$$1\text{-}X = \frac{\text{volume of unreacted core}}{\text{total particle volume}} = \frac{\frac{4}{3} \quad r^3}{\frac{4}{3} \quad R^3} = \frac{r^3}{R^3} \qquad \text{(B-11)}$$

then

$$X = 1 - \frac{r^3}{R^3} = \frac{t}{\tau} \qquad \text{(B-12)}$$

This equation can be used to interpret data for conversion of sorbent with time.

Diffusion Through the Ash Layer is Rate Controlling

The next case, where diffusion through the ash layer controls the rate of reaction, requires a two-step analysis. First, a typical partially reacted particle is characterized; then this relationship is applied for changes in unreacted core radius from R to zero.

First consider a partially reacted particle. Both SO_2 and the boundary of unreacted Na_2CO_3 move inward toward the center of the particle. However, the shrinkage of the core is slower than the diffusion of SO_2 toward the core by about a factor of 1000 (this is roughly the ratio of densities of solid to gas).[1] Thus it can be assumed that at any time the unreacted core is stationary. This steady-state assumption allows the mathematics to be simplified. Other assumptions are that gas film resistance is negligible and that the chemical reaction is instantaneous.

The rate of reaction of SO_2 at any instant is equivalent to the rate of diffusion of SO_2 to the reaction surface (the unreacted core surface).

$$\frac{-dN_{SO_2}}{dt} = 4\pi r^2 Q_{SO_2} \tag{B-13}$$

The flux of SO_2 within the ash layer from Fick's law for equimolar counter diffusion is:

$$Q_{SO_2} = D_V \frac{dC_{SO_2}}{dr} \tag{B-14}$$

Equations B-13 and B-14 can be combined to give:

$$\frac{-dN_{SO_2}}{dt} = 4\pi r^2 \, Dv \frac{dC_{SO_2}}{dr} \tag{B-15}$$

This expression can be integrated as follows:

$$\frac{-dN_{SO_2}}{dt} \int_R^r \frac{dr}{r^2} = 4\pi D_v \int_{C_{SO_2-g} = C_{SO_2-s}}^{C_{SO_2-c} = 0} dC_{SO_2} \tag{B-16}$$

$$\frac{-dN_{SO_2}}{dt} \left(\frac{1}{r} - \frac{1}{R}\right) = 4\pi D_v C_{SO_2-g} \tag{B-17}$$

This expression represents the condition of a reacting particle at any time.

In the second part of the analysis, the size of the unreacted core is changed with time. The value dN_{SO_2} can be expressed in terms of the core radius as was done for the case where gas film diffusion was rate controlling.

Substituting Equation B-5 into Equation B-17 gives

$$\frac{-4\pi\rho r^2 dr}{MW}\left(\frac{1}{r}-\frac{1}{R}\right) = 4\pi D_v C_{SO_2\text{-}g}\, dt \qquad \text{(B-18)}$$

This equation can be written in the integrated form as

$$\frac{-\rho}{MW}\int_{r=R}^{r}\left(\frac{1}{r}-\frac{1}{R}\right) r^2 dr = D_v C_{SO_2\text{-}g}\int_0^t dt \qquad \text{(B-19)}$$

and integrated to give:

$$t = \frac{\rho\, R^2}{6MW\, D_v C_{SO_2\text{-}g}}\left[\,1 - 3\left(\frac{r}{R}\right)^2 + 2\left(\frac{r}{R}\right)^3\,\right] \qquad \text{(B-20)}$$

The time required for complete conversion of a particle (τ) (i.e. to r = 0), is

$$\tau = \frac{\rho\, R^2}{6(MW)\, D_v\, C_{SO_2\text{-}g}} \qquad \text{(B-21)}$$

Therefore,

$$\frac{t}{\tau} = \left[\,1 - 3\left(\frac{r}{R}\right)^2 + 2\left(\frac{r}{R}\right)^3\right] \qquad \text{(B-22)}$$

This can be expressed in terms of fractional conversion by using Equation B-11. Thus Equation B-22 becomes:

$$\frac{t}{\tau} = 1 - 3(1-X)^{2/3} + 2(1-X) \qquad \text{(B-23)}$$

Chemical Reaction is Rate Controlling

In the last case the chemical reaction controls the rate of reaction. For this case it is assumed that the resistance to diffusion of the gas film and through the ash layer are negligible. Thus, $C_{SO_2\text{-}g} = C_{SO_2\text{-}s} = C_{SO_2\text{-}c}$. Therefore, the rate of reaction is proportional to the available surface area of the unreacted core and can be expressed as:

$$\frac{-1}{4\pi r^2}\frac{dN_{Na_2CO_3}}{dt} = \frac{-1}{4\pi r^2}\frac{dN_{SO_2}}{dt} = k_s C_{SO_2-g} \qquad \text{(B-24)}$$

Equation B-5 can be substituted into Equation B-24 to give:

$$\frac{-1}{4\pi r^2}\left(\frac{4\pi\rho r^2 dr}{MW\ dt}\right) = k_s\ C_{SO_2-g} \qquad \text{(B-25)}$$

This relationship can be simplified to

$$\frac{-\rho}{MW}\int_R^r dr = k_s C_{SO_2-g}\int_{t=0}^{t} dt \qquad \text{(B-26)}$$

and integrated and rearranged to yield

$$t = \frac{\rho}{(MW)k_s C_{SO_2-g}}\ (R-r) \qquad \text{(B-27)}$$

The time (τ) required for complete conversion can be obtained when r = 0.

$$\tau = \frac{\rho\ R}{(MW)k_s C_{SO_2-g}} \qquad \text{(B-28)}$$

Thus Equation B-27 can be expressed as

$$\frac{t}{\tau} = 1 - \frac{r}{R} \qquad \text{(B-29)}$$

Equation B-11 can then be used to express Equation B-29 in terms of fractional conversion

$$\frac{t}{\tau} = 1 - (1-X)^{1/3} \qquad \text{(B-30)}$$

REFERENCE FOR APPENDIX B

1. Levenspiel, O. Chemical Reaction Engineering, 2nd edition. John Wiley and Sons, Inc. New York. 1972. pp. 357-377.

APPENDIX C

Conversion Factors

1 ft	=	0.3048 m
1 lb	=	0.454 kg
1000 cfm	=	0.5 m^3/s
1 gal/1000 ft	=	0.13 liters/m
1 Btu	=	1.055 kJ
1 gal	=	3.79 liters
1 ft^3	=	28.32 liters
1 lb-mole	=	453.6 g-mole
1 atm	=	1.013×10^5 Pa
1 $\frac{Btu}{ft^2\text{-}hr\text{-}°F}$	=	5.678 $\frac{J}{m^2\text{-}s\text{-}K}$
1 $\frac{Btu}{lb\text{-}°F}$	=	4.187×10^3 $\frac{J}{kg\ K}$
1 $\frac{ft^2}{sec}$	=	9.29×10^{-2} $\frac{m^2}{S}$
1 $\frac{lb}{ft^3}$	=	16.018 $\frac{kg}{m^3}$
1 $\frac{lb}{ft\text{-}hr}$	=	4.133×10^{-4} Pa-s